TROPICAL PEATLANDS IN WEST KALIMANTAN: FORMATION, CARBON, AND LATE PLEISTOCENE-HOLOCENE HISTORY

by

MONIKA RUWAIMANA

A DISSERTATION

Presented to the Department of Biology
and the Division of Graduate Studies of the University of Oregon
in partial fulfillment of the requirements
for the degree of
Doctor of Philosophy

June 2023

DISSERTATION APPROVAL PAGE

Student: Monika Ruwaimana

Title: Tropical Peatlands in West Kalimantan: Formation, Carbon and Late Pleistocene-Holocene history

This dissertation has been accepted and approved in partial fulfillment of the requirements for the Doctor of Philosophy degree in the Department of Biology:

Scott Bridgham	Chairperson
Daniel Gavin	Advisor
Lauren Hallet	Core Member
Gusti Anshari	Core Member
Lucas Silva	Institutional Representative

and

Krista Chronister	Vice Provost for Graduate Studies

Original approval signatures are on file with the University of Oregon Division of Graduate Studies.

Degree awarded June 2023

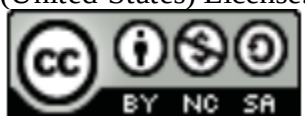

DISSERTATION ABSTRACT

Monika Ruwaimana

Doctor of Philosophy

Department of Biology

June 2023

Title: Tropical Peatlands in West Kalimantan: Formation, Carbon and Late Pleistocene-Holocene History

Peatlands hold an important function in the global carbon cycle. Despite only covering 3–4% of the terrestrial landscape, peatlands disproportionately store 30–40% of the Earth's soil carbon. Temperate and boreal peatlands are mostly well-studied, while tropical peatland is relatively understudied. In the past decades, tropical peatland especially in Southeast Asia has become a center of attention due to frequent disastrous fires. However, its basic properties such as depth, extent, carbon storage, formation, and its potential as an environmental archive are rarely studied. Thus, in this dissertation, I explored a tropical peatland in West Kalimantan, Indonesia, and conducted a stratigraphic study on several peat cores to reveal its ecological history.

We collected 32 peat cores from two main study areas, coastal peatland and inland peatland. We conducted radiocarbon dating and analyses of bulk density, loss-in-ignition, organic geochemistry (C%, N%, $\delta^{13}C$, and $\delta^{15}N$), charcoal counts, and pollen identification. We found that the coastal peatland (6m depth) is thinner than the inland peat (15m), and younger (4,500yr vs 50,000yr). The age and thickness of our inland peat site put it as the deepest and oldest extant peatland in the world, and subsequently as the most carbon-dense ecosystem. In their genesis, coastal peatland has a simple linear age-depth relationship, showing stable accumulation of carbon. In contrast, inland peat shows

a complex history, where we observed age reversals and hiatuses, likely caused by climate variability from the Last Glacial Maximum (LGM) to the Holocene. Our study is the first that utilized multiple cores to create continuous vertical age and geochemical profiles, which revealed an age reversal that was likely caused by flood events. The charcoal record reveals a continuous presence of low severity fire, with increasing late Holocene fire frequency presumably due to increasing anthropogenic influence. Finally, we conducted pollen analysis and created a pollen atlas, which will be used for future palynological work to explore the vegetation change throughout time.

This research highlights not only modern, but also the historical and prehistorical importance of tropical peatland as a dynamic long term carbon storage that withstood the glacial-interglacial climate transition but is currently threatened by deforestation and land-use change. This dissertation includes previously published and unpublished coauthored material.

CURRICULUM VITAE

NAME OF AUTHOR: Monika Ruwaimana

GRADUATE AND UNDERGRADUATE SCHOOLS ATTENDED:

University of Oregon, Eugene, USA
Vrije Universiteit Brussel & Université Libre de Bruxelles, Belgium
Università degli Studi di Firenze, Italy
Universitas Atma Jaya Yogyakarta, Indonesia

DEGREES AWARDED:

Doctor of Philosophy, Biology, 2023, University of Oregon, USA
Master of Science, Ecology, 2016, Vrije Universiteit Brussel, Université Libre de Bruxelles, Università degli Studi di Firenze (under TROPIMUNDO, Erasmus Mundus Joint Master Degree in Tropical Biodiversity and Ecosystems
Bachelor of Science, Biology, 2013, Universitas Atma Jaya Yogyakarta, Indonesia

AREAS OF SPECIAL INTEREST:

Ecology, Pollen, Palynology, Tropical Ecology, Peatland, Forest Fire, Carbon Credit, Soil Science, Mangrove, Sustainable Fisheries, Marine Biology

PROFESSIONAL EXPERIENCE:

Staff, LINI Foundation, Bali, Indonesia, 2013–2014

Faculty, Universitas Atma Jaya Yogyakarta, Indonesia, 2016-Present

GRANTS, AWARDS, AND HONORS:

IPCC (Intergovernmental Panel on Climate Change) Scholarship funded by The Prince Albert II of Monaco Foundation. 28,750 EUR, 2021

AGU Michael H. Freilich Student Visualization Competition Program – Runner up winner 1,000 USD, 2021

William R. Sistrom Memorial Scholarship 1900 USD, 2021

AGU Michael H. Freilich Student Visualization Competition Program – Runner up winner 1,000 USD, 2020

Allan Robertson Grant, International Peat Society 500 EUR, 2020

AICEF (American Indonesian Cultural & Educational Foundation) - Overseas Travel Grant 2500 USD, 2019

Fulbright Doctorate Scholarship 120,000 USD, 2018

VLIR-UOS (the Flemish Interuniversity Council) travel grant, 4,000 EUR, 2016

Erasmus Mundus Category A Full Scholarship in Tropimundo (Erasmus Mundus Masters Course in Tropical Biodiversity and Ecosystems) 44,000 EUR, 2014

Silver Medal at National Science Olympiad, Biology, Ministry of Education, 11,000,000 IDR, 2013

3rd Place at National Science and Technology Olympiad, Department of Youth and Sport, Yogyakarta, 4,000,000 IDR, 2013

Silver Medal at National Science Olympiad, Biology, Ministry of Education, Surabaya, 11,000,000 IDR, 2012

1st Place Research Poster, Science Fair, Indonesia Islam University, Yogyakarta, 500,000 IDR, 2012

2nd Place at Regional Selection Pertamina Science Olympiad 4,500,000 IDR, 2011

PUBLICATIONS:

STYLE QI

Anshari, G.Z., Gusmayanti, E., Afifudin, **M., Ruwaimana**, M., Hendricks, L. and Gavin, D.G., 2022. Carbon loss from a deforested and drained tropical peatland over four years as assessed from peat stratigraphy. CATENA, 208, p.105719.

Ruwaimana, M., Anshari, G.Z., Silva, L.C. and Gavin, D.G., 2020. The oldest extant tropical peatland in the world: a major carbon reservoir for at least 47 000 years. Environmental Research Letters, 15(11), p.114027.

Ruwaimana, M., Satyanarayana, B., Otero, V., Muslim, A.M., Syafiq, M., Ibrahim, S., Raymaekers, D., Koedam, N. and Dahdouh-Guebas, F., 2018. The advantages of using drones over space-borne imagery in the mapping of mangrove forests. PloS one, 13(7), p.e0200288.

Ruwaimana, M. and Yuda, N.A.I.P., 2017. Resolusi Spasial Optimum pada Citra Drone untuk Klasifikasi Spesies Mangrove dengan Metode Maximum Likelihood. Journal of Biota, 2(2).

Ruwaimana, M., Sidharta, B.R. and Atmodjo, P.K., 2015. Comparative study of antibacterial activity of methanol extract of Sinularia, Sarcophyton, and Lobophytum from Tulamben, Bali. KnE Life Sciences, 2(1), pp.654-657.

ACKNOWLEDGMENTS

I am grateful to my supervisor, Dan Gavin, for his professional guidance, moral and material support, and kindness and patience with his students, including myself. He has made me feel welcomed and supported since our first Zoom session when I was finishing my Master's in Brussels, through our trip through Kalimantan's jungle, and finally at the University of Oregon. I am also grateful to Dan and his family for supporting my non-academic projects, such as my food-truck, and for helping me and my family during tough times, such as the immigration issue and Oregon's rare snowstorm.

I am thankful for my committee, Scott Bridgham, Lauren Hallett, Lucas Silva, and Gusti Anshari, for their academic guidance and support. Gusti Anshari was particularly helpful with data collection and processing in Indonesia, and Lauren Hallett was a supportive presence as a fellow mother. Despite unexpected situations such as the pandemic and my family growth, my committee was understanding and supportive.

My labmates, Jamila Baig, Chantel Saban, Geoffrey Johnson, Lauren Hendricks, Buzz Nanavati, Schyler Reiss, Jamie Wright, Natalie Kozlowsky, and Erin Herring, have been great colleagues, helping me with proofreading, presentations, and commiserating over the challenges of research in the face of climate change. I am grateful for my IE2 cohort and their spouses, Lina Aoyama, Sabrina Mostoufi, Max Spencer, Murillo Rodrigues, Kayla Evans, and Sophia Franz, for their camaraderie, and the fun picnics and dinners we shared.

I would like to thank the Indonesian community in Eugene for becoming my family away from home, providing delicious meals, and helping us during tough times. Their unwavering support and generosity will always be remembered. Lastly, I would

like to express my deepest gratitude to my husband, Surya, for always supporting me through this journey. I could not have accomplished this without his love and encouragement. And to my daughter, Aruna, who brings so much joy to our lives and is a constant reminder of what truly matters.

We acknowledge and thank the dedicated efforts of lab and field crew from Universitas Tanjungpura, Nung, Putri, Rabbirl Yarham, Jemani, residents of Putussibau, Hendro and family, and from University of Oregon, Rose Nittler – lab technician. We thank Kathryn Elder (Woods Hole Oceanographic Institute) for interpreting the maximum limiting ages of the radiocarbon measurements. Furthermore, we are grateful for the funding support provided by National Science Foundation award 1561099, an AMINEF Fulbright Doctoral Scholarship, an IPCC Scholarship funded by Prince Albert II of Monaco Foundation, an AICEF (American Indonesian Cultural & Educational Foundation) Overseas Travel Grant, the University of Oregon, and Universitas Atma Jaya Yogyakarta. Finally, it is important to note that all peat cores were collected in a responsible manner, with permission from local authorities and in accordance with local laws.

For Surya and Aruna, my lights.
and
for my ancestral land, Kalimantan.

TABLE OF CONTENTS

LIST OF FIGURES

Figure Page

LIST OF POLLEN MICROSCOPIC PLATES

Plate Page

LIST OF TABLES

Table Page

LIST OF SUPPLEMENTARY FIGURES

Supplementary Figure Page

LIST OF SUPPLEMENTARY TABLES

I. INTRODUCTION

Peatlands are wetland ecosystems defined by their soil characteristic, which is a highly organic peat soil. Most soils only have a thin organic layer on the top, but peatlands often have several meters of organic matter called peat (Baillie, 2001; Paavilainen and Päivänen, 1995). This peat is able to accumulate due to a higher rate of net primary production compared to the rate of decomposition (Moore, 1989). Slow decomposition on the peatland is mainly attributed to a high water level that deprives soil microbes of oxygen (Yu et al., 2010). This highly organic peat consequently stores a high amount of carbon, enabling peatlands to become a major carbon sink (Bridgham et al., 2006; Yu, 2012). Despite covering only approximately 3–5% of terrestrial area globally, peatlands disproportionately store a third to one half of global soil carbon (Joosten and Clarke, 2002; Nichols and Peteet, 2019).

Peatlands occur all over the world, but mainly based on their latitudinal location, they can be divided into temperate/boreal and tropical peatland. Around 84–90% of the peatlands are located in the temperate and boreal regions, while the rest are located in tropical regions (Osaki and Tsuji, 2016). Temperate and tropical peatlands differ starkly in the vegetation types, leading to concomitant differentiation of peat composition; where the temperate peat consists of sphagnum mosses, herbs, shrubs and small trees (Moore and Bellamy, 1974) and the tropical peat forms from rainforest trees and other woody vegetation (Page et al., 1999; Osaki and Tsuji, 2016). Tropical peatlands often store more soil carbon per unit area than temperate peatlands, because tropical peatlands are often deeper, with an average depth of 5 m compared to 2 m for temperate peatlands (Page et al., 2011; Yu, 2012). More than a third (38%) of all tropical peatlands are contained within Indonesia (Gumbricht et al., 2017).

Under natural and undisturbed conditions, these peatlands have functioned for thousands of years as a long-term carbon reservoir (Osaki and Tsuji, 2016). However, hydrological disturbance by climate change or other anthropogenic activity can switch the carbon balance of peatland towards a carbon source (Bridgham et al., 2008). In Indonesian tropical peatlands, large scale forest and escaped agricultural fires over the last three decades have greatly degraded the peatlands and released its carbon. As example, the El Niño fire event in 1997 released up to 2.6 Gt C (Lohman et al., 2007; Page et al., 2002), roughly equal to half of current US annual carbon emission. This fire event followed by subsequent anthropogenic fires that occur consistently

during the monsoon dry season and peaking during El Niño periods (Cattau et al., 2016). From 2000 to 2010 alone, Indonesia lost around 2.7 million ha of peat due to burning and land use change (Miettinen et al., 2012). Despite international attention to fires in tropical peatlands and the important role tropical peatlands play as a carbon reservoir, fundamental properties of peatlands remain poorly understood (e.g., formation, history, extent, depth, and age) (Osaki and Tsuji, 2016). Thus, in this research, we conducted a survey of peatlands in West Kalimantan, Indonesia to describe these fundamental properties and history of tropical peat formation.

In Southeast Asia, peatland could be categorized into coastal and inland peats based on their formation time and their relation to the sea level change (Dommain et al., 2011). The coastal peat formed after the current sea level stabilized around 7–8 ka, while the inland peat possibly initiated earlier. Thus, inland peat is often older and deeper than the coastal peat (Dommain et al., 2014; Neuzil, 1997). Our study sites are located in West Kalimantan, a province of Indonesia with approximately 1.6 million ha of peat (Anda et al., 2021; Ritung et al., 2011). This province contains the Kapuas River—the longest river in Indonesia—which defines two distinct peatland regions, inland peatland on the upstream floodplain, and coastal peatland on the river delta; thus this area is a great site as it encompasses both types of tropical peatland. With the samples and data collected from that site, we answered the following research questions:

1. Initiation and formation of peatland. Inland and coastal peatlands form differently based on their relationship with the past climate and sea level changes (Dommain et al., 2014, 2011). When did the different types (inland and coastal) of tropical peatland start to form, and what is the link with climate and sea level change? This question is answered in chapter 2 and published on Environmental Research Letters in 2020 with co-authors Gusti Anshari, Lucas Silva, and Dan Gavin.

2. Tropical peatlands' carbon dynamics throughout time. Multiple factors such as climate, fire and humans affect carbon dynamics in peatlands, therefore, impacting the global carbon cycle (Bridgham et al., 2008; Cochrane, 2003; Page et al., 2011). Interplay of these factors cause variation of peat accumulation rates, and subsequently carbon sequestration rates (Page et al., 2004; Young et al., 2021). How can the chemical and physical stratigraphy of peat layers explain the temporal dynamics of peat accumulation

and carbon sequestration in the tropical peatlands of West Kalimantan? This question is answered in chapter 3 and submitted to the journal Ecosystems in November 2022 with co-authors Gusti Anshari and Dan Gavin, and is currently under review.

3. Tropical peatland vegetation change. Vegetation composition and climate have changed over time in tropical peatlands and by conducting palynological analysis, we could infer those changes (Anshari et al., 2001; Haberle et al., 2010; Yulianto et al., 2005). What are the pollen and spore types that are preserved in this peatland, how has the vegetation changed, and how have these changes resulted from past climate changes? These questions require detailed study of the pollen stratigraphy, a challenging task as the palynoflora of tropical peatlands is poorly described. These questions are addressed in chapter 4 and the paper will be published on the journal of Quaternary International with co-authors Daniel Gavin, Gusti Anshari, and Kartika Hapsari.

References

Anda, M., Ritung, S., Suryani, E., Sukarman, Hikmat, M., Yatno, E., Mulyani, A., Subandiono, R.E., Suratman, Husnain, 2021. Revisiting tropical peatlands in Indonesia: Semi-detailed mapping, extent and depth distribution assessment. Geoderma 402, 115235. https://doi.org/10.1016/j.geoderma.2021.115235

Anshari, G., Peter Kershaw, A., van der Kaars, S., 2001. A Late Pleistocene and Holocene pollen and charcoal record from peat swamp forest, Lake Sentarum Wildlife Reserve, West Kalimantan, Indonesia. Palaeogeography, Palaeoclimatology, Palaeoecology, Quaternary Environmental Change in the Indonesian Region 171, 213–228. https://doi.org/10.1016/S0031-0182(01)00246-2

Baillie, I.C., 2001. Soil survey staff 1999, soil taxonomy: a basic system of soil classification for making and interpreting soil surveys, agricultural handbook 436, Natural Resources Conservation Service, USDA, Washington DC, USA, pp. 869. Wiley Online Library.

Bridgham, S.D., Megonigal, J.P., Keller, J.K., Bliss, N.B., Trettin, C., 2006. The carbon balance of North American wetlands. Wetlands 26, 889–916.

Bridgham, S.D., Pastor, J., Dewey, B., Weltzin, J.F., Updegraff, K., 2008. Rapid carbon response of peatlands to climate change. Ecology 89, 3041–3048.

Cattau, M.E., Harrison, M.E., Shinyo, I., Tungau, S., Uriarte, M., DeFries, R., 2016. Sources of anthropogenic fire ignitions on the peat-swamp landscape in Kalimantan, Indonesia. Global Environmental Change 39, 205–219.

Cochrane, M.A., 2003. Fire science for rainforests. Nature 421, 913–919. https://doi.org/10.1038/nature01437

Dommain, R., Couwenberg, J., Glaser, P.H., Joosten, H., Suryadiputra, I.N.N., 2014. Carbon storage and release in Indonesian peatlands since the last deglaciation. Quaternary Science Reviews 97, 1–32. https://doi.org/10.1016/j.quascirev.2014.05.002

Dommain, R., Couwenberg, J., Joosten, H., 2011. Development and carbon sequestration of tropical peat domes in south-east Asia: links to post-glacial sea-level changes and Holocene climate variability. Quaternary Science Reviews 30, 999–1010. https://doi.org/10.1016/j.quascirev.2011.01.018

Gumbricht, T., Roman-Cuesta, R.M., Verchot, L., Herold, M., Wittmann, F., Householder, E., Herold, N., Murdiyarso, D., 2017. An expert system model for mapping tropical wetlands and peatlands reveals South America as the largest contributor. Global Change Biology 23, 3581–3599.

Haberle, S.G., Behling, H., Dupont, L., Kirleis, W., 2010. Introduction: Tropical palaeoecology and global change. Global Change Biology 16, 1645–1646. https://doi.org/10.1111/j.1365-2486.2010.02231.x

Joosten, H., Clarke, D., 2002. Wise use of mires and peatlands: background and principles including a framework for decision-making. International Peat Society; International Mire Conservation Group, Jyväskylä] : [Greifswald.

Lohman, D.J., Bickford, D., Sodhi, N.S., 2007. The Burning Issue. Science 316, 376.

Miettinen, J., Hooijer, A., Shi, C., Tollenaar, D., Vernimmen, R., Liew, S.C., Malins, C., Page, S.E., 2012. Extent of industrial plantations on Southeast Asian peatlands in 2010 with analysis of historical expansion and future projections. GCB Bioenergy 4, 908–918. https://doi.org/10.1111/j.1757-1707.2012.01172.x

Moore, P.D., 1989. The ecology of peat-forming processes: a review. International Journal of Coal Geology 12, 89–103.

Moore, P.D., Bellamy, D.J., 1974. Peatlands. Springer.

Neuzil, S.G., 1997. Onset and rate of peat and carbon accumulation in four domed ombrogenous peat deposits, Indonesia. Biodiversity and sustainability of tropical peatland.

Nichols, J.E., Peteet, D.M., 2019. Rapid expansion of northern peatlands and doubled estimate of carbon storage. Nature Geoscience 12, 917–921.

Osaki, M., Tsuji, N., 2016. Tropical peatland ecosystems. Springer.

Paavilainen, E., Päivänen, J., 1995. Peatland forestry: ecology and principles. Springer Science & Business Media.

Page, S.E., Rieley, J.O., Banks, C.J., 2011. Global and regional importance of the tropical peatland carbon pool. Global Change Biology 17, 798–818. https://doi.org/10.1111/j.1365-2486.2010.02279.x

Page, S.E., Rieley, J.O., Shotyk, Ø.W., Weiss, D., 1999. Interdependence of peat and vegetation in a tropical peat swamp forest. Philosophical Transactions of the Royal Society of London B: Biological Sciences 354, 1885–1897. https://doi.org/10.1098/rstb.1999.0529

Page, S.E., Siegert, F., Rieley, J.O., Boehm, H.-D.V., Jaya, A., Limin, S., 2002. The amount of carbon released from peat and forest fires in Indonesia during 1997. Nature 420, 61–65. https://doi.org/10.1038/nature01131

Page, S.E., Wűst, R. a. J., Weiss, D., Rieley, J.O., Shotyk, W., Limin, S.H., 2004. A record of Late Pleistocene and Holocene carbon accumulation and climate change from an equatorial peat bog (Kalimantan, Indonesia): implications for past, present and future carbon dynamics. J. Quaternary Sci. 19, 625–635. https://doi.org/10.1002/jqs.884

Ritung, S., Wahyunto, W., Nugroho, K., Sukarman, S., Hikmatullah, H., Suparto, S., Tafakrenanto, C., 2011. Peta Lahan Gambut Indonesia Skala 1:250.000, December 2. ed. Balai Besar Penelitian dan Pengembangan Sumberdaya Lahan Pertanian, Badan Penelitian dan Pengembangan Pertanian, Bogor.

Young, D.M., Baird, A.J., Gallego-Sala, A.V., Loisel, J., 2021. A cautionary tale about using the apparent carbon accumulation rate (aCAR) obtained from peat cores. Sci Rep 11, 9547. https://doi.org/10.1038/s41598-021-88766-8

Yu, Z., Loisel, J., Brosseau, D.P., Beilman, D.W., Hunt, S.J., 2010. Global peatland dynamics since the Last Glacial Maximum. Geophysical Research Letters 37.

Yu, Z.C., 2012. Northern peatland carbon stocks and dynamics: a review. Biogeosciences 9, 4071–4085. https://doi.org/10.5194/bg-9-4071-2012

Yulianto, E., Rahardjo, A.T., Noeradi, D., Siregar, D.A., Hirakawa, K., 2005. A Holocene pollen record of vegetation and coastal environmental changes in the coastal swamp forest at Batulicin, South Kalimantan, Indonesia. Journal of Asian Earth Sciences 25, 1–8.

II. THE OLDEST EXTANT TROPICAL PEATLAND IN THE WORLD: A MAJOR CARBON RESERVOIR FOR AT LEAST 47,000 YEARS

Published as Ruwaimana, M., Anshari, G.Z., Silva, L.C. and Gavin, D.G., 2020. The oldest extant tropical peatland in the world: a major carbon reservoir for at least 47,000 years. *Environmental Research Letters*, 15(11), p.114027.

MR, GDG, and GZA conceptualized the study, devised the methodology and conducted the field investigation. DGG, GZA and LCRS supervised and provided resources. DGG & MR acquired the funding. MR curated, analyzed, and visualized the data. MR wrote the original draft, all authors discussed the results and contributed to the final manuscript.

Introduction

Tropical peatlands in Indonesia have become a large source of carbon emissions due to land clearance, drainage and disastrous forest fires over the past three decades. For example, the El Niño related fire event in 1997 released up to 2.6 Gt C (Lohman et al., 2007; Page et al., 2002), roughly equal to half of current US annual carbon emissions, and subsequent anthropogenic fires occur consistently during the dry season and peaking during El Niño periods (Cattau et al., 2016). From 2000 to 2010 alone, around 2.7 million ha of peatlands in Indonesia is deforested and degraded (Miettinen et al., 2011). However, over at least the past several thousand years, tropical peatlands have functioned as a carbon sink, currently storing more than 104,7 Gt carbon (Dargie et al., 2017). The history of peatland formation, and fundamental properties of their extent, depth, and age remain poorly constrained for large parts of Southeast Asia. For example, improvements in mapping methods have shown original studies underestimated peatlands extent and depth (Osaki and Tsuji, 2016). In addition, little is known of the ages of tropical peatland initiation, which constrains the peat carbon stock and provides crucial information regarding the past climates suitable for peat growth (Treat et al., 2019).

Despite their importance on a global scale, tropical peatlands are much less studied compared to their temperate and boreal counterparts (Osaki and Tsuji, 2016; Yu, 2012). Globally, out of 3983 dated peatland sites, only 198 are from the tropics, and only 80 of those are

in Southeast Asia, despite the fact that this area contains the deepest and most extensive peat areas in the tropics (Gumbricht et al., 2017; Treat et al., 2017). Tropical peatlands in Southeast Asia can be divided into coastal peatland, which established after ca. 8 ka (thousand calibrated radiocarbon years before present) when sea level decreased and stabilized, and inland peatland which formed much earlier during the Late Pleistocene (Dommain et al., 2011). The peatlands in this area initiate within broad inundated basins, eventually accumulating sufficient organic matter to form raised dome structures that support tropical forests (Anderson, 1963). Peatlands usually form and accumulate faster during the warm and wet climates of the interglacial period (Fischer et al., 2018). While temperate peatlands were overrun and degraded by ice sheets during glacial periods, tropical peat may have remained intact, despite possible degradation due to a colder and drier climate (Treat et al., 2019). In this study, we highlight the differences of formation times and depth profiles between coastal and inland peatlands, and how the climate possibly affected peat formation. As there is not yet any estimate of the carbon stored in the inland peat of West Borneo, we provide the first estimation of the timing of peat genesis and carbon accumulated since then.

Materials and Methods

Study Area

Sampling sites are located on West Kalimantan, a province of Indonesia with approximately 1,7 million ha of peat (Ritung et al., 2011; Ritung and Subagjo, 2004). This province contains the Kapuas River—the longest river in Indonesia—which defines two distinct peatland regions, inland peatland on the upstream floodplain, and coastal peatland on the river deltas. We expect these two regions will have distinct characteristics, because based on their elevation, the upstream region always remained as land during the Holocene, meanwhile the delta region was affected by sea level changes (Dommain et al., 2014).

We laid two main transects across two peat domes, Rasau Jaya in the Kapuas delta region, and a dome south of Putussibau in the Upper Kapuas Basin region (Fig 1). In addition to these two transects, we also collected several cores from three other areas (Ketapang, Gunung Palung and Sentarum). The samples from Sentarum were collected in 2011, while the other samples were collected during 2017–2019. Among these sites, Sentarum and Gunung Palung are

protected within national parks, while other locations are disturbed by burning, clear cutting and replaced by abandoned forest or plantation.

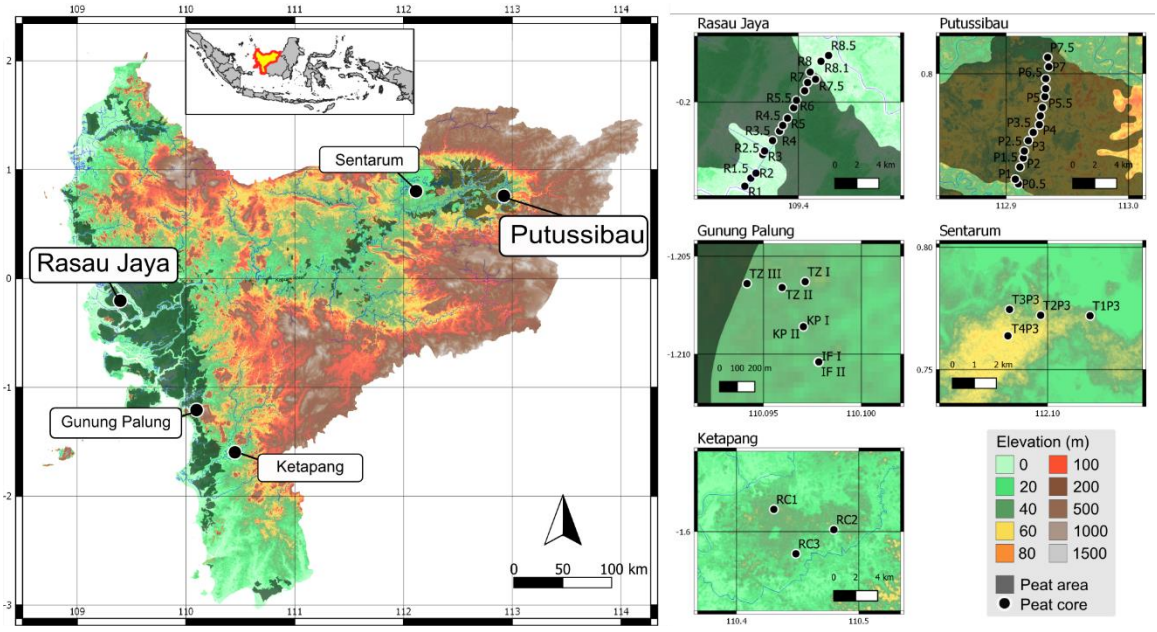

Figure 2.1. Sampling location map with detailed coring site on the subsets. Two main transects located in Putussibau (inland peat) and Rasau Jaya (coastal peat). Other sites are sampled randomly.

Sampling Method

We collected peat cores using Russian peat corers. We used a 52 mm diameter Russian peat corer to obtain samples down to the mineral layer. At the main transects in Rasau Jaya (Kapuas delta) and Putussibau (Upper Kapuas), we collected two sets of cores spaced at ca. 1-km. One core was used for carbon and bulk density analysis and one core for other peat properties. For the first core, in each 25-cm segment we subsampled 10 cm for bulk density and loss-on-ignition analysis. For the second core, in 5-cm contiguous samples, we sampled 20 cm^3 from the center of the core, so the outer part of the core does not contaminate the sample. We stored the samples in sterile bags and kept them at 4°C except during transport. In between the main sampling sites we took an additional core with only purpose of measuring the peat depth and therefore did not take samples.

We had technical difficulty in cores P3, P4, and P5, where we were unable to collect samples to the bottom of the peat as we repeatedly encountered a layer of buried hardwood at ca. 10–11 m depth. This hardwood layer twisted and opened the corer when we tried to collect samples from this depth. The layer was encountered in at least ten locations over a ca. 30 m^2 area

around sampling points. Therefore, in these cases we changed the objective to obtaining samples as deep as possible rather than contiguously through the woody layer (See Fig. 3). In core P3, we were able to collect a 5-cm segment sample from the bottom of the peat at the depth of 15 m. However, at core P4 and P5, we did not reach the mineral layer at the depth of 15 m, which is the maximum depth reached by our corer. Therefore, we assume that the bottom of the peat is topographically flat with the adjacent site (P3.5), resulting in estimated depths at P4 of 17 m and at P5 of 16.9 m. This estimate is also supported by one of the author's (G.Z.A.) ongoing coring project who found a peat depth of 18 m roughly 1 km west of our transect (RSS GmbH, 2018).

Radiocarbon Dating

We used 5-cm segment samples for radiocarbon dating the base of the peat cores. We sieved 1 cc bulk peat to obtain the 125–500 μm fraction, which was then treated with HCl and KOH rinses. For some samples (RC cores from Ketapang), we also picked out larger material (>500 μm) to date. We sent 25 samples to the NOSAMS Woods Hole facility and 7 samples (from Sentarum sites) to Waikato in New Zealand (See Table S1 for the details). We calibrated the dates following IntCal13 (Reimer et al., 2013).

Various materials may produce different ages due to peat layer dynamics. For example, pollen and macrofossil material have yielded consistent ages because they tend to stay at the same layer, however the bulk peat material might date younger than the actual age due to root intrusion (Wüst et al., 2008). To test the effect of material type on radiocarbon ages, we dated two types of material from the RC cores. In our comparisons from two cores (RC1 and RC3), there were insignificant differences (<100 years) between ages derived from bulk material and plant macrofossils (> 500 μm). In a third core (RC2), we found that the woody material was 1200 years older than the bulk peat. As these results disagree with Wüst et al. (2018), we decided to date only woody material sieved from bulk peat (125–500 μm) for the core transects.

Elevation Measurement and Peat Profile

We used RTK GPS to measure the elevation of the transect points across the peat domes in Rasau Jaya and Putussibau. At each site, we collected multiple sessions of 20 to 60 minutes of raw GPS data as RINEX files using a Garmin GPSMAP 66. To obtain the ellipsoid elevation, we post-processed the RINEX files using RTK-Lib software with data from Continuously Operating

Reference Stations in Putussibau and Pontianak and atmospheric correction data from Global Navigation Satellite Systems (GNSSs). We retained only observations with high positional accuracy rated as Q1 and Q2 in RTK-Lib. Using the Earth Gravitational Model 2008 (EGM2008), we adjusted the ellipsoid elevation to elevation above mean sea level.

Carbon Stock Estimation

We estimated the total carbon stock of peats in the Upper Kapuas Basin following equations by Yu (2012) and Lawson et al. (2015), where the carbon stock is calculated from area, depth, bulk density and carbon content (See Supplementary 1 for detailed calculation). As there is uncertainty of the total peat coverage in this region, we estimated the carbon stock from two maps of peat area: Global Forest Watch (2,461.32 km^2) and Badan Restorasi Gambut (BRG, Peat Restoration Agency) of the Indonesian Government (3,833.2 km^2; Fig S2.1). For the average depth of the peat, we used two values. One is the average depth of our 14 sampling points, and the other is the estimated depth from a simple relationship between peat depth and distance to the peat edge (estimated from the transect cores) and extrapolated to all peatlands in the upper Kapuas. The bulk density value is directly from the measurement of 10-cm subsamples every 25 cm of the core. Sample volume was measured using water displacement of tightly wrapped samples. To obtain the carbon content, we used the LOI of the bulk-density samples (normally >95%) and published values for percent total organic carbon of peat at similar sites (Agus et al., 2010; Anshari et al., 2010) to estimate the carbon density and finally carbon concentration. As we have two values of area and two values of depth, we calculated four estimates of the carbon stock.

Results

Peat Basal Radiocarbon Dates

We obtained 32 radiocarbon dates from 5 sites, of which 26 are basal dates (Table S.1). The oldest calibrated age from each site ranges from 4.5 ka to 47.8 ka (Fig. 2). Overall, we found a weak correlation between age and depth of the peat (See Table S.2.2). Basal radiocarbon dates at Rasau Jaya show similar ages across the transect, while basal radiocarbon dates at Putussibau show that ages tend to be older at the center of the dome. We also observed that the inland peat is much deeper compared to coastal peat (Fig 3).

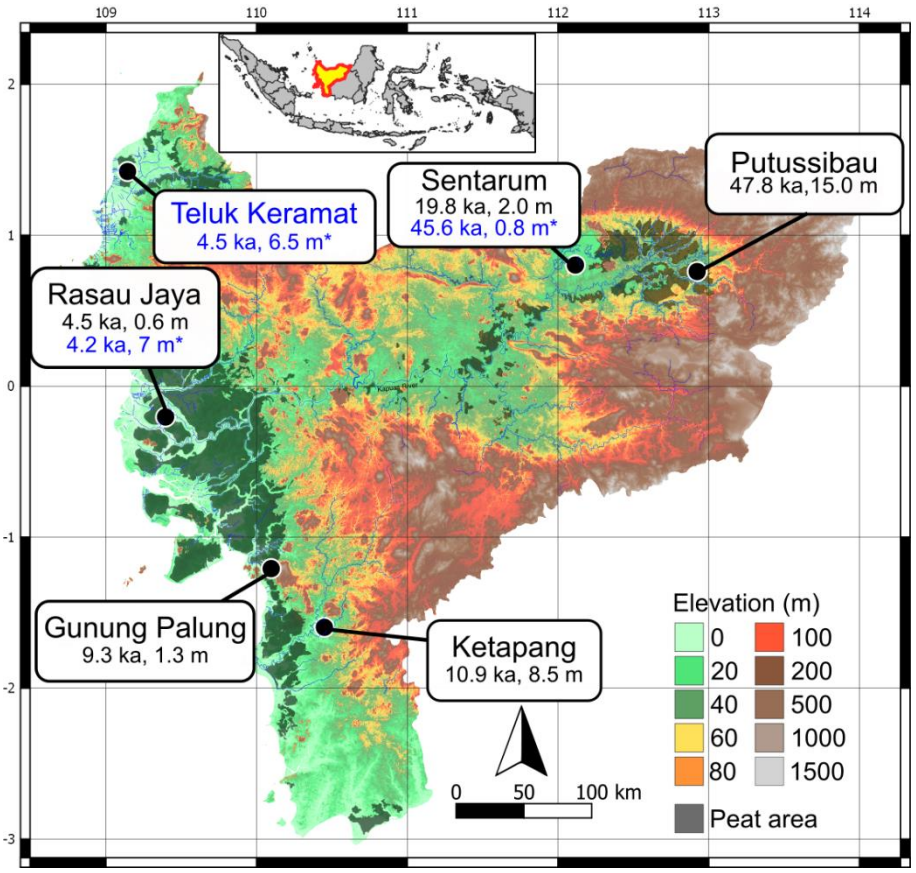

Figure 2.2. Oldest peat basal radiocarbon date from each site. Boxes show the oldest median calibrated age and the corresponding peat depth found at each location. Teluk Keramat and Rasau Jaya are coastal peatlands near sea level. *Blue dates are from previous studies at Rasau Jaya (Anshari et al., 2010), Sentarum (Anshari et al., 2001) and Teluk Keramat (Neuzil, 1997).

At Rasau Jaya, five basal radiocarbon dates from cores with depths of 0.6 to 5 m show ages of 4.0–4.5 ka. We found a negative correlation between depth and basal age in this area, due to the deepest core R3 is located in very degraded peat, and only 60 cm peat remains. At Putussibau, we obtained five dates between 18 and 48 ka, with an upper estimation of >50 ka for the oldest date (See Table S.1, core ID P4).

At Sentarum, the oldest date is from a shallow peat (19.8 ka at 2 m depth), while the deepest peat (14 m) is only aged 13.5 ka. A previous study in this area shows a date of 45.6 ka at a depth of only 0.8 m (Anshari et al., 2004). At Gunung Palung, despite its closeness to the coastline (12 km), we found a quite old age (9.3 ka), indicating that this site is categorized as inland peatland. However, the peat is extremely shallow for an inland peat (e.g., TZII at 0.9 m,

8.1 ka and TZIII at 1.3 m, 9.3 ka). The Ketapang site is located further inland than Gunung Palung (45 km from coastline) and has a depth of 8.5 m and an age of 10.9 ka.

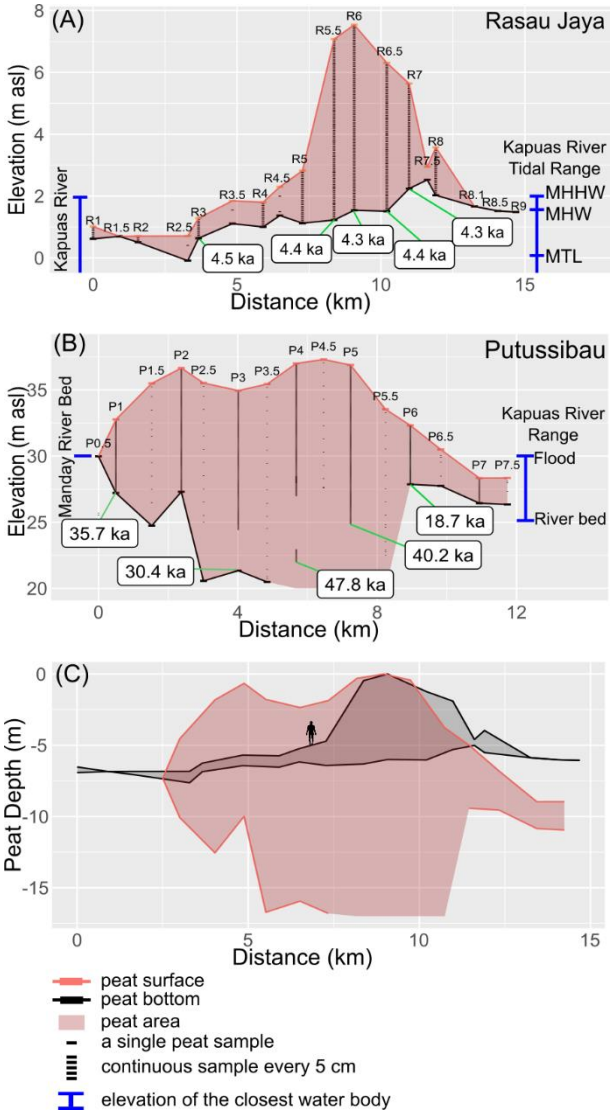

Figure 2.3. Dome profiles from (A) coastal peat and (B) inland peat. (C) Scaled comparison at the bottom with a 170 cm human for scale. Four sampling points (P4, P4.5, P5 and P5.5) at Putussibau did not reach the basal mineral layer, as shown by the black line. Elevation is the altitude above the mean sea level and distance is the position of cores along the transect. Detailed transect maps are available in Fig. S1. Blue bars show river levels and flood stages (unknown for Manday River), and the tidal range at Rasau Jaya.

Carbon Stock Estimation

We estimated the carbon stock in the Upper Kapuas basin region based on our Putussibau transect depth, because the great depth and age found in our cores suggest this region is a

potentially a large and long-term carbon store. Of the four estimates from different peat extent and mean depths, our lowest estimate is 0.78 ± 0.47 Gt C while our highest estimate is 2.14 ± 0.62 Gt C (Table 1). The large range resulted from the 55% larger extent of the BRG map and the difference in average depths estimated directly from the sampling sites (10.35 m) or estimated from a depth model (~5.5 m). We also estimated the carbon density per area by dividing the carbon stock by total area. If using the more recent BRG map and the potentially more accurate modelled depth estimates, the estimate for carbon density is 2790 ± 1440 Mg C/ha.

Table 2.1. Estimate of carbon stock and carbon density in Upper Kapuas Basin based on two different map (Global Forest Watch and Badan Restorasi Gambut) and different depths (average sampling site and modelled)

Area and depth value sources	Total carbon stock (Petagram) ± 95% CI	Carbon stock per area (Mg C/ha) ± 95% CI
GFW map, sampling-sites depth	1.37 ± 0.40	5,590 ± 1,610
BRG map, sampling-sites depth	2.14 ± 0.62	
GFW, modelled depth	0.78 ± 0.47	3,180 ± 1,910
BRG, modelled depth	1.07 ± 0.55	2,790 ± 1,440

Discussion

Peat depth and age at coastal and inland sites

Most of the 25 million hectares of tropical peatlands in Southeast Asia have been deforested and/or drained, leading to widespread subsidence and carbon dioxide emissions (Hoyt et al., 2020). Understanding when and how peatland formed in this region is therefore crucial for prevention and reversal of subsidence and carbon loss going forward. West Kalimantan (Borneo) contains 1.7 million ha of mapped peatlands, and approximately 39% is inland peatland (based on the map from BRG). However, only three radiocarbon-dated peat cores have been previously published: in the Sentarum Lake system dating to 45.6 ka (thousands of years, calibrated, before present) (Anshari et al., 2004), at Rasau Jaya dating to 4.1 ka (Anshari et al., 2010) and at Teluk Keramat dating to 4.5 ka (Neuzil, 1997). Thus, 32 radiocarbon dates from this study help to provide a better picture about the age of the peatlands in this region.

We found that coastal and inland peat domes may achieve thicknesses of 4–6 m and >17 m, respectively, confirming earlier studies (Anderson, 1963; Cameron et al., 1989; Page et al., 2011). While peat age may explain the large differences in peat thickness, we should also consider the human impact on peat depth. Shallower depths (<1 m) at the southern six km of the Rasau Jaya transect indicate a major disturbance that caused peat loss. This area was extensively cultivated and burned following development for agricultural by the Indonesian government transmigration program in the 1970s. Only 20–30% organic content remain in this area (and technically are no longer categorized as peat) compared to >90% organic content in the relatively intact dome center at 4–6 m depth. In contrast, Putussibau was only partially disturbed since the 1990s, with 2–4 m peat depth at the edge and approximately 17–18 m at the center.

The ages of the domes are also extremely different. The coastal Rasau Jaya basal dates are all approximately 4 ka, similar to the Teluk Keramat coastal peat (Fig. 2), indicating simultaneous formation of the peatlands. This is consistent with late Holocene sea level decline that resulted in replacement of mangrove by forested peatlands, a processes underlying most Bornean and Sumatran coastal peats (Fujimoto et al., 2019; Dommain et al. 2014). Here, high tide often reaches 1.35 m (Kästner et al., 2017). Thus, during the highest tides the degraded portions of this peat are inundated or saturated with brackish water, possibly reducing the agricultural value of this land. This tidal influence and salt water intrusion are exacerbated by anthropological peat drainage and sea level rise, and possibly develops a high energy environment that halts future peat accumulation (Whittle and Gallego-Sala, 2016). This peat loss resulted in a negative correlation between peat depth and age at Rasau Jaya (Table S2.2). The Gunung Palung site, despite its thin peat and its proximity to the coast, is categorized as inland peat as it is much older (9.3 ka) than the sea level rise of the mid-Holocene. However, it is much thinner compared to the nearby inland peat in Ketapang, suggesting historical peat loss within this national park.

In contrast to the coastal peatlands, the inland Putussibau dome has basal ages ranging from 18 to 48 ka. There is some chance that the addition of modern carbon into the deeper peat can occur through root exudates and dissolved organic carbon, decreasing the radiocarbon ages. However, we dated woody fragments >125 microns that were treated with several KOH measurements, and we found no large or consistent difference between dates of different size fractions, thus we consider these dates as the best possible estimate of peat initiation

(Supplementary Table S2). The oldest date at Putussibau calibrated to the limit of the Intcal13 calibration curve, at ca 48 ka, with maximum limit at >50 ka: the date was statistically different from concurrently-run organic carbon blanks and therefore remains constrained within the radiocarbon time scale. This date places the inland peatland in Putussibau as the oldest intact and active peatland (Treat et al., 2017). This oldest dated sample comes from the depth of 15 m, while we predict that the peat in Upper Kapuas Basin could reach 17–18 m. Thus, a better method than hand-operated peat corers is required to obtain samples and date carbon deposited at the base of the peat.

Regardless of methodological limitations, the basal radiocarbon dates reported here show that the age of deposition was older at the center of the dome, which indicates that the peat started to form from a point of depression at the center, possibly an oxbow lake, that became terrestrialized by the peat and then expanded laterally (Belyea and Baird, 2006; Foster and Wright Jr, 1990). We also noticed that the base of the peat is approximately 5 m below the Kapuas river bed, which could indicate river-bed aggradation and water-table rise since the glacial period. This increasing water table probably released the hydrological limitation of peat upward growth (Belyea and Baird, 2006; Ingram, 1982), thus enabling the peat to grow up to 17–18 m depth. Half of the Putussibau dome lies below the river level, indicating its importance as a hydrological buffer, where the wetland system in the Upper Kapuas Basin stores approximately twice the volume of the water in the Kapuas River and its floodplain lakes (Law et al., 2015). Recent land-use change and peat degradation near Putussibau is possibly linked with the increasing frequency of flooding events (Wells et al., 2016).

At the Sentarum site, negative correlation between depth and age (Kendall's $\tau = -0.833$) suggests that peat formation and growth are very heterogenous across space and time in this area. The discrepancies between age and depth implies a dynamic in peat dome growth and degradation even in the absence of human causes, where old peat stopped accumulating or even degraded as new domes formed elsewhere. A possible cause for this heterogeneity is the adjacent large seasonal lake system where local peat initiation may be linked to the spatial and temporal heterogeneity of water levels within this large lake system (Hidayat et al., 2017).

Climate History and Peat Formation

Coastal and inland peat formation in Southeast Asia region react differently to climate (Dommain et al., 2011). Coastal peat mainly formed at the earliest after sea level stabilization ca. 8 ka (Dommain et al., 2011; Treat et al., 2019), while our results shows that inland peat possibly started to form much earlier at >50 ka. To explain subsequent effects of climate to the peat formation, we combined our data with other 37 radiocarbon dates available from Borneo (See Table S.1). We aligned our basal dates with the geographically closest climate record from cave stalagmites in Gunung Buda located 460 km to the NE of our Putussibau site (Fig. 4; Carolin et al., 2016).

Based on the comparison between peatlands initiation time and the climate, we observe a inland peat-formation hiatus around 20–30 ka, generally aligned with the glacial maximum (Clark et al., 2009). Moreover, higher δ18O concentration in the cave record around 25–17 ka indicates lower precipitation and a colder climate during this period. A sea-surface temperature reconstruction also shows cooler temperatures and a warm-up shortly after 20 ka (Mohtadi et al., 2010). These records are consistent with a cooler Northern Hemisphere, which shifted the Inter Tropical Convergence Zone (ITCZ) southward, creating stronger monsoon precipitation over Australia, and a drier climate over Kalimantan (Denniston et al., 2013). A colder and drier climate likely resulted in a hiatus of new peatland initiation and possibly a negative carbon balance on existing peat surfaces. This hiatus period overlaps with a previous study of peat stratigraphy from South Kalimantan, where the peat accumulation underwent a hiatus from 27–14 ka (Wüst et al., 2008). Out of 37 peat basal dates from various studies in Borneo, only one formed during this hiatus period (Page et al., 2004). Despite the peat-formation hiatus, the climate during this period seems sufficiently wet to sustain the existing peatlands, which is consistent with a pollen record (Anshari et al., 2001) and biogeographic evidence for continuous forest cover through the glacial period (Bird et al., 2005; Suraprasit et al., 2019).

Around 15–7 ka, we observed a cluster of peat initiation events at Ketapang and Gunung Palung. This peat formation was possibly caused by a long increase in precipitation through the early Holocene, when the northern hemisphere warmed and the ITCZ advanced northward, which was coupled with the sea-level rise from deglaciation (Griffiths et al., 2013). At a finer temporal resolution, the apparent association of peat initiation at Sentarum and Putussibau with Heinrich Events (abrupt Northern-hemisphere cold intervals during the Pleistocene) suggests an

opposite climatic relationship, though how these events are expressed in the local hydroclimate is not understood.

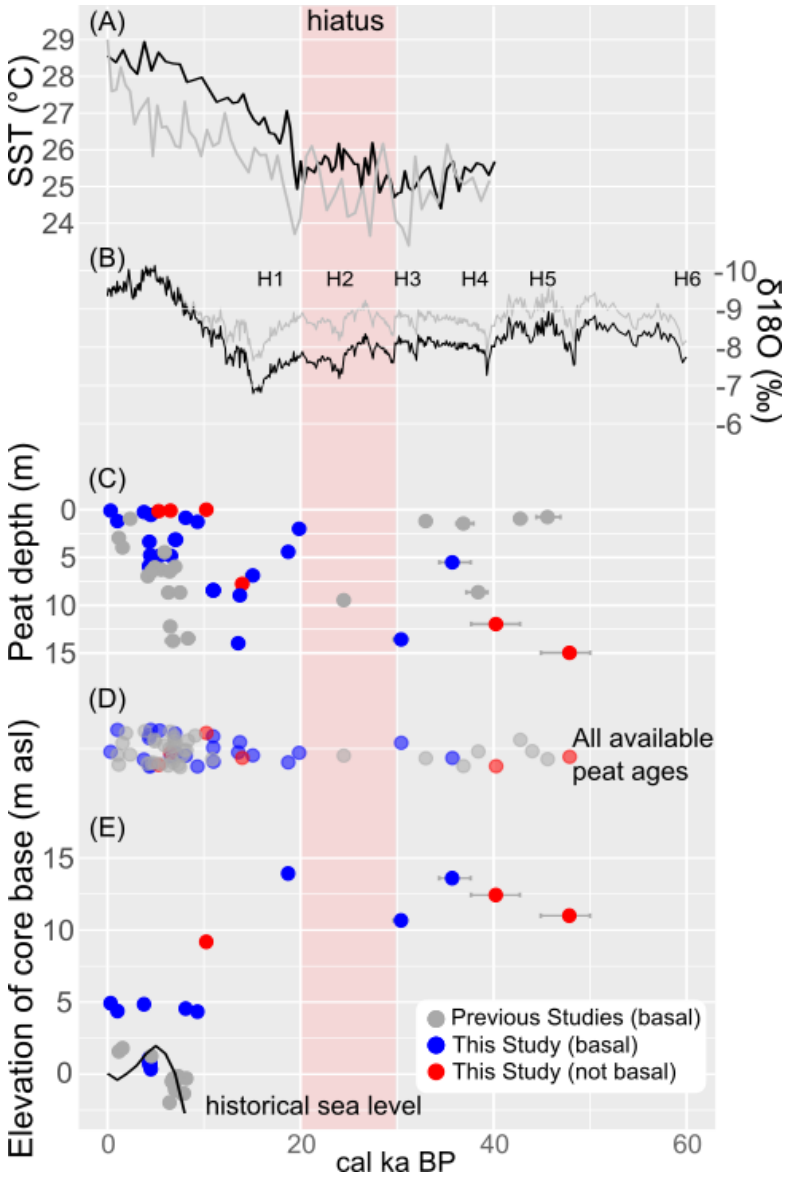

Figure 2.4. Peat age and depth in West Kalimantan plotted in relation to climate proxies. (A) Reconstructed sea surface temperatures are from benthic and planktonic Mg/Ca ratio in two cores off coast of Sumatra (Mohtadi et al., 2010). (B) Speleothem δ18O is from Gunung Mulu National Park with gray line showing δ18O adjusted for the effect of ice cover (Carolin et al., 2016), where less negative peaks are possibly related with Heinrich Events (Hemming, 2004). (C) Basal ages and peat depth from Borneo. Blue points indicate dates from this study, and grey points indicate dates from previous studies (see Table S1). (D) All available peat basal ages in Borneo. (E) Basal age and peat elevation. Light red background indicates the hiatus period of peat formation. Historical sea level reconstructed from mangrove sediment in Peninsular Malaysia (Tam et al., 2018). Peat basal elevation and peat depth were not reported for all sites.

After sea level stabilization at 8 ka, we started to observe coastal peat formation, although our sample in Rasau that shows the age of 4.5 ka probably formed later after the Kapuas River delta accumulated enough land for peat to grow. However, relative to their young age, the coastal peats are quite deep, indicating that they grow much faster (possibly due to a warmer and wetter climate), a finding consistent with other studies of peat growth rate across Southeast Asia (Dommain et al., 2014; Page et al., 2004). Future radiocarbon dating across the vertical plane of the core will show further how the climate affected peat growth and dynamics after peat initiation.

Carbon Stock Estimation

With our limited data, we predict that the inland peatland in the Upper Kapuas basin contains at least 0.78 ± 0.47 Gt C and a maximum of 2.14 ± 0.62 Gt C (Table 1). The total peat carbon stock of Indonesia is estimated to be at 25.33 Gt C and on Borneo at 9.08 Gt C (Warren et al., 2017). However, the Warren et al. (2017) estimate lumped peat at >3 m as a single depth class. As we observe in the field, and based on our modelling, the depth of inland peatland is often underestimated by prior studies.

Our method that produced the lowest estimate of carbon density (using modelled depth from the BGR map), still shows a mean estimate of 2790 ± 1440 Mg C/ha. We do not include the above-ground biomass in this value as we did not collect vegetation biomass data since our transects are located on secondary forests which were recently burned and/or deforested. Some areas were already transformed either to abandoned bush fern field or small plantations. A previous study in the Sentarum region shows that the carbon density average at 156 Mg C/ha for above ground biomass and 3,228 Mg C/ha below ground biomass (Anshari et al., 2012). Most of the carbon of this tropical ecosystem is stored in the soil.

Our carbon density estimate shows that the Upper Kapuas Basin is more than twice as deep (and more than twice the C stock) than the average Indonesian peat (Osaki and Tsuji, 2016; Page et al., 2011). This also shows that this inland peatland is more C-dense than boreal peats (average 600–700 Mg C/ha) (Yu, 2012) or the most C-dense forested peats in the Amazon (1390 Mg C/ha) (Draper et al., 2014). Thus, not only have these deep inland peats provided a carbon sink that has persisted from glacial to interglacial climates, they are likely the most carbon-dense ecosystem in the world.

Conclusion

In this study, we provide new data that improve our understanding of tropical peatlands initiation and carbon accumulation. Most of the peatlands of Borneo formed <20 ka, however, we found a peat deposit of greater depth (ca. 18 m) and age (>48,000 years) in a large, understudied peatland region, suggesting that peatlands older than the glacial maximum are more extensive than previously estimated (Treat et al., 2019). Our findings point to a new possibility to use these old and deep peat deposits as a long-term environmental archive. We also note that not all old peats are deep. Some shallow peats, 1–2 m in depth, had an old age (>10 ka). Typically, peat of this age is at least 5 m thick, thus indicating extreme peat loss and/or subsidence. Additional radiocarbon dates at the top of cores could reveal the timing and the cause of disturbances to this peat. Finally, our results highlight the importance of inland peatlands for conservation and climate change mitigation. Due to their exceptionally high carbon density, disturbance on this ecosystem can release a large amount of stored carbon. For our site, we estimate that for each hectare of peat that is lost ~2800 Mg C could be released to the atmosphere. While only 7% of the inland peat in West Kalimantan has been logged and converted to plantations to date (Miettinen et al., 2011), 76% occurs outside protected areas (Fig. S4). Despite their small extent, the deep inland peats of Kalimantan are a long-term carbon reservoir and hydrological buffer that requires immediate conservation and restoration.

In the next chapter, we will focus more in depth on peat domes, by conducting stratigraphic analysis on the peat soil core to reveal the changes over time/depth on soil physical and chemical properties, as well as charcoal analysis that reveals fire occurrence in this ecosystem. This in turn provides information on how the peat changes and interacts with the climate and with humans. It also suggests a new potential of a bigger-than-predicted impact of peatland fire on past climate.

References

Agus, F., Hairiah, K., Mulyani, A., 2010. Measuring carbon stock in peat soils: practical guidelines. World Agroforestry Centre.

Anderson, J., Muller, J., 1975. Palynological study of a Holocene peat and a Miocene coal deposit from NW Borneo. Review of Palaeobotany and Palynology 19, 291–351.

Anderson, J.A.R., 1963. The structure and development of the peat swamps of Sarawak and Brunei. Jour. Trop. Geogr. 18, 7–16.

Anshari, G., Gusmayanti, E., Afifudin, M., Widhanarto, G., 2012. A Study of Carbon Balance in Customary Peat Forest (Hutan Nung) in Taman Nasional Danau Sentarum (No. ENV0100-USA19-DM3, TA: USA193000). CIFOR.

Anshari, G., Peter Kershaw, A., van der Kaars, S., 2001. A Late Pleistocene and Holocene pollen and charcoal record from peat swamp forest, Lake Sentarum Wildlife Reserve, West Kalimantan, Indonesia. Palaeogeography, Palaeoclimatology, Palaeoecology, Quaternary Environmental Change in the Indonesian Region 171, 213–228. https://doi.org/10.1016/S0031-0182(01)00246-2

Anshari, G., Peter Kershaw, A., Van Der Kaars, S., Jacobsen, G., 2004. Environmental change and peatland forest dynamics in the Lake Sentarum area, West Kalimantan, Indonesia. J. Quaternary Sci. 19, 637–655. https://doi.org/10.1002/jqs.879

Anshari, G.Z., Afifudin, M., Nuriman, M., Gusmayanti, E., Arianie, L., Susana, R., Nusantara, R.W., Sugardjito, J., Rafiastanto, A., 2010. Drainage and land use impacts on changes in selected peat properties and peat degradation in West Kalimantan Province, Indonesia. Biogeosciences 7, 3403–3419.

Balesdent, J., Basile-Doelsch, I., Chadoeuf, J., Cornu, S., Derrien, D., Fekiacova, Z., Hatté, C., 2018. Atmosphere–soil carbon transfer as a function of soil depth. Nature 559, 599–602. https://doi.org/10.1038/s41586-018-0328-3

Belyea, L.R., Baird, A.J., 2006. Beyond "the limits to peat bog growth": Cross-scale feedback in peatland development. Ecological Monographs 76, 299–322.

Bird, M.I., Taylor, D., Hunt, C., 2005. Palaeoenvironments of insular Southeast Asia during the Last Glacial Period: a savanna corridor in Sundaland? Quaternary Science Reviews 24, 2228–2242. https://doi.org/10.1016/j.quascirev.2005.04.004

Cameron, C.C., Esterle, J.S., Palmer, C.A., 1989. The geology, botany and chemistry of selected peat-forming environments from temperate and tropical latitudes. International Journal of Coal Geology 12, 105–156. https://doi.org/10.1016/0166-5162(89)90049-9

Carolin, S.A., Cobb, K.M., Lynch-Stieglitz, J., Moerman, J.W., Partin, J.W., Lejau, S., Malang, J., Clark, B., Tuen, A.A., Adkins, J.F., 2016. Northern Borneo stalagmite records reveal West Pacific hydroclimate across MIS 5 and 6. Earth and Planetary Science Letters 439, 182–193. https://doi.org/10.1016/j.epsl.2016.01.028

Cattau, M.E., Harrison, M.E., Shinyo, I., Tungau, S., Uriarte, M., DeFries, R., 2016. Sources of anthropogenic fire ignitions on the peat-swamp landscape in Kalimantan, Indonesia. Global Environmental Change 39, 205–219.

Clark, P.U., Dyke, A.S., Shakun, J.D., Carlson, A.E., Clark, J., Wohlfarth, B., Mitrovica, J.X., Hostetler, S.W., McCabe, A.M., 2009. The Last Glacial Maximum. Science 325, 710–714. https://doi.org/10.1126/science.1172873

Dargie, G.C., Lewis, S.L., Lawson, I.T., Mitchard, E.T., Page, S.E., Bocko, Y.E., Ifo, S.A., 2017. Age, extent and carbon storage of the central Congo Basin peatland complex. Nature 542, 86–90.

Denniston, R.F., Wyrwoll, K.-H., Asmerom, Y., Polyak, V.J., Humphreys, W.F., Cugley, J., Woods, D., LaPointe, Z., Peota, J., Greaves, E., 2013. North Atlantic forcing of millennial-scale Indo-Australian monsoon dynamics during the Last Glacial period. Quaternary Science Reviews 72, 159–168. https://doi.org/10.1016/j.quascirev.2013.04.012

Dommain, R., Couwenberg, J., Glaser, P.H., Joosten, H., Suryadiputra, I.N.N., 2014. Carbon storage and release in Indonesian peatlands since the last deglaciation. Quaternary Science Reviews 97, 1–32. https://doi.org/10.1016/j.quascirev.2014.05.002

Dommain, R., Couwenberg, J., Joosten, H., 2011. Development and carbon sequestration of tropical peat domes in south-east Asia: links to post-glacial sea-level changes and Holocene climate variability. Quaternary Science Reviews 30, 999–1010. https://doi.org/10.1016/j.quascirev.2011.01.018

Draper, F.C., Roucoux, K.H., Lawson, I.T., Mitchard, E.T., Coronado, E.N.H., Lähteenoja, O., Montenegro, L.T., Sandoval, E.V., Zaráte, R., Baker, T.R., 2014. The distribution and amount of carbon in the largest peatland complex in Amazonia. Environmental Research Letters 9, 124017.

Fischer, H., Meissner, K.J., Mix, A.C., Abram, N.J., Austermann, J., Brovkin, V., Capron, E., Colombaroli, D., Daniau, A.-L., Dyez, K.A., Felis, T., Finkelstein, S.A., Jaccard, S.L., McClymont, E.L., Rovere, A., Sutter, J., Wolff, E.W., Affolter, S., Bakker, P., Ballesteros-Cánovas, J.A., Barbante, C., Caley, T., Carlson, A.E., Churakova, O., Cortese, G., Cumming, B.F., Davis, B.A.S., de Vernal, A., Emile-Geay, J., Fritz, S.C., Gierz, P., Gottschalk, J., Holloway, M.D., Joos, F., Kucera, M., Loutre, M.-F., Lunt, D.J., Marcisz, K., Marlon, J.R., Martinez, P., Masson-Delmotte, V., Nehrbass-Ahles, C., Otto-Bliesner, B.L., Raible, C.C., Risebrobakken, B., Sánchez Goñi, M.F., Arrigo, J.S., Sarnthein, M., Sjolte, J., Stocker, T.F., Velasquez Alvárez, P.A., Tinner, W., Valdes, P.J., Vogel, H., Wanner, H., Yan, Q., Yu, Z., Ziegler, M., Zhou, L., 2018. Palaeoclimate constraints on the impact of 2 °C anthropogenic warming and beyond. Nature Geosci 11, 474–485. https://doi.org/10.1038/s41561-018-0146-0

Foster, D.R., Wright Jr, H.E., 1990. Role of ecosystem development and climate change in bog formation in central Sweden. Ecology 71, 450–463.

Fujimoto, K., Miura, M., Kobayashi, S., Simbolon, H., 2019. Habitat evolution of a peat swamp forest and belowground carbon sequestration during the Holocene along the coastal lowland in Central Sumatra, Indonesia. Prog Earth Planet Sci 6, 41. https://doi.org/10.1186/s40645-019-0288-8

Griffiths, M.L., Drysdale, R.N., Gagan, M.K., Zhao, J., Hellstrom, J.C., Ayliffe, L.K., Hantoro, W.S., 2013. Abrupt increase in east Indonesian rainfall from flooding of the Sunda Shelf ~9500 years ago. Quaternary Science Reviews, Linking Southern Hemisphere records and past circulation patterns: the AUS-INTIMATE project 74, 273–279. https://doi.org/10.1016/j.quascirev.2012.07.006

Gumbricht, T., Roman-Cuesta, R.M., Verchot, L., Herold, M., Wittmann, F., Householder, E., Herold, N., Murdiyarso, D., 2017. An expert system model for mapping tropical wetlands and peatlands reveals South America as the largest contributor. Global Change Biology 23, 3581–3599.

Hansen, M.C., Potapov, P.V., Moore, R., Hancher, M., Turubanova, S.A., Tyukavina, A., Thau, D., Stehman, S.V., Goetz, S.J., Loveland, T.R., 2013. High-resolution global maps of 21st-century forest cover change. science 342, 850–853.

Hemming, S.R., 2004. Heinrich events: Massive late Pleistocene detritus layers of the North Atlantic and their global climate imprint. Reviews of Geophysics 42. https://doi.org/10.1029/2003RG000128

Hidayat, H., Teuling, A.J., Vermeulen, B., Taufik, M., Kastner, K., Geertsema, T.J., Bol, D.C.C., Hoekman, D.H., Haryani, G.S., Van Lanen, H.A.J., Delinom, R.M., Dijksma, R., Anshari, G.Z., Ningsih, N.S., Uijlenhoet, R., Hoitink, A.J.F., 2017. Hydrology of inland tropical lowlands: the Kapuas and Mahakam wetlands. Hydrol. Earth Syst. Sci. 21, 2579–2594. https://doi.org/10.5194/hess-21-2579-2017

Hope, G., Chokkalingam, U., Anwar, S., 2005. The stratigraphy and fire history of the Kutai Peatlands, Kalimantan, Indonesia. Quaternary Research, Late Quaternary Tropical Ecosystem Dynamics 64, 407–417. https://doi.org/10.1016/j.yqres.2005.08.009

Hoyt, A.M., Chaussard, E., Seppalainen, S.S., Harvey, C.F., 2020. Widespread subsidence and carbon emissions across Southeast Asian peatlands. Nature Geoscience 13, 435–440. https://doi.org/10.1038/s41561-020-0575-4

Ingram, H.A.P., 1982. Size and shape in raised mire ecosystems: a geophysical model. Nature 297, 300–303.

Kästner, K., Hoitink, A.J.F., Vermeulen, B., Geertsema, T.J., Ningsih, N.S., 2017. Distributary channels in the fluvial to tidal transition zone. Journal of Geophysical Research: Earth Surface 122, 696–710.

Law, E.A., Bryan, B.A., Meijaard, E., Mallawaarachchi, T., Struebig, M., Wilson, K.A., 2015. Ecosystem services from a degraded peatland of Central Kalimantan: implications for policy, planning, and management. Ecological Applications 25, 70–87. https://doi.org/10.1890/13-2014.1

Lawson, I.T., Kelly, T.J., Aplin, P., Boom, A., Dargie, G., Draper, F.C.H., Hassan, P.N.Z.B.P., Hoyos-Santillan, J., Kaduk, J., Large, D., Murphy, W., Page, S.E., Roucoux, K.H., Sjögersten, S., Tansey, K., Waldram, M., Wedeux, B.M.M., Wheeler, J., 2015. Improving estimates of tropical peatland area, carbon storage, and greenhouse gas fluxes. Wetlands Ecol Manage 23, 327–346. https://doi.org/10.1007/s11273-014-9402-2

Lohman, D.J., Bickford, D., Sodhi, N.S., 2007. The Burning Issue. Science 316, 376.

Maxwell, T.M., Silva, L.C.R., 2020. A State Factor Model for Ecosystem Carbon–Water Relations. Trends in Plant Science 25, 652–660. https://doi.org/10.1016/j.tplants.2020.02.007

Maxwell, T.M., Silva, L.C.R., Horwath, W.R., 2018. Predictable Oxygen Isotope Exchange Between Plant Lipids and Environmental Water: Implications for Ecosystem Water Balance Reconstruction. Journal of Geophysical Research: Biogeosciences 123, 2941–2954. https://doi.org/10.1029/2018JG004553

Miettinen, J., Shi, C., Liew, S.C., 2011. Deforestation rates in insular Southeast Asia between 2000 and 2010. Global Change Biology 17, 2261–2270.

Mohtadi, M., Steinke, S., Lückge, A., Groeneveld, J., Hathorne, E.C., 2010. Glacial to Holocene surface hydrography of the tropical eastern Indian Ocean. Earth and Planetary Science Letters 292, 89–97. https://doi.org/10.1016/j.epsl.2010.01.024

Neuzil, S.G., 1997. Onset and rate of peat and carbon accumulation in four domed ombrogenous peat deposits, Indonesia. Biodiversity and sustainability of tropical peatland.

Notohadiprawiro, T., 2006. Peat deposition, an idle stage in the natural cycling of Nitrogen, and its possible activationfor agriculture. Proceedings of the nitrogen cycling in south-east Asian wet moonsoonal ecosystem 14.

Osaki, M., Tsuji, N., 2016. Tropical peatland ecosystems. Springer.

Page, S.E., Rieley, J.O., Banks, C.J., 2011. Global and regional importance of the tropical peatland carbon pool. Global Change Biology 17, 798–818. https://doi.org/10.1111/j.1365-2486.2010.02279.x

Page, S.E., Siegert, F., Rieley, J.O., Boehm, H.-D.V., Jaya, A., Limin, S., 2002. The amount of carbon released from peat and forest fires in Indonesia during 1997. Nature 420, 61–65. https://doi.org/10.1038/nature01131

Page, S.E., Wűst, R. a. J., Weiss, D., Rieley, J.O., Shotyk, W., Limin, S.H., 2004. A record of Late Pleistocene and Holocene carbon accumulation and climate change from an equatorial peat bog (Kalimantan, Indonesia): implications for past, present and future carbon dynamics. J. Quaternary Sci. 19, 625–635. https://doi.org/10.1002/jqs.884

Reimer, P.J., Bard, E., Bayliss, A., Beck, J.W., Blackwell, P.G., Ramsey, C.B., Buck, C.E., Cheng, H., Edwards, R.L., Friedrich, M., 2013. IntCal13 and Marine13 radiocarbon age calibration curves 0–50,000 years cal BP. Radiocarbon 55, 1869–1887.

Ritung, S., Wahyunto, W., Nugroho, K., Sukarman, S., Hikmatullah, H., Suparto, S., Tafakrenanto, C., 2011. Peta Lahan Gambut Indonesia Skala 1:250.000, December 2. ed. Balai Besar Penelitian dan Pengembangan Sumberdaya Lahan Pertanian, Badan Penelitian dan Pengembangan Pertanian, Bogor.

Ritung, W., Subagjo, H., 2004. Peta Sebaran Lahan Gambut, Luas dan Kandungan Karbon di Kalimantan/Map of Peatland Distribution Area and Carbon Content in Kalimantan. Wetlands International-Indonesia Programme & Wildlife Habitat Canada (WHC).

RSS GmbH, 2018. Kapuas Hulu peat remapping final report: Mapping peat extent and depth of 16 Peat Hydrological Units within the Kapuas Hulu Basin (No. 12.2216.0–001.00). Remote Sensing Solution GmbH, FORCLIME.

Silva, L.C.R., 2017. Carbon sequestration beyond tree longevity. Science 355, 1141–1141. https://doi.org/10.1126/science.aan0109

Silva, L.C.R., Lambers, H., 2020. Soil-plant-atmosphere interactions: structure, function, and predictive scaling for climate change mitigation. Plant Soil. https://doi.org/10.1007/s11104-020-04427-1

Staub, James R., Gastaldo, R.A., 2003. Late Quaternary incised-valley fill and deltaic sediments in the Rajang River Delta. Tropical Deltas of Southeast Asia-Sedimentology, Stratigraphy, and Petroleum Geology 76, 71–87.

Staub, J.R., Esterle, J.S., 1994. Peat-accumulating depositional systems of Sarawak, East Malaysia. Sedimentary Geology 89, 91–106. https://doi.org/10.1016/0037-0738(94)90085-X

Suraprasit, K., Jongautchariyakul, S., Yamee, C., Pothichaiya, C., Bocherens, H., 2019. New fossil and isotope evidence for the Pleistocene zoogeographic transition and hypothesized savanna corridor in peninsular Thailand. Quaternary Science Reviews 221, 105861. https://doi.org/10.1016/j.quascirev.2019.105861

Tam, C.-Y., Zong, Y., Hassan, K. bin, Ismal, H. bin, Jamil, H. binti, Xiong, H., Wu, P., Sun, Y., Huang, G., Zheng, Z., 2018. A below-the-present late Holocene relative sea level and the glacial isostatic adjustment during the Holocene in the Malay Peninsula. Quaternary Science Reviews 201, 206–222. https://doi.org/10.1016/j.quascirev.2018.10.009

Tie, Y.L., Esterle, J.S., 1991. Formation of lowland peat domes in Sarawak, Malaysia. Proceedings of the International Symposium on Tropical Peatland 81–89.

Treat, C.C., Broothaerts, N., Dalton, A.S., Dommain, R., Douglas, T., Drexler, J., Finkelstein, S.A., Grosse, G., Hope, G., Hutchings, J.A., Jones, M.C., Kleinen, T., Kuhry, P., Lacourse, T., Lahteenoja, O., Loisel, J., Notebaert, B., Payne, R.J., Peteet, D.M., Sannel, A.B.K., Stelling, J., Strauss, J., Swindles, G., Talbot, J., Tarnocai, C., Verstraeten, G., Williams, C.J., Xia, Z., Yu, Z., Brovkin, V., 2017. (Table S2) Global dataset of peatland basal ages. https://doi.org/10.1594/PANGAEA.873065

Treat, C.C., Kleinen, T., Broothaerts, N., Dalton, A.S., Dommain, R., Douglas, T.A., Drexler, J.Z., Finkelstein, S.A., Grosse, G., Hope, G., 2019. Widespread global peatland establishment and persistence over the last 130,000 y. Proceedings of the National Academy of Sciences 116, 4822–4827.

Ward, B.M., Wong, C.I., Novello, V.F., McGee, D., Santos, R.V., Silva, L.C.R., Cruz, F.W., Wang, X., Edwards, R.L., Cheng, H., 2019. Reconstruction of Holocene coupling between the South American Monsoon System and local moisture variability from speleothem δ18O and 87Sr/86Sr records. Quaternary Science Reviews 210, 51–63. https://doi.org/10.1016/j.quascirev.2019.02.019

Warren, M., Hergoualc'h, K., Kauffman, J.B., Murdiyarso, D., Kolka, R., 2017. An appraisal of Indonesia's immense peat carbon stock using national peatland maps: uncertainties and potential losses from conversion. Carbon Balance Manage 12, 12. https://doi.org/10.1186/s13021-017-0080-2

Wells, J.A., Wilson, K.A., Abram, N.K., Nunn, M., Gaveau, D.L.A., Runting, R.K., Tarniati, N., Mengersen, K.L., Meijaard, E., 2016. Rising floodwaters: mapping impacts and perceptions of flooding in Indonesian Borneo. Environmental Research Letters 11, 064016. https://doi.org/10.1088/1748-9326/11/6/064016

Whittle, A., Gallego-Sala, A.V., 2016. Vulnerability of the peatland carbon sink to sea-level rise. Sci Rep 6, 28758. https://doi.org/10.1038/srep28758

Wilford, G.E., 1959. Radiocarbon age determinations of quaternary sediments in Brunei and northeast Sarawak. British Borneo Geological Survey, Annual Report.

Wüst, R.A., Jacobsen, G.E., von der Gaast, H., Smith, A.M., 2008. Comparison of radiocarbon ages from different organic fractions in tropical peat cores: insights from Kalimantan, Indonesia. Radiocarbon 50, 359–372.

Yu, Z.C., 2012. Northern peatland carbon stocks and dynamics: a review. Biogeosciences 9, 4071–4085. https://doi.org/10.5194/bg-9-4071-2012

Yulianto, E., Rahardjo, A.T., Noeradi, D., Siregar, D.A., Hirakawa, K., 2005. A Holocene pollen record of vegetation and coastal environmental changes in the coastal swamp forest at Batulicin, South Kalimantan, Indonesia. Journal of Asian Earth Sciences 25, 1–8.

III. INTERPLAY OF CLIMATE, FIRES, FLOODS, AND ANTHROPOGENIC IMPACTS ON THE FORMATION AND CARBON ACCUMULATION OF COASTAL AND INLAND TROPICAL PEATLANDS IN WEST KALIMANTAN, INDONESIA

Submitted to *Ecosystems* (Style of *Ecosystems*)

Co-authored material (with D.G. Gavin H and G.Z. Anshari). The paper was written entirely by me, with my coauthors providing editorial assistance.

MR, GDG, and GZA conceptualized the study, devised the methodology and conducted the field investigation. DGG and GZA supervised and provided resources. DGG & MR acquired the funding. MR curated, analyzed, and visualized the data. MR wrote the original draft, all authors discussed the results and contributed to the final manuscript.

Introduction

Peatland normally functions as a carbon sink, removing carbon from the atmosphere and sequestering it in the form of undecayed stable soil organic matter that may continually accumulate for thousands of years (Gallego-Sala and others, 2018). However, many factors can stop peat accumulation, or even release stored carbon back into the atmosphere (Loisel and others, 2020; Turetsky and others, 2002). Most of the temperate peatland that formed during past interglacial periods was degraded by advancing ice sheets and cold and dry glacial climates, and thus most of the temperate and boreal peatland is younger than 11,000 years (the Holocene) when the climate was warm enough for peatland to form (Treat and others, 2019; Yu, 2012). This is not the case for tropical peatland where ice sheets did not directly affect the peat, and where forested peatland potentially accumulated through the glacial maximum (Anshari and others, 2001; Page and others, 2004; Ruwaimana and others, 2020). However, several other inter-related factors can affect tropical peat accumulation, such as climate, fires, floods, and humans.

The three major tropical peatland regions are found in Southeast Asia, the Amazon Basin, and the Congo Basin (Osaki and Tsuji, 2016). Compared to the latter two that have only recently started to be explored and studied, tropical peatland in Southeast Asia is relatively well studied, especially for the accessible coastal peat (Page and others, 2011; Ribeiro and others, 2021). In

general, peatland in Southeast Asia can be divided into two categories - inland peatland and coastal peatland (Dommain and others, 2011; Morley, 2013). Inland peatland, composed of ombrogenous peat domes, forms in poorly-drained basins located above the current sea level and were never affected by sea level changes over the glacial period (Morley, 2013). The oldest radiocarbon dates from inland peatland approach the limit of radiocarbon dating, at more than 50,000 years old (Anshari and others, 2001; Ruwaimana and others, 2020). These inland peat areas remain little studied despite their great depth and immense carbon stock (Ruwaimana et al. 2020). Coastal peatland formed after sea level stabilization ca. 7000 year ago, thus this peatland is often younger (Dommain and others, 2011). Some peatlands, such as the Sebangau Peatland in Central Kalimantan is a continuous mix of both types (Page and others, 2004), but in some areas such as the Upper Kapuas Peatland of West Kalimantan, the peat is located 300–900 km upstream from the coast (Anshari and others, 2001; Ruwaimana and others, 2020).

Peat accumulation and subsequently its carbon sequestration is a balance between primary productivity and decomposition (Yu and others, 2010). For peat to accumulate in ombrogenous peatlands, the climate must be warm and wet enough to support high primary productivity, precipitation must maintain a high soil water level to prevent peat decay, and in the case of tropical peatland, organic matter must develop recalcitrant aromatic compounds that help stabilize the peat at warm temperatures (Hodgkins and others, 2018). However, even though the tropics experienced less cooling through the glacial periods, climate change during glacial-interglacial periods has indeed affected peat accumulation (Hapsari and others, 2017). We suggest that when the climate was colder and precipitation was lower, the peat carbon sequestration might have halted or even shifted into a carbon source when the water level was low, exposing the peat material to oxygen and decomposition. Age profiles of peat cores often show abrupt changes as much as ten thousand years (Anshari and others, 2001; Hapsari and others, 2017; Page and others, 2004; Wüst and others, 2008), which suggest peat accumulation hiatuses are a common occurrence. However, their cause and links to climate is often overlooked.

Fire is an important disturbance on current tropical peatland ecosystems (Cochrane, 2003; Page and others, 2010). In Southeast Asia, especially in Indonesia and Malaysia, peatland is often converted to oil palm or pulp wood plantations, involving draining and burning peatland (Dohong and others, 2017; Posa and others, 2011). Peatland fire in Indonesia in 1997 alone

released approximately 2.4 Gt carbon (Page and others, 2002), and lesser fire years such as 2019 still released 0.7 GtC (Datta and Krishnamoorti, 2022). These fires are often ongoing for weeks and month, causing what is called Southeast Asian Haze on 1997, 2002, 2006, 2009, 2013, 2014, 2015 and 2019 (Page and Hooijer, 2016). Despite this current major concern, fire is often dismissed as a historical natural force in peatland, as a pristine peatland is often perceived as a waterlogged and high humidity environment where fire rarely or never occurs (Cochrane, 2003). However, recent paleoecological studies of tropical peat cores have found charcoal evidence of non-anthropogenic fires over the Holocene (Cole and others, 2019; Hapsari and others, 2022).

The upper Kapuas River peatlands are affected by a flood cycle that follows the El Niño - Southern Oscillation (ENSO) (Hidayat et al., 2017). During the La Niña, extreme rainfall causes floods which raises a river level up to 10 meters, while on the other hand during the El Niño, the river bed is often exposed and some of the connected lake systems such as Lake Sentarum dry out (Anshari and others, 2004; Hidayat and others, 2017). The oscillation between dry and wet periods might affect peat formation, as drought could lead to peat decay, while floods could erode and deposit peat material and thus reshape peat topography. Some peat cores have a mineral or clay layer inserted between the peat layers, indicating deposition from a flood event (Gastaldo, 2010; Hapsari and others, 2017). While peat domes may reach elevations well above the reach of floods, in some locations traces of oxbow lakes indicate river meandering had a different spatial extent in the past and could have affected peat formation.

Human impact is also an undeniable factor affecting the peatland environment. Kalimantan was occupied by modern humans since at least 50 ka (thousands of years before present) (Reynolds and Barker, 2014). However, early human populations, part of the Melanesian migration, were largely hunter and gatherers, employing only a small degree of forest management and influence on land cover (Pyatt and others, 2005). Thus, their impact to the peatland was likely small. However, migration from Asia arrived multiple times to Kalimantan, with a major immigration during the Austronesian expansion beginning approximately 7 ka. Agriculture began during this period for crops such as yam, taro, millet and rice (Blench, 2010; Gao and others, 2020; Yew and others, 2018).

In this study, using a newly collected set of radiocarbon-dated cores from coastal and inland peatlands in West Kalimantan (Indonesia), we analyze the peat stratigraphy, accumulation history, and geochemical indicators of peat degradation. We also analyze the charcoal

stratigraphy as a proxy of fire presence, how its occurrence might relate to climate and human impact, and how the effects of modern human-caused fire and past fires on peatland differ. These datasets allow us to examine the similarities and differences of these two types of peatlands. We expect that the peat accumulation and fire regime was different before and after Austronesian expansion, was different during and after the glacial-maximum climatic period. We also expect that the coastal peat was more affected by human impact, especially anthropogenic fire, compared to the inland peat.

Material and Method

Study Area

West Kalimantan has approximately between 1.5 and 1.7 million ha of peat (Anda and others, 2021; Ritung and others, 2011). The peatland region here is defined by the Kapuas River— the longest river in Indonesia— with scattered domed peat areas in the upstream basin and flood plain, and a larger peatland on the extensive river deltas. The upstream region always remained above sea level during the Quaternary, meanwhile the coastal region was affected by sea level changes and delta formation (Dommain and others, 2011). Thus, their age is extremely different with the coastal peat dating to approximately 4.5–5 ka, while the inland peat dates to more than 50 ka (Ruwaimana and others, 2020). We laid one transect across each peat dome in the coastal and inland region (Figure 1). The samples were collected in 2019.

Sampling Method

We collected peat cores using 55 mm diameter Russian peat corers to obtain samples down to the mineral layer. Coring sites were spaced approximately 2 km apart. 17 points were cored at Rasau Jaya (coastal peatland) and 15 points were cored at Putussibau (inland peatland). At Rasau Jaya, we collected peat core samples from 8 points (R1-R8, Fig 1), and on the remaining 9 points we used the cores to determine peat depth. At Putussibau, we collected samples from 7 points (P1-P7, Fig 1) and at the remaining points we photographed cores, noted the presence of rare minerogenic layers, and determined the peat depth.

At each sample point where we collected cores, we obtained a pair of cores. For the first core, in each 25 cm segment we subsampled 10 cm for bulk density, loss-on-ignition, and carbon

and nitrogen elemental analysis. For the second core, we sampled the center of the core in contiguous 5 cm segments, so the outer part of the core did not contaminate the sample. We stored the samples in sterile whirl-pak bags. In between the main sampling sites, we took additional cores for the only purpose of measuring the peat depth. We had technical difficulties for cores P3, P4, and P5, where we were unable to collect samples to the mineral layer as we repeatedly encountered a layer of impenetrable wood at ca. 10–11 m depth that twisted and opened the corer. We cored additional locations within a radius of several tens of meters, but wood layers were persistent. Therefore, in these cases we changed the objective to obtaining samples as deep as possible rather than contiguously through the woody layer. In core P3, we were able to collect a 5 cm segment sample from the bottom of the peat at the depth of 15 m for radiocarbon dating. However, our maximum corer extension only reached 15 m, and at sites P4 and P5 we still did not reach the mineral layer at 15 m. In this case, we assume that the mineral layer is topographically flat with the adjacent site (P3.5), resulting in estimated depths at P4 of 17 m and at P5 of 16.9 m. An ongoing coring project by one of the authors (G.Z.A.) found a peat depth of 18 m roughly 1 km west of our transect supports this estimate (RSS GmbH, 2018). The elevation of each core site was determined using RTK GPS with an error of ±2–10 cm (Ruwaimana and others, 2020).

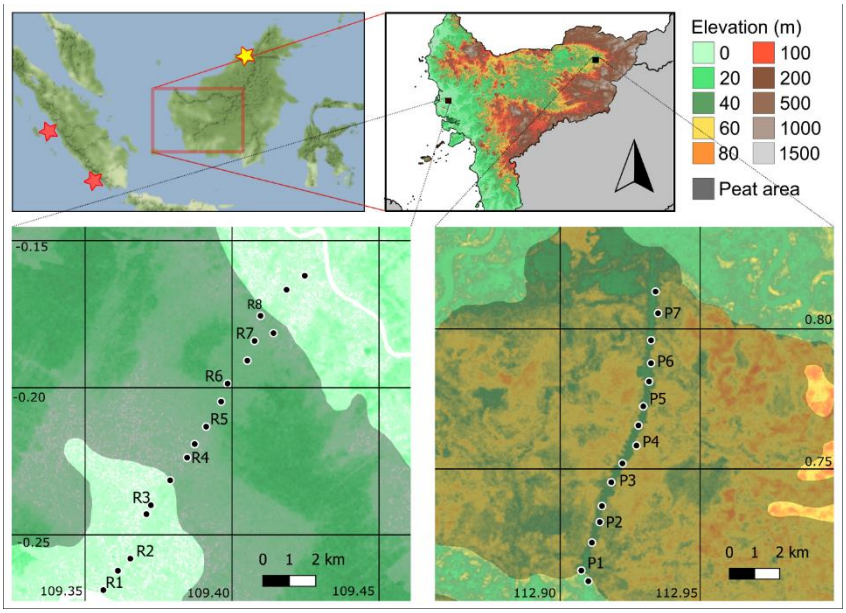

Figure 3.1. Map of sampling locations. Two transects across the peatland dome are placed on Putussibau (inland peat) and Rasau Jaya (coastal peat). Peat area (light grey overlay) is from a coarse resolution remote-sensing

estimation (Global Forest Watch, 2018) and in some places does not correspond with ground truth observations. Note that the remotely-sensed elevation data, the only available data for these sites, contain artifacts due to canopy cover, as seen as forest clearance along the road on the Putussibau transect. Red stars mark the location of ocean cores for reconstructed sea surface temperatures from benthic and planktonic Mg/Ca ratio (Mohtadi and others, 2010) and the yellow star marks the location of a speleothem δ18O as proxy of precipitation at Gunung Mulu National Park (Carolin and others, 2016)

Sample Analyses

Bulk density, loss-on-ignition (LOI), and elemental analysis (C%, N%, δ13C and δ15N) were conducted every 25 cm. For bulk density, we used the entire 10 cm core segment, wrapped the sample tightly with saran wrap, and immersed it briefly in a graduated cylinder filled with water to obtain the volume. Later, the whole sample was oven dried for 2–3 days at 70°C until the weight was constant. For LOI, the sample was finely ground, and 3–4 g of the sample placed in crucible in a muffle furnace at 500°C for 4 hours or until the organic matter turns to ash. For elemental analyses, we measured approximately 5–10 mg of sample in tin capsules. Carbon and nitrogen concentrations and stable isotopes were measured at the Stable Isotope Facility at the University of California Davis.

Radiocarbon dating was conducted from the 5-cm segment samples. We sieved 1 cm^3 bulk peat to obtain the 125–500 µm fraction, then treated it with 10% HCl and 10% KOH rinses. Intensive radiocarbon dating was conducted down-core on the three deepest cores in each study area (P3, P4, P5, R5.5, R6, and R6.5). We obtained dates in five submissions so that each submission iteratively narrows down the times of inflections and hiatuses in the age-depth relationship. We also obtained dates from the core bases from three additional cores at Putissibau and two additional cores at Rasau Jaya. In total we radiocarbon dated 41 samples (Table S1). We sent the samples to either the NOSAMS Laboratory (Woods Hole, MA) or DirectAMS (Bothell WA). We calibrated the radiocarbon dates following IntCal20 using the rcarbon package in R (Crema and Bevan, 2021). We then used Bayesian age-depth modelling in rbacon (Blaauw and others, 2019) to create age-depth models (Fig 2).

Charcoal analysis was also conducted on contiguous samples from the three cores from each area. From each of the 5-cm segment samples, we sieved 1 cm^3 bulk peat subsample to obtain the 125–500 µm fraction and then treated it with 3% H2O2 for 12 hours to lighten non-charcoal organic matter. We categorized charcoal into 13 morphotypes (Dussol and others, 2021)

which we then grouped into three main categories (woody; herb/grass/leaf; and other, Fig 3, Fig S3.6 and S3.7). We found the most abundant charcoal in the "lattice" and "framework" morphotypes (Dussol et al.) which were usually partially charred (i.e., partially dark black). We handpicked this charcoal morphotype and conducted 13C NMR (Nuclear Magnetic Resonance) spectroscopy to confirm that this type of charcoal particle has the geochemical signature of pyrogenic carbon. As a control, we also conducted NMR analysis on non-charred material from our sample, and on charcoal that we created in the furnace using our sample.

Results

Age-depth Chronology

Six cores were modelled for their age. The Rasau Jaya site (coastal peat) was formed at approximately 4.5 ka with the maximum depth of 6 m. Most of the peat especially on the edge of the peat dome was already degraded, thus we picked the three middle deepest cores for vertical radiocarbon dating (R5.5, R6 and R6.5) and created age-depth models on those cores. The age-depth relation is relatively linear with a maximum age of 4.5 ka (Fig 2).

The Putussibau site (inland peat) is much deeper and older than the coastal peat. Cores P3, P4 and P5 were radiocarbon dated along the vertical profile (Table S1). Core P3 has a maximum depth of 1360 cm and dated at 30.2 ka at the bottom. Core P4's maximum depth is unknown but the deepest sample we obtained at 1500 cm dated at 47.9 ka. Core P5's maximum depth is also unknown and the deepest sample at 1200 cm dated at 39.5 ka. Abrupt changes in radiocarbon ages suggests that hiatuses are present in all the cores: one hiatus in P3, and two hiatuses in each P4 and P5. These hiatuses have similar age, with the first hiatus at ca. 20–30 ka (cores P4 and P5 only), and the second hiatus at ca. 2–10 ka. There are also age reversals in cores P3 and P4 indicative of slumped or redeposited peat, which we modeled as instantaneous deposition. After accounting for this slump, only one radiocarbon date is an outlier in the modeled age-depth relationships (Fig 2).

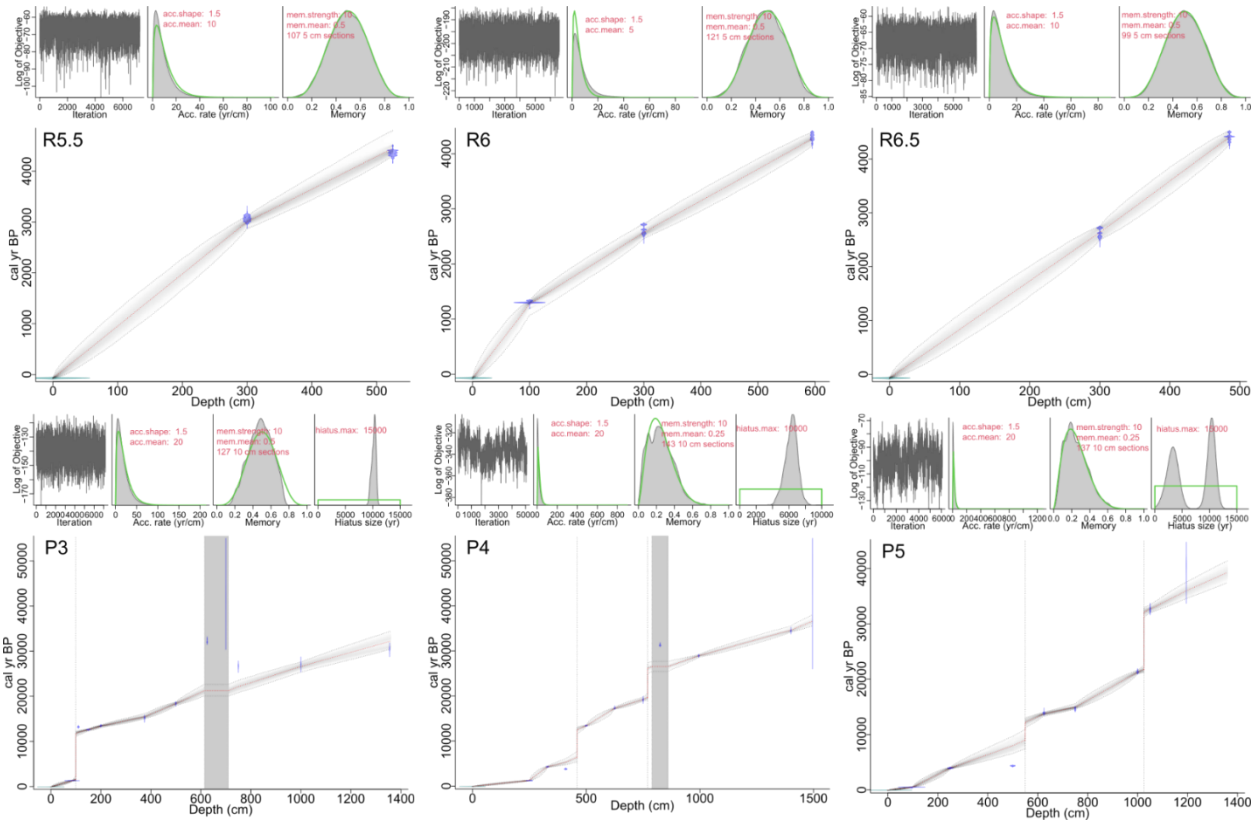

Figure 3.2. Bacon Age-Depth model output of three deepest cores form each site (Rasau Jaya: R55, R6, R65, Putussibau: P3, P4 and P5). Each model shows the types of The Bayesian modeling

Age Profile

We interpolated the ages from the intensively dated cores with radiocarbon dates from other cores to create an age profile on the cross-section created by the transect of cores (Fig. 3). At Rasau Jaya, as expected due to relatively linear age-depth relationship, age isolines are uniformly spaced within the less disturbed peat. However, we did not date the surface of cores R1-R5. The peat in these sites is quite compacted and heavily mixed due to current agricultural activity, thus likely will date to a modern age. The interpolation of ages resulted in closely spaced age isolines. However, it is important to note that the linear age-depth relationship may not hold true, particularly at the surface where compaction is prevalent and the potential for missing late Holocene peat exists due to recent peat degradation and fire. The interpolation of ages created tightly spaced age isolines, but we do not that the linear age-depth relation is the case especially at the surface where is there is a lot of compaction and there is a high possibility of missing late Holocene peat due to recent peat degradation and fire.

At Putussibau, the age profile is more complex, where there is an age reversal on two main cores (P3 and P4) that occur at the same elevation in the profile. This age reversal also is supported by a basal age of core P1 and P2 which are about the same age (35–40 ka) and located at the same elevation with the age reversal. We also observed hiatuses where the age changes abruptly, especially at core P3 where the age jumped from 13 ka to 1.3 ka. There is also a depression along the transect at core P3 which might indicate the loss of several meters of peat (Fig. 3).

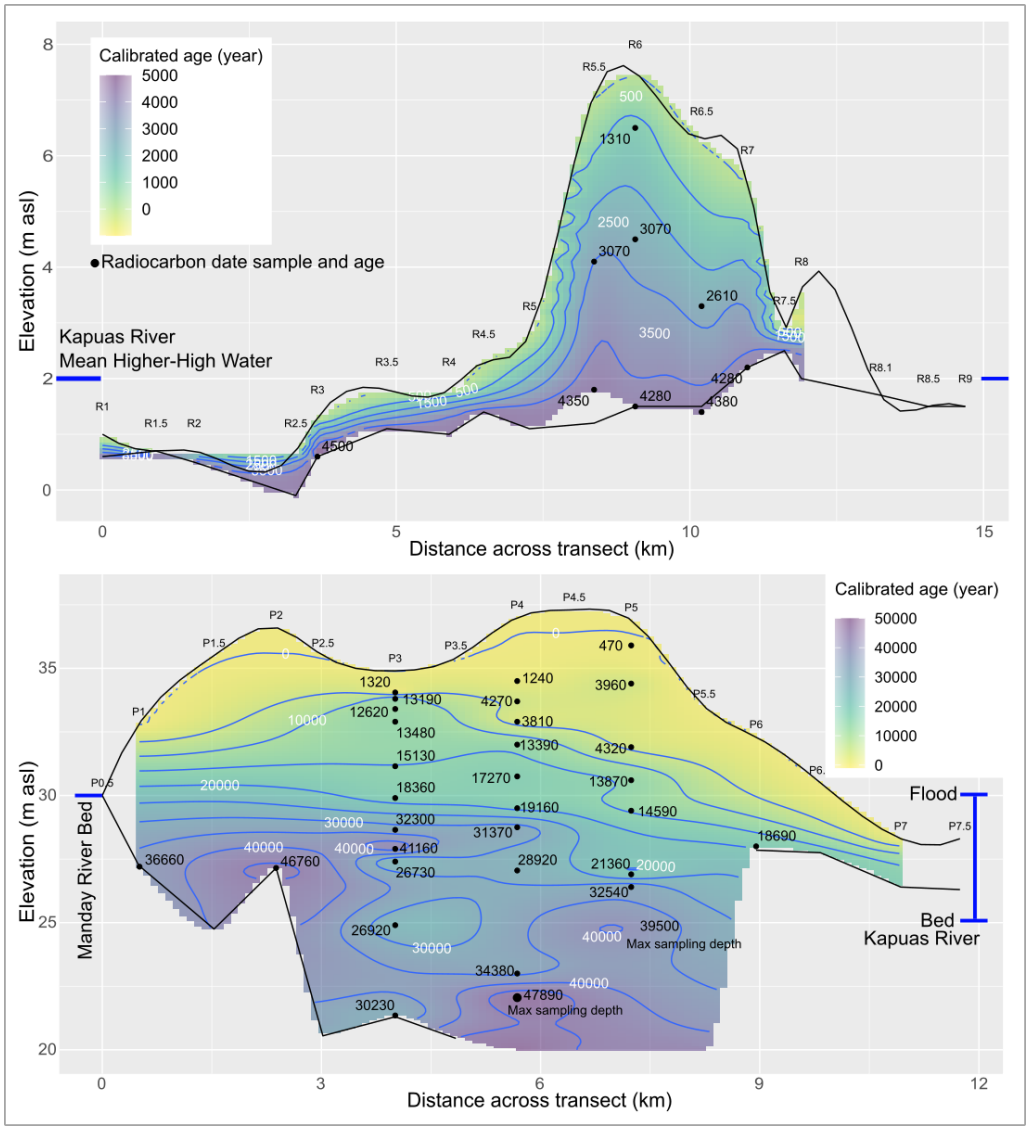

Figure 3.3. Age Profiles of Rasau Jaya and Putussibau peat domes. Black dots indicate the radiocarbon samples. All cores in Rasau Jaya reach the mineral layer, but cores P3.5 to P5.5 at Putussibau did not reach the mineral layer, thus we radiocarbon dated the deepest sample available. Surface profile created based on RTK-GPS.

Peat Geochemistry and Accumulation

All cores are highly organic with %C >50%, loss-on-ignition >95%, bulk density ca. 0.2 g/cm^3, and C:N ratio >40, except for an area of shallow peat at Rasau Jaya with more compact and less organic peat (Figs S1, S2). δ13C of total organic C varied little by depth, remaining between -29 to -31‰ (Fig S1). δ15N varied from -3 to 5‰, with high values near the surface at both sites.

At Rasau Jaya, peat accumulated at the rate ranging from 0.5–1 mm/y, where core R5.5 and R6 shows faster accumulation (>1 mm/yr) at the older age (1.5–4.5 ka) and slowing down afterward. Core R6.5 shows a constant accumulation rate at 0.75 mm/y. aCAR (apparent carbon accumulation rate) ranges from 20–50 g C/m^2/y, where all cores show slightly increased aCAR after 1 ka (Fig 4).

At Putussibau, the peat accumulation rate shows more variation. At 35–20 ka, the accumulation rate is around 0.5-0.7 mm/y and decreasing down to 0.2-0.3 mm/y around 20–10 ka. There is a small increase of accumulation around 15 ka to 0.5 mm/y, and then decreases again. During the early Holocene, there is a complete hiatus in all three cores, so the accumulation rate at that time is unknown. Afterward, the accumulation rate remains low at 0.3-0.5 mm/y until recently at 1 ka when the accumulation rate increase to 1.0 mm/y (Fig 4). Putussibau has quite uniform BD and %C, thus the aCAR closely follows the peat accumulation rate.

Charcoal

The charcoal from both sites is dominated by herb and leaf charcoal, which account for 83% of the total charcoal counted (Fig 4). One particular morphotype, called "lattice", is dominating (Fig S3.6 and S3.7). This type is defined as flat and thin, partially black and translucent, dull, and with visible cellular structure (Dussol and others, 2021). NMR results confirmed that these herbaceous charcoal sample contains both aromatic and aliphatic chemical structures which confirm that this sample is indeed partially charred (Fig S4).

Woody charcoal accounts for about 12% of the total charcoal sample, and other charcoal types account for 5% of the sample. We aligned the total concentration (pieces/cm^3), charcoal accumulation rate (pieces/cm^2/year), woody charcoal accumulation rate and herb/leaf charcoal accumulation rate with paleoclimate records from the region (Fig 4).

At Rasau Jaya, charcoal is rarely present around 3–4.5 ka, and started to increase toward modern time and peaking at ca. 1 ka. Surprisingly there is low charcoal abundance in the uppermost core sample. At Putussibau, charcoal is consistently present in all samples. Peak values of woody and herb/leaf charcoal co-occur in each core. Major peaks occur at ca. 26–27 ka, 13–14 ka and at 1 ka.

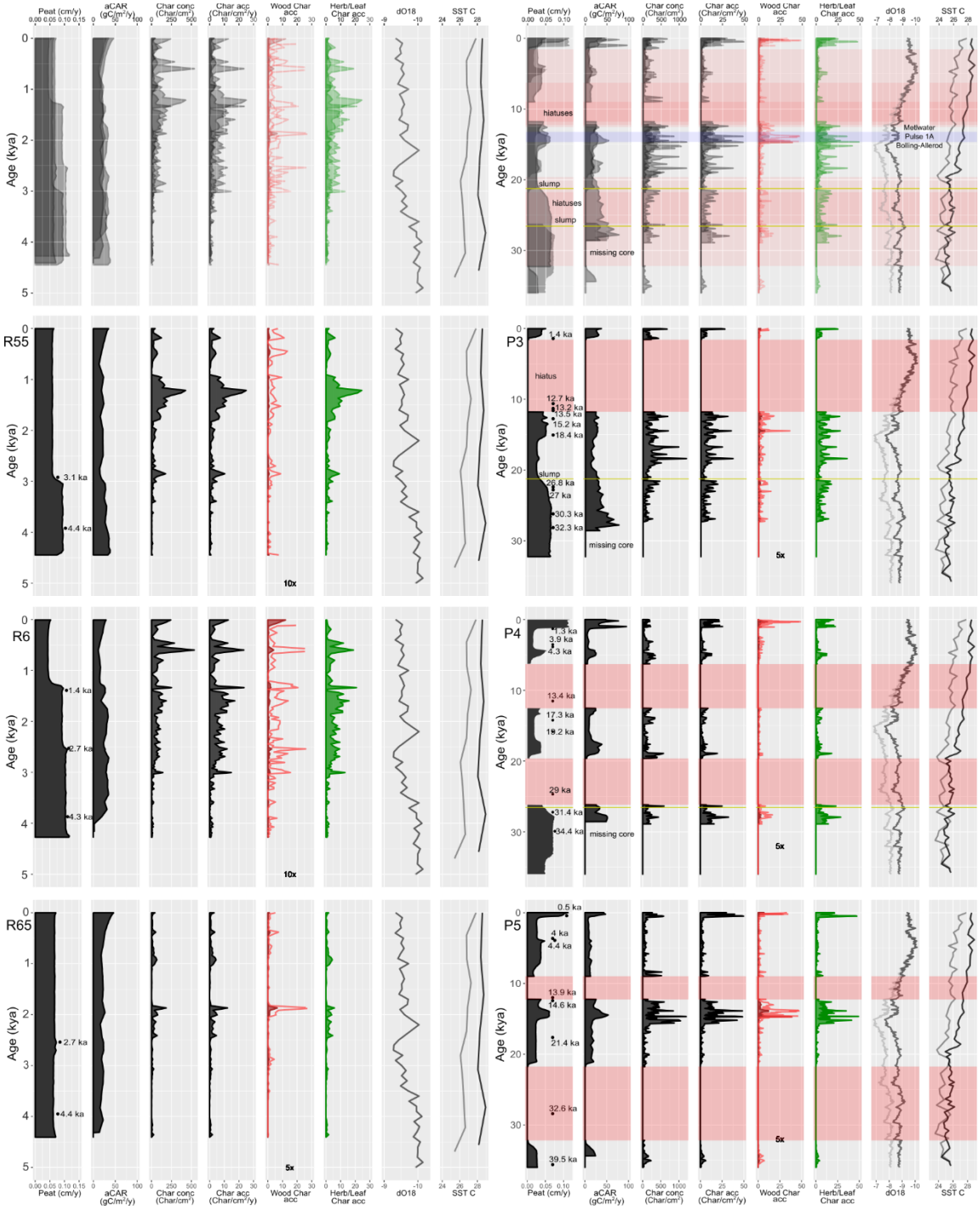

Figure 3.4. Combined cores (top row) and breakdown of each core (bottom three rows) from Rasau Jaya and Putussibau. Each core shows the peat accumulation rate, apparent carbon accumulation rate (aCAR), charcoal concentration, total charcoal accumulation rate, wood charcoal accumulation rate, herbaceous and leaf charcoal accumulation rate, and two paleoclimate records. δ18O from the Gunung Buda cave is a proxy of precipitation (lower values to the right indicates more precipitation). Light grey line shows the original data and black line show ice-volume corrected values (Carolin and others, 2016). The sea surface temperature from two cores off the coast of Sumatra is based on the benthic and planktonic Mg/Ca ratio (Mohtadi and others, 2011). Red shaded areas indicate missing peat that was modeled as hiatuses. Age in Y axis is based on rBacon modelling, Black dots on peat accumulation columns shows each individual radiocarbon date measurement calibrated with rCarbon.

Discussion

The high C:N ratio (>40) indicate a terrestrial peat existed at all times, with no periods of lakes (Meyers and Lallier-vergés, 1999). Also, the low δ13C (less than -29‰) indicates dominance by C3 plants at all times. The C:N ratio at Putussibau (73±26; 1σ) is higher than at Rasau (47±12, 1σ), which indicates that the peatland at Rasau is more degraded as more decomposed peat will have smaller C:N ratio value due to preferential loss of C over N in microbial decomposition (Krüger and others, 2015).

Coastal Peatland (Rasau Jaya)

Coastal peatlands are expected to form after the sea level stabilization within the last 7000 yr (Dommain and others, 2011). At the Rasau Jaya site, the bottom of the cores show that the peat started to form at 4.5 ka. However, the peat probably did not form immediately as the river delta first needed to form, followed by mangrove vegetation, which finally aggraded to form organic peats (Hunt and Premathilake, 2012; Yulianto and others, 2005). During this time, paleoclimate proxies indicates that precipitation was only slightly decreasing (Carolin and others, 2016) and sea surface temperature was relatively stable (Mohtadi and others, 2010) except for the recent modern anthropogenic climate change which increase the SST (Martono, 2016). Due to this stable climate, the peat accumulation shows a linear age-depth relation, with faster peat accumulation in the bottom half of the core (0.7–1.0 mm/y) and slowing down toward the modern age (0.5 mm/y), following the trend in precipitation (Fig 4). However, aCAR is relatively constant at 20–30 g C/m^2/y throughout the cores, until around 600–700 years ago, where all the cores show increases in aCAR to 30–50 g C/m^2/y. This could be an indication of peat compaction on the last few centuries, as the bulk density on the peat surface is relatively

higher and no radiocarbon dates were obtained through this interval to account for such compaction (Fig S1). This also could be the result of slow C loss deeper in the profile, which would cause the CAR to increase near the core top (Young and others, 2021).

While peat accumulation appeared to be uniform in space and time except for the last millennium, fire changed greatly through time. Before 3 ka, charcoal is only present in low numbers, when the peat had just started to establish with a high peat accumulation rate. After 3 ka, fire prevalence increased and peaked around 1.2 ka. While most paleoclimate records are too coarse to evaluate a climate link to these fire periods (Fig 4), in general over the last 4000 years, a warmer ENSO phase caused multiple drought events in this region (Biagioni and others, 2015; Carolin and others, 2016; Konecky and others, 2016; Partin and others, 2007; Rodysill and others, 2013) which could possibly decrease the peat accumulation rate and increase fire prevalence.

Beside the climate drivers, anthropogenic impacts are also potentially a strong driver of fire on this peatland. Borneo Island was inhabited by people since 50 ka and received a constant influx of human migration especially when the land bridge was connected to mainland Asia (Reynolds and Barker, 2014). However, early immigrants were largely hunter and gatherers, thus probably had minimal fire use (Pyatt and others, 2005). Rice cultivation arrived in this region at ca. 4 ka, and started to become intensive around 2.5–2 ka. Rice agriculture involved swidden agriculture with heavy fire use for land clearing (Ma and others, 2020; Zheng and others, 2021), thus probably causing the increase in charcoal. Moreover, around 1.5-0.75 ka, kingdoms in Indonesia started to form and establish a trading-post route along the coastal region of Kalimantan. One of the largest kingdoms, Majapahit, was expanding around 1290s to 1520s, or 0.66 to 0.43 ka (Gin, 2015; Smith and Smith, 2011). There is the possibility that Majapahit and earlier kingdoms harvested the coastal forest for boat building, and increased agriculture along the coastline of Borneo, thus causing the charcoal peaks at 1.2 ka and 0.7 ka. Similar to our results, (Hope and others, 2005) observed in a Kutai (East Kalimantan) peatland evidence for human-induced fires within the last millennia.

Following the peak in fire in the last millennium, we expected the amount of charcoal to continue increasing toward the modern time, however this is not the case. The city of Pontianak, located just ca. 20 km north of our site, was established in the 17th century and population continued to increase in the region (Sirrullah, 2019). During the 1970s the Indonesian

government relocated thousands of people from Java to Rasau Jaya as a part of transmigration program and to establish plantations, mainly of crops tolerant of peat such as aloe vera and pineapple (Septiyani, 2014). The development of human settlement started from the southern edge of the dome where the peat is thinner and easier to build upon (Arif, 2019). This development depleted the peat edge in the area of cores R1-R5, leaving behind less than one meter of decomposed and compact sapric peats (Fig S1). Fire is still heavily used for agriculture, as burning produces ashes that neutralize the soil acidity, which is a cheaper alternative to limestone to improve peat soil for agriculture. Thus, we were expecting high amounts of charcoal at the core surface of these sites. The lack of recent charcoal record on at the core tops may mean that the fires were smoldering peat fires that either produced no charcoal or the charcoal was consumed in subsequent fires during planting seasons. This interpretation is supported by higher δ15N (ca. 3‰; Fig S3.4) on the peat surface at Rasau Jaya, as combustion of peat may release δ15N-depleted gases (Davidson et al. 2014; Hapsari 2021).

Inland Peatland (Putussibau)

Inland peat in the Upper Kapuas Basin, including Putussibau, was established more than 50 ka and persisted through several climate changes including the Last Glacial Maximum (Anshari and others, 2001; Ruwaimana and others, 2020; Yu and others, 2010). The base of the Putussibau peat dome has ages ranging from 36 ka near the Manday River to > 45 ka near the deepest peats at transect-km 6 to 7 (Fig 3). Given this long history, this site is expected to have a more complex age-depth model. Indeed, the age model indicates periods of rapid peat accumulation, an age reversal in two cores, and hiatuses in all cores (amounting to 30.6% of the time of the three cores). We interpret this history using geochemical (C and N) and charcoal indicators and with respect to climate history and the potential for flood disturbances.

Peat Age Reversal Indicates Flood

An age reversal occurred in cores P4 between 28–19 ka and P3 between 26–18 ka. In the Bacon age-depth modelling, we treated the age reversals as slumps of redeposited older peat material. The radiocarbon dates in the slump are dated from 30–41 ka and based on the age profiles (Fig 3). Usually, age reversal is caused by the mobility of vegetation biomass where younger vegetation parts such as roots penetrate the deeper zone, and when the sample is taken,

this young part is collected. However, upon further analysis, the slump material was found to have the same horizontal elevation and likely spans between the core sites. Other soil physical and chemical analysis such as C%, CD, N%, C/N, and BD (Fig S3.2 and S3.3) also support a different origin of the slumped material, with higher carbon (less decomposed) and denser than the peat above or below. We also observed the presence of silt materials in the other cores at the same elevation with the age reversal (Fig S3.9). This probably indicates a single or multiple flooding events eroded peat material or wood from the banks of the Manday River and deposited this material, along with silt, at the core sites. Other than the meandering of large rivers, flooding rarely erodes intact peat material supporting dense vegetation. However, there is a possibility that fires and dried out peat, during a cooler climate when vegetation cover was less dense, lowered the elevation of the peat surface (Anshari and others, 2001; Bird and others, 2005). These factors loosened the peat material, thus enabling the peat and/or detrital wood to flood onto the dome surface.

The modern elevation of the Manday River (30 m) lies above the elevation of this age reversal (27–29 m a.s.l.). In fact, peat was cored up to 10 m below the modern river elevation. This peat has similar texture and geochemistry as Holocene peats. It is likely that the Manday River bed was at a lower elevation prior to the LGM, and aggraded over millennia, thus affecting the water table and supporting the development of the very deep peatlands. There may be other links between the patterns of aggradation and incision of the Manday and Kapuas rivers affecting periods of peat accumulation and peat loss, assuming water table distal from the rivers is affected by river bed elevation. Future work should address the links between fluvial geomorphology and peatland history.

This age reversal coincided with the Last Glacial Maximum. An age inversion was also reported at 20–10 ka at the Sebagau Peatland in Central Borneo (Page and others, 2004) and at 11 ka in Central Sumatra (Hapsari and others, 2017), which suggest the inversion is quite a common occurrence and dynamic in these tropical peatlands. The peat comprising the reversal is more compacted and with higher bulk density and higher carbon content. A hiatus may also have occurred at this time, as peat only started to accumulate again around 18–19 ka. This hiatus may be from eroded peat from a flood, or from a nutrient limitation, as the peat in this zone has a high C/N and is rather low in N.

Fire History

Our composite charcoal record from three cores begins at 28 ka, starting with high values and decreasing until the LGM at 24 ka. During the LGM, peat accumulation and carbon accumulation decreased as vegetation became sparser due to colder and drier climate (Bird and others, 2005; Hunt and others, 2012). Moreover, lower precipitation, and thus less thunderstorms and lightning, may have reduced the fire ignition rate. After the LGM, charcoal was fluctuating at low levels for several centuries, suggesting that the fire is a constant presence on pristine inland peat. Charcoal started to increase approximately 20 ka and reaches the highest level at ca. 15–13 ka. During this period even though humans were already present at various caves across Kalimantan, there is little archaeological evidence of human agricultural activity, and their impact on peatland ecosystem might be negligible (Pyatt and others, 2005; Reynolds and Barker, 2014). However, there are potential climatic causes for this period of fire. Around 20 ka, the δ18O record shows a decrease in precipitation, thus probably causing more available dry peat material for combustion. However, when δ18O shows sudden precipitation increase at 15–13 ka, instead of decreasing charcoal, the charcoal accumulation increased. This time is coincident with Bolling-Allerod warming and Meltwater Pulse 1A. Although Bolling-Allerod is largely recorded in the Northern Hemisphere and caused increased precipitation in coastal Asia (Wen and others, 2016), its impact on climate in the tropical region is largely unstudied. Warmer temperature and increasing sea levels might also have increased fire on pristine peat (Hapsari and others, 2017), possibly by shifting the ITCZ northward and creating more thunderstorms, potentially causing more lightning and generating more fire. Thus, increased precipitation also would increase the peat accumulation rate due to higher productivity and a higher water table. Increased charcoal at times of increased peat growth was also observed in a core from Sumatra (Hapsari and others, 2022)

The fires that occurred at the Putussibau peatlands were likely low severity litter fires very close to the core site rather than dispersed from upland forest 20–30 km away. This is supported by the abundance of lattice and herb/leaf charcoal types relative to blocky wood charcoal, and the high accumulation rate of the charcoal, often more than 25 pieces/cm^2/y. These fires were also local to the core site, as burning of peat surface creates abundant charred material in the peat deposit, up to 25–50 pieces/cm^2/y (Huber and others, 2004; Huber and Markgraf, 2003). For comparison, lake sediments in high-severity fire regimes are often <2 pieces/cm^2/y

due to dispersal and dilution in lakes (Higuera and others, 2007). NMR analysis of this charcoal type confirms our interpretation of it being partially burned herb and leaf material (Fig S3.8). In addition to the NMR results, the abundance of partially burned lattice charcoal is supported by the reported combustion factor (proportion of above-ground fuel mass consumed in fire) for tropical peatland in Kalimantan, which ranges from 0.4 to 0.7, indicating large amount of unburnt peat remains following fire (Krisnawati and others, 2021).

At the inland Putussibau site, in the most recent peat at the core tops, we found surprisingly more charcoal compared to the coastal site. This charcoal is an indication the presence of modern fire. There is no clear historical record when this area began to be settled, but we observe that the charcoal started to increase at approximately 1 ka. The Upper Kapuas Region was already inhabited by Dayak people that mainly were farming on the river floodplain, and in the 18th century the Kingdom of Selimbau established Putussibau city, located approximately 15 km north of the sampling site (Prasojo, 2017; Suprianto and others, 2021). Recent development of rubber and oil palm has caused some of the peat, especially areas with road access, to be converted into plantations. However, due to the poor quality of the peat, these plantations are unproductive and most of them were abandoned when the samples were collected in 2019 (personal observation and communication with local farmers). Thus, fires during the last millennium at Putussibau may have been used for clearing (as shown by higher levels of wood charcoal, Fig S3.6), but likely not continuously as the farming is not productive on this deep peat dome.

Drought or Fire-Caused Hiatuses in Peat Accumulation

There are a range of scenarios for the causes of the hiatuses observed in the peat stratigraphy. One scenario is that there was a long-term decline in productivity and/or increase in peat respiration during a drier climatic period. Lower precipitation during the LGM likely resulted from the lower sea level that exposed the Karimata Strait that connected Borneo, Sumatra, and Java Islands into a large landmass, potentially with a savanna corridor (Bird and others, 2005). This change in land area to the west of Borneo may have reduced precipitation at the study site (Kershaw and others, 2001). Currently, ca. 40% rainfall in this region is recycled by evaporation from land and the remaining ca. 60% comes from evaporation from the South China Sea and the Java Sea (Tuinenburg and others, 2020). Thus, when sea level was lower, the

study site was further from the sea, and thus received less precipitation. This is supported by the Gunung Buda δ18O speleothem record, showing generally drier conditions before the Holocene and during the earlier period of hiatus (Carolin and others, 2016; Partin and others, 2007). Lower precipitation in turn lowered plant productivity and paused the peat accumulation, as well as lowered the ground water level and exposed the existing peat to the atmosphere to decompose. In this case, hiatuses or even peat degradation continued for several thousand years until the climate allowed the peat to grow back.

Another scenario is that hiatuses are the result of single or several intense fire events. Under this scenario, peat was continually accumulating even during the low precipitation periods, consistent with previous studies that the Putussibau area is a rainforest glacial refugium despite it being somewhat drier during the LGM (Anshari and others, 2001; Bird and others, 2005). However, at a certain point a large fire event burned up several meters of the peat column, thus creating a gap of thousands of years in the peat record. One single event of fire could potentially smolder down to 50–60 cm depth and potentially deeper depending on the soil water level (Konecny and others, 2016; Usup and others, 2004). Recent modern clearing fire has been observed to smolder as deep as the road foundation at a 2–3 m depth (Wahyudi Hidayat, Putussibau Regence official, personal communication, July 26th 2019). These past events, potentially consuming several thousand years of peat, released an equal amount of carbon compared to recent fires. For example, in core P5 where the most recent hiatus lasted for ca. 3000 years, and assuming an aCAR of 20 g C/m^2/year, if burned in a series of fire events this site would have released 600 t C/ha. As comparison, severe peat fire event in 1997 in Indonesia released 200–250 t C/ha (Boehm and others, 2022; Page and others, 2002), a milder fire in 2006 released 29.6 t C/ha (Ballhorn and others, 2009), and a reburn of a peatland in Central Kalimantan released 64 t C/ha (Konecny and others, 2016). Thus, high amount of carbon loss in our core is likely the result of multiple fire events.

We may use the evidence of fire history and peat degradation to support which scenario, or combination of scenarios, was the more likely cause of the hiatuses. The two older hiatuses at cores P4 and P5 ended at similar time around 21–20 ka, and afterward there was an increase in the charcoal count, which could indicate fire events in conjunction with the regionally drier conditions could be the cause of these hiatuses, consuming a different amount of peat at each site. Three younger hiatuses at all cores started at the similar time around 12 ka but ended at

different times. Peat growth may have slowed down or stopped during this period. Although in general δ18O shows increase in rainfall through the early Holocene (Carolin and others, 2016), a high-resolution lake core with from Loagan Bunut, Sarawak, 350 km north of the study site, shows that there are periods of drier climate and more fire 9250–8890, 7900 and 7600–7545 cal. BP (Hunt and Premathilake, 2012). This short period of drought might happen multiple times and potentially cause hiatuses from a combination of drought and severe fire.

Under the peat-degradation scenario for hiatuses, we would expect that indicators of peat degradation would be correlated with aCAR, in general, down core. For example, δ13C may decrease from the selective loss of labile 13C-rich carbohydrates, 15N may increase from selective use of 14N by microbes, and C:N decreases from carbon respiration (Ramdzan and others, 2022; Spiker and Hatcher, 1984) (Ramdzan, Spiker). However, there is little support from the stratigraphic correlation of these indicators (Figs S1, S2). At Rasau Jaya, aCAR varies little, and only d15N is high near the peat surface, resulting from recent fires as mentioned above. At Putussibau, while aCAR varies down-core, there is no clear correlation of aCAR with any of these indicators.

Conclusions

Coastal peat is younger and shallower than inland peat. As coastal peat is formed during a relatively stable climate, the age-depth relationship is quite linear. This is in contrast with inland peat, where we find age reversals and hiatuses. Despite stable peat accumulation rate in coastal peat, the fire regime varied greatly, likely due to combination of ENSO phases and increasing anthropogenic impact, especially the rise of agricultural practice is this region. For both areas, the charcoal type is dominated by partially burned, herbaceous charcoal. This suggests that the fire was probably a low severity surface and shallow fire. High amount of charcoal also suggest that the fires were local.

Age reversals have been observed in various deep tropical peat cores, however, their causes are often dismissed as a contaminated radiocarbon sample or not investigated. By analyzing multiple cores with different distance from the river, we rule out contamination and deduced that there was a flood that causing this reversal. Two scenarios may explain the hiatuses in the peat core. The first is a long period of no peat accumulation and slow decomposition. Reduced precipitation and cooler climate reduced the primary productivity and lowered the water

level, and subsequently lowered the peat accumulation rate and exposed the existing peat to decomposition. The second scenario is a single or multiple fire events removed several thousand years of peat accumulation.

We currently cannot confirm which scenario is more likely without more study of peat degradation indicators. For example, Garcin and others (2022) used a suite of peat degradation indicators to support a climate, not fire, caused hiatus in a peat core from the Congo Basin. Regardless of the exact cause of the hiatuses in our cores, the amount of carbon released in each event (ca. 600 t/ha for a 3000-yr hiatus) is greater than that from the most intense modern fire years. If our results are representative of the 6630 km^2 of deep peatlands of the upper Kapuas Basin, the carbon fluxes implied for these hiatuses reach globally significant values (> 1.5 Gt CO2). We note that the end of the first hiatus period, at ca. 20 ka, is close to the timing of initiation of the post-glacial increase of atmospheric CO2 at 19 ka. In addition, the hiatuses during the mid to late Holocene occur during a period of rising atmospheric CO2, which has previously been attributed to a terrestrial carbon source (Ruddiman, 2003). Thus, our results are consistent with previous research highlighting Indonesian peatlands as a globally important for the carbon cycle, (Datta and Krishnamoorti, 2022; Krisnawati and others, 2021; Page and others, 2002) functioning as a terrestrial carbon sink during the Last Glacial Maximum and as a CO2 source during the early postglacial period and during the Holocene.

In the next chapter, we will focus more on the biological proxy from the peat layers. We will list and identify all the pollen and spore types found in the peat samples. This will address a research gap on tropical pollen; there are only a few materials currently available and published. This work will be a foundation for our future project on pollen in tropical peatland.

References

Anda, M., Ritung, S., Suryani, E., Sukarman, Hikmat, M., Yatno, E., Mulyani, A., Subandiono, R.E., Suratman, Husnain, 2021. Revisiting tropical peatlands in Indonesia: Semi-detailed mapping, extent and depth distribution assessment. Geoderma 402, 115235. https://doi.org/10.1016/j.geoderma.2021.115235

Anshari, G., Peter Kershaw, A., van der Kaars, S., 2001. A Late Pleistocene and Holocene pollen and charcoal record from peat swamp forest, Lake Sentarum Wildlife Reserve, West Kalimantan, Indonesia. Palaeogeography, Palaeoclimatology, Palaeoecology, Quaternary Environmental Change in the Indonesian Region 171, 213–228. https://doi.org/10.1016/S0031-0182(01)00246-2

Anshari, G., Peter Kershaw, A., Van Der Kaars, S., Jacobsen, G., 2004. Environmental change and peatland forest dynamics in the Lake Sentarum area, West Kalimantan, Indonesia. J. Quaternary Sci. 19, 637–655. https://doi.org/10.1002/jqs.879

Arif, M., 2019. AWAL KEHIDUPAN MASYARAKAT TRANSMIGRASI DI RASAU JAYA 1. MASA: Journal of History 1.

Ballhorn, U., Siegert, F., Mason, M., Limin, S., 2009. Derivation of burn scar depths and estimation of carbon emissions with LIDAR in Indonesian peatlands. Proceedings of the National Academy of Sciences 106, 21213–21218. https://doi.org/10.1073/pnas.0906457106

Biagioni, S., Krashevska, V., Achnopha, Y., Saad, A., Sabiham, S., Behling, H., 2015. 8000 years of vegetation dynamics and environmental changes of a unique inland peat ecosystem of the Jambi Province in Central Sumatra, Indonesia. Palaeogeography, Palaeoclimatology, Palaeoecology 440, 813–829. https://doi.org/10.1016/j.palaeo.2015.09.048

Bird, M.I., Taylor, D., Hunt, C., 2005. Palaeoenvironments of insular Southeast Asia during the Last Glacial Period: a savanna corridor in Sundaland? Quaternary Science Reviews 24, 2228–2242. https://doi.org/10.1016/j.quascirev.2005.04.004

Blaauw, M., Christen, J.A., Vazquez, J.E., Belding, T., Theiler, J., Gough, B., Karney, C., Blaauw, M.M., 2019. Package 'rbacon.'

Blench, R., 2010. Was there an Austroasiatic presence in Island Southeast Asia prior to the Austronesian expansion? Bulletin of the Indo-Pacific Prehistory Association 30, 133–144.

Boehm, H.-D., Siegert, D., Rieley, F., Page, J., 2022. Fire impacts and carbon release on tropical peatlands in Central Kalimantan, Indonesia 1.

Carolin, S.A., Cobb, K.M., Lynch-Stieglitz, J., Moerman, J.W., Partin, J.W., Lejau, S., Malang, J., Clark, B., Tuen, A.A., Adkins, J.F., 2016. Northern Borneo stalagmite records reveal West Pacific hydroclimate across MIS 5 and 6. Earth and Planetary Science Letters 439, 182–193. https://doi.org/10.1016/j.epsl.2016.01.028

Cochrane, M.A., 2003. Fire science for rainforests. Nature 421, 913–919. https://doi.org/10.1038/nature01437

Cole, L.E.S., Bhagwat, S.A., Willis, K.J., 2019. Fire in the swamp forest: Palaeoecological insights into natural and human-induced burning in intact tropical peatlands. Front. For. Glob. Change 2. https://doi.org/10.3389/ffgc.2019.00048

Crema, E.R., Bevan, A., 2021. INFERENCE FROM LARGE SETS OF RADIOCARBON DATES: SOFTWARE AND METHODS. Radiocarbon 63, 23–39. https://doi.org/10.1017/RDC.2020.95

Datta, A., Krishnamoorti, R., 2022. Understanding the Greenhouse Gas Impact of Deforestation Fires in Indonesia and Brazil in 2019 and 2020. Frontiers in Climate 4.

Dohong, A., Aziz, A.A., Dargusch, P., 2017. A review of the drivers of tropical peatland degradation in South-East Asia. Land Use Policy 69, 349–360. https://doi.org/10.1016/j.landusepol.2017.09.035

Dommain, R., Couwenberg, J., Joosten, H., 2011. Development and carbon sequestration of tropical peat domes in south-east Asia: links to post-glacial sea-level changes and Holocene climate variability. Quaternary Science Reviews 30, 999–1010. https://doi.org/10.1016/j.quascirev.2011.01.018

Dussol, L., Vannière, B., Purdue, L., Orange, F., Testé, M., Castanet, C., Garnier, A., Lemonnier, E., Théry-Parisot, I., 2021. How to highlight slash-and-burn agriculture in ancient soils? A modern baseline of agrarian fire

imprint in the Guatemalan lowlands using charcoal particle analysis. Journal of Archaeological Science: Reports 35, 102725. https://doi.org/10.1016/j.jasrep.2020.102725

Gallego-Sala, A.V., Charman, D.J., Brewer, S., Page, S.E., Prentice, I.C., Friedlingstein, P., Moreton, S., Amesbury, M.J., Beilman, D.W., Björck, S., Blyakharchuk, T., Bochicchio, C., Booth, R.K., Bunbury, J., Camill, P., Carless, D., Chimner, R.A., Clifford, M., Cressey, E., Courtney-Mustaphi, C., Vleeschouwer, F.D., Jong, R. de, Fialkiewicz-Koziel, B., Finkelstein, S.A., Garneau, M., Githumbi, E., Hribjlan, J., Holmquist, J., Hughes, P.D.M., Jones, C., Jones, M.C., Karofeld, E., Klein, E.S., Kokfelt, U., Korhola, A., Lacourse, T., Roux, G.L., Lamentowicz, M., Large, D., Lavoie, M., Loisel, J., Mackay, H., MacDonald, G.M., Makila, M., Magnan, G., Marchant, R., Marcisz, K., Cortizas, A.M., Massa, C., Mathijssen, P., Mauquoy, D., Mighall, T., Mitchell, F.J.G., Moss, P., Nichols, J., Oksanen, P.O., Orme, L., Packalen, M.S., Robinson, S., Roland, T.P., Sanderson, N.K., Sannel, A.B.K., Silva-Sánchez, N., Steinberg, N., Swindles, G.T., Turner, T.E., Uglow, J., Väliranta, M., Bellen, S. van, Linden, M. van der, Geel, B. van, Wang, G., Yu, Z., Zaragoza-Castells, J., Zhao, Y., 2018. Latitudinal limits to the predicted increase of the peatland carbon sink with warming. Nature Climate Change 1. https://doi.org/10.1038/s41558-018-0271-1

Gao, Y., Dong, G., Yang, X., Chen, F., 2020. A review on the spread of prehistoric agriculture from southern China to mainland Southeast Asia. Science China Earth Sciences 63. https://doi.org/10.1007/s11430-019-9552-5

Garcin, Y., Schefuß, E., Dargie, G.C., Hawthorne, D., Lawson, I.T., Sebag, D., Biddulph, G.E., Crezee, B., Bocko, Y.E., Ifo, S.A., Mampouya Wenina, Y.E., Mbemba, M., Ewango, C.E.N., Emba, O., Bola, P., Kanyama Tabu, J., Tyrrell, G., Young, D.M., Gassier, G., Girkin, N.T., Vane, C.H., Adatte, T., Baird, A.J., Boom, A., Gulliver, P., Morris, P.J., Page, S.E., Sjögersten, S., Lewis, S.L., 2022. Hydroclimatic vulnerability of peat carbon in the central Congo Basin. Nature 1–6. https://doi.org/10.1038/s41586-022-05389-3

Gastaldo, R.A., 2010. Peat or no peat: Why do the Rajang and Mahakam Deltas differ? International Journal of Coal Geology, Hermann W. Pfefferkorn Commemorative Volume 83, 162–172. https://doi.org/10.1016/j.coal.2010.01.005

Gin, O.K., 2015. Borneo in the early modern period: c. late fourteenth to c. late eighteenth centuries, in: Early Modern Southeast Asia, 1350-1800. Routledge, pp. 116–130.

Global Forest Watch, 2018. Indonesia Peat Land [WWW Document]. URL http://data.globalforestwatch.org/datasets/d52e0e67ad21401cbf3a2c002599cf58_10?geometry=79.244%2C-8.804%2C145.997%2C6.528

Hapsari, K.A., Biagioni, S., Jennerjahn, T.C., Reimer, P.M., Saad, A., Achnopha, Y., Sabiham, S., Behling, H., 2017. Environmental dynamics and carbon accumulation rate of a tropical peatland in Central Sumatra, Indonesia. Quaternary Science Reviews 169, 173–187. https://doi.org/10.1016/j.quascirev.2017.05.026

Hapsari, K.A., Jennerjahn, T., Nugroho, S.H., Yulianto, E., Behling, H., 2022. Sea level rise and climate change acting as interactive stressors on development and dynamics of tropical peatlands in coastal Sumatra and South Borneo since the Last Glacial Maximum. Global Change Biology 28, 3459–3479. https://doi.org/10.1111/gcb.16131

Hidayat, H., Teuling, A.J., Vermeulen, B., Taufik, M., Kastner, K., Geertsema, T.J., Bol, D.C.C., Hoekman, D.H., Haryani, G.S., Van Lanen, H.A.J., Delinom, R.M., Dijksma, R., Anshari, G.Z., Ningsih, N.S., Uijlenhoet, R., Hoitink, A.J.F., 2017. Hydrology of inland tropical lowlands: the Kapuas and Mahakam wetlands. Hydrol. Earth Syst. Sci. 21, 2579–2594. https://doi.org/10.5194/hess-21-2579-2017

Higuera, P.E., Peters, M.E., Brubaker, L.B., Gavin, D.G., 2007. Understanding the origin and analysis of sediment-charcoal records with a simulation model. Quaternary Science Reviews 26, 1790–1809. https://doi.org/10.1016/j.quascirev.2007.03.010

Hodgkins, S.B., Richardson, C.J., Dommain, R., Wang, H., Glaser, P.H., Verbeke, B., Winkler, B.R., Cobb, A.R., Rich, V.I., Missilmani, M., Flanagan, N., Ho, M., Hoyt, A.M., Harvey, C.F., Vining, S.R., Hough, M.A., Moore, T.R., Richard, P.J.H., Cruz, F.B.D.L., Toufaily, J., Hamdan, R., Cooper, W.T., Chanton, J.P., 2018. Tropical peatland carbon storage linked to global latitudinal trends in peat recalcitrance. Nat Commun 9, 1–13. https://doi.org/10.1038/s41467-018-06050-2

Hope, G., Chokkalingam, U., Anwar, S., 2005. The stratigraphy and fire history of the Kutai Peatlands, Kalimantan, Indonesia. Quaternary Research, Late Quaternary Tropical Ecosystem Dynamics 64, 407–417. https://doi.org/10.1016/j.yqres.2005.08.009

Huber, U.M., Markgraf, V., 2003. Holocene fire frequency and climate change at Rio Rubens Bog, southern Patagonia, in: Fire and Climatic Change in Temperate Ecosystems of the Western Americas. Springer, pp. 357–380.

Huber, U.M., Markgraf, V., Schäbitz, F., 2004. Geographical and temporal trends in Late Quaternary fire histories of Fuego-Patagonia, South America. Quaternary Science Reviews 23, 1079–1097. https://doi.org/10.1016/j.quascirev.2003.11.002

Hunt, C.O., Gilbertson, D.D., Rushworth, G., 2012. A 50,000-year record of late Pleistocene tropical vegetation and human impact in lowland Borneo. Quaternary Science Reviews 37, 61–80. https://doi.org/10.1016/j.quascirev.2012.01.014

Hunt, C.O., Premathilake, R., 2012. Early Holocene vegetation, human activity and climate from Sarawak, Malaysian Borneo. Quaternary International 249, 105–119. https://doi.org/10.1016/j.quaint.2011.04.027

Kershaw, P., Penny, D., van der Kaars, S., Anshari, G., Thamotherampillai, A., 2001. Vegetation and climate in lowland southeast Asia at the Last Glacial Maximum. pp. 227–236.

Konecky, B., Russell, J., Bijaksana, S., 2016. Glacial aridity in central Indonesia coeval with intensified monsoon circulation. Earth and Planetary Science Letters 437, 15–24. https://doi.org/10.1016/j.epsl.2015.12.037

Konecny, K., Ballhorn, U., Navratil, P., Jubanski, J., Page, S.E., Tansey, K., Hooijer, A., Vernimmen, R., Siegert, F., 2016. Variable carbon losses from recurrent fires in drained tropical peatlands. Global Change Biology 22, 1469–1480. https://doi.org/10.1111/gcb.13186

Krisnawati, H., Adinugroho, W.C., Imanuddin, R., Suyoko, Weston, C.J., Volkova, L., 2021. Carbon balance of tropical peat forests at different fire history and implications for carbon emissions. Science of The Total Environment 779, 146365. https://doi.org/10.1016/j.scitotenv.2021.146365

Krüger, J.P., Leifeld, J., Glatzel, S., Szidat, S., Alewell, C., 2015. Biogeochemical indicators of peatland degradation – a case study of a temperate bog in northern Germany. Biogeosciences 12, 2861–2871. https://doi.org/10.5194/bg-12-2861-2015

Loisel, J., Gallego-Sala, A.V., Amesbury, M.J., Magnan, G., Anshari, G., Beilman, D., Benavides, J.C., Blewett, J., Camill, P., Charman, D.J., Chawchai, S., Hedgpeth, A., Kleinen, T., Korhola, A., Large, D., Mansilla, C.A., Müller, J., van Bellen, S., West, J.B., Yu, Z., Bubier, J., Garneau, M., Moore, T., Sannel, A.B.K., Page, S., Väliranta, M., Bechtold, M., Brovkin, V., Cole, L.E.S., Chanton, J.P., Christensen, T.R., Davies, M.A., De Vleeschouwer, F., Finkelstein, S.A., Frolking, S., Galka, M., Gandois, L., Girkin, N., Harris, L.I., Heinemeyer, A., Hoyt, A.M., Jones, M.C., Joos, F., Juutinen, S., Kaiser, K., Lacourse, T., Lamentowicz, M., Larmola, T., Leifeld, J., Lohila, A., Milner, A.M., Minkkinen, K., Moss, P., Naafs, B.D.A., Nichols, J., O'Donnell, J., Payne, R., Philben, M., Piilo, S., Quillet, A., Ratnayake, A.S., Roland, T., Sjögersten, S., Sonnentag, O., Swindles, G.T., Swinnen, W., Talbot, J., Treat, C., Valach, A.C., Wu, J., 2020. Expert assessment of future vulnerability of the global peatland carbon sink. https://doi.org/10/01656

Ma, T., Rolett, B.V., Zheng, Z., Zong, Y., 2020. Holocene coastal evolution preceded the expansion of paddy field rice farming. Proceedings of the National Academy of Sciences 117, 24138–24143. https://doi.org/10.1073/pnas.1919217117

Martono, M., 2016. Seasonal and Inter Annual Variation of Sea Surface Temperature in the Indonesian Waters. Forum Geografi 30, 120–129.

Meyers, P.A., Lallier-vergés, E., 1999. Lacustrine sedimentary organic matter records of late Quaternary paleoclimates. Journal of Paleolimnology 21, 345–372. https://doi.org/10.1023/A:1008073732192

Mohtadi, M., Oppo, D.W., Steinke, S., Stuut, J.-B.W., De Pol-Holz, R., Hebbeln, D., Lückge, A., 2011. Glacial to Holocene swings of the Australian-Indonesian monsoon. Nature Geosci 4, 540–544. https://doi.org/10.1038/ngeo1209

Mohtadi, M., Steinke, S., Lückge, A., Groeneveld, J., Hathorne, E.C., 2010. Glacial to Holocene surface hydrography of the tropical eastern Indian Ocean. Earth and Planetary Science Letters 292, 89–97. https://doi.org/10.1016/j.epsl.2010.01.024

Morley, R.J., 2013. Cenozoic ecological history of South East Asian peat mires based on the comparison of coals with present day and Late Quaternary peats. Journal of Limnology 72, e3.

Osaki, M., Tsuji, N., 2016. Tropical peatland ecosystems. Springer.

Page, S., Hoscilo, A., Langner, A., Tansey, K., Siegert, F., Suwido, L., Rieley, J., 2010. Tropical peatland fires in Southeast Asia, in: Cochrane, M.A. (Ed.), Tropical Fire Ecology: Climate Change, Land Use and Ecosystem Dynamics. Springer Science & Business Media, pp. 263–287.

Page, S.E., Hooijer, A., 2016. In the line of fire: the peatlands of Southeast Asia. Philosophical Transactions of the Royal Society B: Biological Sciences 371, 20150176. https://doi.org/10.1098/rstb.2015.0176

Page, S.E., Rieley, J.O., Banks, C.J., 2011. Global and regional importance of the tropical peatland carbon pool. Global Change Biology 17, 798–818. https://doi.org/10.1111/j.1365-2486.2010.02279.x

Page, S.E., Siegert, F., Rieley, J.O., Boehm, H.-D.V., Jaya, A., Limin, S., 2002. The amount of carbon released from peat and forest fires in Indonesia during 1997. Nature 420, 61–65. https://doi.org/10.1038/nature01131

Page, S.E., Wűst, R. a. J., Weiss, D., Rieley, J.O., Shotyk, W., Limin, S.H., 2004. A record of Late Pleistocene and Holocene carbon accumulation and climate change from an equatorial peat bog (Kalimantan, Indonesia): implications for past, present and future carbon dynamics. J. Quaternary Sci. 19, 625–635. https://doi.org/10.1002/jqs.884

Partin, J.W., Cobb, K.M., Adkins, J.F., Clark, B., Fernandez, D.P., 2007. Millennial-scale trends in west Pacific warm pool hydrology since the Last Glacial Maximum. Nature 449, 452–455. https://doi.org/10.1038/nature06164

Posa, M.R.C., Wijedasa, L.S., Corlett, R.T., 2011. Biodiversity and Conservation of Tropical Peat Swamp Forests. BioScience 61, 49–57. https://doi.org/10.1525/bio.2011.61.1.10

Prasojo, Z.H., 2017. Religious and Cultural Existences Within the Communities of Upper Kapuas Riverside of West Kalimantan. al-albab 6, 197. https://doi.org/10.24260/alalbab.v6i2.931

Pyatt, F.B., Wilson, B., Barker, G.W., 2005. The chemistry of tree resins and ancient rock paintings in the Niah Caves, Sarawak (Borneo): some evidence of rain forest management by early human populations. Journal of Archaeological Science 32, 897–901. https://doi.org/10.1016/j.jas.2005.01.010

Ramdzan, K.N.M., Moss, P.T., Heijnis, H., Harrison, M.E., Yulianti, N., 2022. Application of palaeoecological and geochemical proxies in the context of tropical peatland degradation and restoration: A review for Southeast Asia. Wetlands 42, 95. https://doi.org/10.1007/s13157-022-01618-7

Reynolds, T., Barker, G., 2014. Reconstructing Late Pleistocene climates, landscapes, and human activities in northern Borneo from excavations in the Niah Caves.

Ribeiro, K., Pacheco, F.S., Ferreira, J.W., Sousa-Neto, E.R., Hastie, A., Krieger Filho, G.C., Alvalá, P.C., Forti, M.C., Ometto, J.P., 2021. Tropical peatlands and their contribution to the global carbon cycle and climate change. Glob. Change Biol. 27, 489–505. https://doi.org/10.1111/gcb.15408

Ritung, S., Wahyunto, W., Nugroho, K., Sukarman, S., Hikmatullah, H., Suparto, S., Tafakrenanto, C., 2011. Peta Lahan Gambut Indonesia Skala 1:250.000, December 2. ed. Balai Besar Penelitian dan Pengembangan Sumberdaya Lahan Pertanian, Badan Penelitian dan Pengembangan Pertanian, Bogor.

Rodysill, J.R., Russell, J.M., Crausbay, S.D., Bijaksana, S., Vuille, M., Edwards, R.L., Cheng, H., 2013. A severe drought during the last millennium in East Java, Indonesia. Quaternary Science Reviews 80, 102–111. https://doi.org/10.1016/j.quascirev.2013.09.005

RSS GmbH, 2018. Kapuas Hulu peat remapping final report: Mapping peat extent and depth of 16 Peat Hydrological Units within the Kapuas Hulu Basin (No. 12.2216.0–001.00). Remote Sensing Solution GmbH, FORCLIME.

Ruddiman, W.F., 2003. The Anthropogenic Greenhouse Era Began Thousands of Years Ago. Climatic Change 61, 261–293. https://doi.org/10.1023/B:CLIM.0000004577.17928.fa

Ruwaimana, M., Anshari, G.Z., Silva, L.C.R., Gavin, D.G., 2020. The oldest extant tropical peatland in the world: a major carbon reservoir for at least 47,000 years. Environ. Res. Lett. https://doi.org/10.1088/1748-9326/abb853

Septiyani, D., 2014. Para transmigran di Desa Rasau Jaya I Kabupaten Kubu Raya Kalimantan Barat Tahun 1971-1979. Journal of Indonesian History 3.

Sirrullah, S. bin S., 2019. Sejarah Kesultanan Kadriah Pontianak 1778-2017 M. UIN Sunan Ampel Surabaya.

Smith, F.A., Smith, H.F., 2011. A shadowy state in Borneo: where was Tanjungpura? Borneo Research Bulletin 42, 89–103.

Spiker, E.C., Hatcher, P.G., 1984. Carbon isotope fractionation of sapropelic organic matter during early diagenesis. Organic Geochemistry 5, 283–290. https://doi.org/10.1016/0146-6380(84)90016-0

Suprianto, B., Prasojo, Z.H., Witro, D., 2021. The History of Islamic Kingdoms in Kapuas Hulu District: A Manuscript Translation of Pangeran Kesoema Anom Soeria Negara. Heritage of Nusantara: International Journal of Religious Literature and Heritage 10, 274–309.

Treat, C.C., Kleinen, T., Broothaerts, N., Dalton, A.S., Dommain, R., Douglas, T.A., Drexler, J.Z., Finkelstein, S.A., Grosse, G., Hope, G., 2019. Widespread global peatland establishment and persistence over the last 130,000 y. Proceedings of the National Academy of Sciences 116, 4822–4827.

Tuinenburg, O.A., Theeuwen, J.J.E., Staal, A., 2020. High-resolution global atmospheric moisture connections from evaporation to precipitation. Earth System Science Data 12, 3177–3188. https://doi.org/10.5194/essd-12-3177-2020

Turetsky, M., Wieder, K., Halsey, L., Vitt, D., 2002. Current disturbance and the diminishing peatland carbon sink. Geophysical Research Letters 29, 21-1-21–4. https://doi.org/10.1029/2001GL014000

Usup, A., Hashimoto, Y., Takahashi, H., HAYASAKA, H., 2004. Combustion and thermal characteristics of peat fire in tropical peatland in Central Kalimantan, Indonesia. Tropics 14, 1–19.

Wen, X., Liu, Z., Wang, S., Cheng, J., Zhu, J., 2016. Correlation and anti-correlation of the East Asian summer and winter monsoons during the last 21,000 years. Nat Commun 7, 11999. https://doi.org/10.1038/ncomms11999

Wüst, R.A., Jacobsen, G.E., von der Gaast, H., Smith, A.M., 2008. Comparison of radiocarbon ages from different organic fractions in tropical peat cores: insights from Kalimantan, Indonesia. Radiocarbon 50, 359–372.

Yew, C.-W., Lu, D., Deng, L., Wong, L.-P., Ong, R.T.-H., Lu, Y., Wang, X., Yunus, Y., Aghakhanian, F., Mokhtar, S.S., Hoque, M.Z., Voo, C.L.-Y., Abdul Rahman, T., Bhak, J., Phipps, M.E., Xu, S., Teo, Y.-Y., Kumar, S.V., Hoh, B.-P., 2018. Genomic structure of the native inhabitants of Peninsular Malaysia and North Borneo suggests complex human population history in Southeast Asia. Hum Genet 137, 161–173. https://doi.org/10.1007/s00439-018-1869-0

Young, D.M., Baird, A.J., Gallego-Sala, A.V., Loisel, J., 2021. A cautionary tale about using the apparent carbon accumulation rate (aCAR) obtained from peat cores. Sci Rep 11, 9547. https://doi.org/10.1038/s41598-021-88766-8

Yu, Z., Loisel, J., Brosseau, D.P., Beilman, D.W., Hunt, S.J., 2010. Global peatland dynamics since the Last Glacial Maximum. Geophysical Research Letters 37.

Yu, Z.C., 2012. Northern peatland carbon stocks and dynamics: a review. Biogeosciences 9, 4071–4085. https://doi.org/10.5194/bg-9-4071-2012

Yulianto, E., Rahardjo, A.T., Noeradi, D., Siregar, D.A., Hirakawa, K., 2005. A Holocene pollen record of vegetation and coastal environmental changes in the coastal swamp forest at Batulicin, South Kalimantan, Indonesia. Journal of Asian Earth Sciences 25, 1–8.

Zheng, Z., Ma, T., Roberts, P., Li, Z., Yue, Y., Peng, H., Huang, K., Han, Z., Wan, Q., Zhang, Y., Zhang, X., Zheng, Y., Saito, Y., 2021. Anthropogenic impacts on Late Holocene land-cover change and floristic biodiversity loss in tropical southeastern Asia. Proceedings of the National Academy of Sciences 118, e2022210118. https://doi.org/10.1073/pnas.2022210118

IV. POLLEN AND SPORES RECORDED IN A LATE PLEISTOCENE-HOLOCENE INLAND TROPICAL PEAT DEPOSIT IN WEST KALIMANTAN, INDONESIA

In preparation (Style of *Quaternary International*)

Co-authored material (with Daniel G. Gavin, Gusti Z. Anshari, K. Anggi Hapsari and Rebecca J. Hamilton). The experimental work was performed by me. The paper was written entirely by me, with DGG, GZA and KAH providing editorial assistance. KAH and RJH contributed to pollen and spore identification.

Introduction

Tropical peatland is a type of wetland ecosystem where accumulating organic material is stabilized by a combination of water saturation, low oxygen levels, and a change in chemical properties (Osaki and Tsuji, 2016; Hodgkins et al., 2018). This organic material deposit traps carbon and stores various valuable paleoecology and paleoclimate proxies within its layers, such as pollen, charcoal, testate amoeba, metals, and various stable isotopes (Blackford, 2000; Bindler, 2006). One of the important biological proxies that is archived in the peat core is pollen and spores (Chambers and Charman, 2004). A relatively large number of pollen and spore studies have been conducted in northern temperate peat compared to the tropical peat. For example, of the 411 peat and wetland stratigraphy studies are registered in the Neotoma Paleoecology Database (Williams et al., 2018), 336 are located at mid- to high-latitudes, while only 64 are located in tropical and subtropical regions. Of these 64 studies, no peat stratigraphic study in Indonesia is yet entered into the Neotoma database, although there are several peat pollen stratigraphy studies in Indonesia that are not registered there (Anshari, Kershaw and van der Kaars, 2001; Anshari et al., 2004; Yulianto et al., 2005; Biagioni et al., 2015; Hapsari et al., 2017, 2018).

Moreover, tropical peatland also has a higher plant biodiversity than its temperate counterpart, but there are only a few studies that focus on cataloging the tropical peatland pollen flora in Southeast Asia. Two of these studies are pioneering studies that were conducted in the early 20th century (Polak, 1933, 1949), and the most recent study was conducted almost a half century ago (Anderson and Muller, 1975). Due to limited reference material for pollen identification, not only specifically for tropical peat pollen, but also for any palynoflora in

Indonesia (Poliakova and Behling, 2016), a notable percentage of pollen and spores in stratigraphic studies of peatland remain unidentified or only identified to family level. For example, a study by Biagioni et al. (2015) resulted in 242 pollen and spore types, of which 87 specimens were unidentified. A study by Cole et al., (2015) resulted in 179 types; 10 types were unidentified, and of the identified ones 30% of the taxa were identified to family and 70% identified to genus level. Studies by Anshari et al. (2001, 2004) resulted in 123 pollen and spore types, of which approximately 10% were identified to species level, 65% to genus level, and 25% to family level. A study by Hapsari et al. (2017, 2018) identified 63 pollen and spore types, of which 60% identified to genus level and 40% were identified to family level. A study by Yulianto et al. (2005) resulted in 77 pollen and spore types, of which 11 were unidentified, while most identified taxa were mostly at the genus and family level. While some member of the same plant family or genus might occupy a similar niche and provide similar ecological function, some have wide ranges of habitat, distribution, trait, and even life form (e.g., Myrtaceae, Fabaceae, Melastomataceae) (Lemmens et al., 1995, Soerianegara et al., 1993 and Sosef et al., 1998). For example, member of the common peat-swamp forest family, Dipterocarpaceae, could also grow on coastal (e.g., *Shorea parvistipulata*, *S. splendida*), riparian (e.g., *Vatica rassak*, *S. macrophylla*), or hill forest (e.g., *Anisoptera thurifera*, *Dipterocarpus grandiflorus*, *Hopea celebica*) (Hamilton et al., 2019). Thus, it remains important to achieve more detailed pollen and spore grain identification.

Photographic documentation of encountered fossil pollen and spore grains is rarely done. Out of the studies listed above, only one peat stratigraphy study by Cole et al. (2015) provided in their supplementary material photographs of the most common pollen taxa, though the images are only from one angle thus it is difficult to do the identification based on these images. A study by Poliakova and Behling (2016) does provide documentation of fossil pollen grains, however, this study is not focused on peatland, and the detail on grain descriptions are not given. With this current situation, a palynologist studying peat pollen must look through multiple references, thus increasing the difficulty of identification and, likely, increasing the number of unidentified but ecologically important pollen and spores.

Thus, we conducted this study to catalog fossil pollen and spores from a 30,000 year- old peat core. Moreover, as this core has experienced various climates from the Last Glacial Maximum to the warm modern Holocene, this core possibly contains a wider range of plant

types as the composition of the plant community changes following climate changes. We also provide a morphological description such as aperture morphology, exine sculpturing, and size measurements. Pollen stratigraphic studies are starting to be more common in Southeast Asia, and thus future studies that focus on peatland will benefit from the peat fossil pollen and spore catalogue presented here.

Regional Setting

This study focuses on peatland in Putussibau Regence, West Kalimantan, Indonesia. Peatland in this region has been accumulating for at least 50,000 years with maximum thickness of approximately 15–18 m, making it the oldest and deepest extant peatland in the world (Ruwaimana et al., 2020). This peatland is located on interfluves approximately 450 km upstream from the outlet of the Kapuas River, the longest river in Indonesia. Compared to most of the coastal peat in Indonesia that only accumulated since approximately 7500 years before present, after sea level stabilized (Dommain, Couwenberg and Joosten, 2011), the Putussibau peatland, currently located 30 m above the sea level, thus was not affected directly by past changes of sea level. The peat is predicted to accumulate even during the Last Glacial Maximum. Despite some peat loss due to prehistoric and modern fire events, this peatland still has the potential to provide stratigraphic records that encompass the time before the Last Glacial Maximum until now.

Generally, on Kalimantan Island the five most abundant families are Dipterocarpaceae, Euphorbiaceae, Myrtaceae, Sapotaceae and Lauraceae and five most abundant genera are Shorea, Syzygium, Diospyros, Madhuca and Dipterocarpus (Slik et al., 2003). However, the plant composition in peatland is different due to its unique high organic and low nutrient soil. In Kalampangan peat in Central Kalimantan, the dominant species are *Combretocarpus rotundatus* (Anisophylleaceae), *Palaquium cochlorifolium* (Sapotaceae), *Callophyllum canum* (Callophyllaceae), *Ctenolophon parvifolius* (Ctenolophonaceae), and *Cratoxylum glaucum* (Hypericaceae) (Osaki and Tsuji, 2016; Tuah et al., 2003). Meanwhile, other peatland in Central Kalimantan, Sebangau Peat is dominated by *Palaquium* spp, comp. (Sapotaceae), *Syzygium densinervium* (Myrtaceae), *Xanthophyllum palembanicum* (Polygalaceae), *Hydnocarpus* sp. (Achariaceae) and *Shorea guiso* (Dipterocarpaceae) (Simbolon and Mirmanto, 2000; Yulianto et al., 2005;). Specifically, on our site, Putussibau, there is no formal report of peatland vegetation

list yet. However, the closest vegetation record around Putussibau is from Danau Sentarum. This site is located approximately 30km downstream from Putussibau, thus we could infer that their vegetation is similar. Tree inventory on Danau Sentarum resulting on 31 families, including Dipterocarpaceae, Myristicaceae, Burseraceae, Clusiaceae, Fabaceae, Euphorbiaceae, Elaeocarpaceae, Anacardiaceae, Sapotaceae, Annonaceae, Sapindaceae, Myrtaceae, and Meliaceae, (Anshari et al., 2012). Some species that has the highest importance value on transects are *Dryobalanops* sp. (Dipterocarpaceae), *Elaeocarpus palembanicus* (Elaeocarpaceae), *Santiria oblongifolia* (Burseraceae), *Palaquium* sp. (Sapotaceae), *Shorea* sp. (Dipterocarpaceae), *Sindora bruggemanii* (Fabaceae), *Garcinia* sp. (Clusiaceae) and *Gluta* sp (Anacardiaceae). As this area is affected by fire, after fire the most prominent pioneer species are *Croton cf. ensifolius* (Euphorbiaceae), *Ixora mentangis* (Rubiaceae), *Timonius salicifolius* (Rubiaceae), and the herbs *Polygonum spp*. (Polygonaceae) (Dennis et al., 2000)

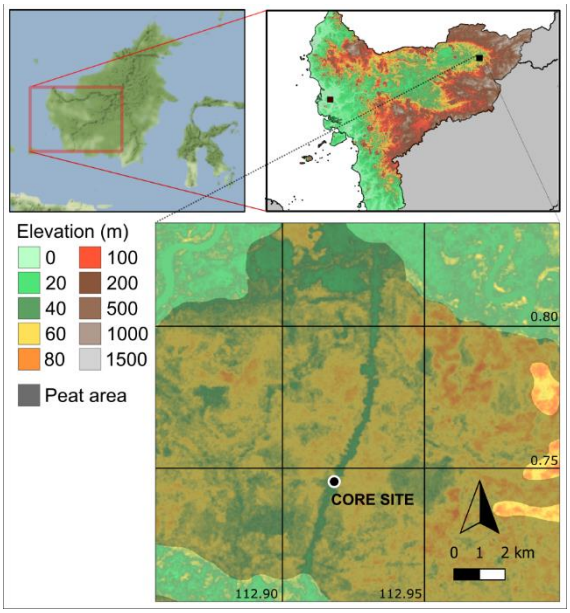

Figure 4.1. Map of peat core sampling location. Note that the elevation data in this map reflects canopy height, and thus reveals the road corridor along which core was obtained.

Material and Method

We collected peat cores (0.780N; 112.925E, Fig 4.1) using a 55 mm diameter Russian peat corer to obtain samples down to the mineral layer. We extract 1 cm^2 sample every 25 cm, with a standard protocol by (Faegri et al., 1989). We sieved the samples at 150 µm to remove the

larger fraction. Sample was then treated following the protocol by Chambers and van Geel, (2011) with some modification, where we did 5–10 times warm 10% KOH rinses to remove the peat material and excluded the HF treatment due to the low inorganic material content. Pollen and spores were photographed using 100 x 10 magnification under immersion oil with a Zeiss Binocular Microscope and AmScope digital camera. For each sample, around 100-150 pollen and spore grains are photographed; each grain is photographed twice with different angle, mostly from polar side and from equatorial side. Pollen preservation was good at all depths. The base of the core is dated to 30,230 years cal BP (calibrated with IntCal20)

We made pollen and spore identification using photographs from previous studies and online resources. We use online database Australia Pollen and Spore Atlas (APSA) and selected taxa found in Maritime Southeast Asia region (Haberle, 2018). We also utilized published pollen atlas paper from northern Borneo that covers peatland and all other types of ecosystems (Anderson and Muller, 1975; Jones, 2012). We also compare our pollen with pollen and spores from marine sediments atlas as one of their sediment sources is peatlands in Central Kalimantan (Poliakova and Behling, 2016). One of the most common families in Kalimantan is Dipterocarpaceae; we use this family's pollen identification guide from Hamilton et al. (2019). We also use an unpublished pollen and spore photo collection from the late Prof. Edward J. Cushing, which contain approximately 3,000 sample from Indonesia, which about 300 are from Kalimantan. Due to the limitation of image resolution, we described the pollen and spore grains on their aperture morphology, exine sculpturing, and size measurements (Punt et al., 2007; Grant-Downton, 2009).

Most of the pollen measurements are the equatorial and polar diameters (Faegri, 1989). Some exceptions are pollen and spores with a triangular shape (e.g., trilete) and or those with an almost perfectly spherical shape, without a clear polar or equatorial distinction, are described by their largest diameter. Their maximum, median and minimum dimensions are based on the largest diameter of several specimens. Monolete pollen and spores are described based on their length and width (Barrington, 2020).

Result and Discussion

In total, 286 morphotypes were identified from 6435 sample photographs. 260 morphotypes are pollen and 26 are spores. Currently, 170 types (59%) are identified to family level,86 types

(30%) to genus level, and none to species level. These identification results are tentative as we are still waiting for identification from our collaborators. The smallest grains are Myrtaceae pollen (4 µm, Plate 9.18) and the largest grains are monolete spores (75 µm length, Plate 1.1). All the pollen and spore identifications, morphological descriptions, and measurements are listed in Table 1. The morphotypes are presented in 18 photographic plates in scale with each other, grouped by aperture morphology and exine sculpturing.

Table 4.1. List of pollen morphotype and its identification.

Plate ID	Family	Genus	Morphological Description	Size
Plate 1.1	Indet	Indet	Monolete, Reticulate	Length 75µm, Width 40µm
Plate 1.2	Indet	Indet	Monolete, Psilate	Length 41–57µm, Width 28–29µm
Plate 1.3	Indet	Indet	Monolete, Psilate	Length 57–63µm, Width 32–36µm
Plate 1.4	Indet	Indet	Monolete, Psilate	Length 40–45µm, Width 25–27µm
Plate 1.5	Indet	Indet	Monolete, Granulate	Length 39–43µm, Width 23–24µm
Plate 1.6	Indet	Indet	Monolete, Psilate	Length 37–29µm, Width 17–20µm
Plate 1.7	Indet	Indet	Monolete, Psilate	Length 42–43µm, Width 20–22µm
Plate 1.8	Indet	Indet	Monolete, Psilate	Length 31–32µm, Width 18–19µm
Plate 1.9	Indet	Indet	Monolete, Psilate	Length 32–35µm, Width 22–25µm
Plate 1.10	Davalliaceae	*Davzlia* sp.	Monolete, Verrucate	Length 50–54µm, Width 34–38 µm
Plate 1.11	Indet	Indet	Monolete, Psilate	Length 15–16µm, Width 28–29µm
Plate 1.12	Indet	Indet	Monolete, Verrucate	Length 40–41µm, Width 26–28µm
Plate 1.13	Indet	Indet	Monolete, Reticulate	Length 33µm, Width 18µm
Plate 1.14	Indet	Indet	Monolete, Verrucate	Length 44µm, Width 35µm
Plate 1.15	Indet	Indet	Monolete, Fimbriate	Length 33µm, Width 23µm
Plate 1.16	Indet	Indet	Monolete, Verrucate	Length 37µm, Width 22µm
Plate 1.17	Indet	Indet	Monolete, Verrucate	Length 29µm, Width 20–21µm
Plate 2.1	Cyatheaceae	*Cyathea* sp.	Trilete, Psilate	Min 32µm, Med 35µm, Max 37µm
Plate 2.2	Cyatheaceae	*Cyathea* sp.	Trilete, Psilate	Min 29µm, Med 30µm, Max 34µm
Plate 2.3	Indet	Indet	Trilete, Psilate	Min 24µm, Med 26µm, Max 31µm
Plate 2.4	Lycopodiaceae	*Lycopodiella* sp.	Trilete, Reticulated	Min 24µm, Med 25µm, Max 27µm
Plate 2.5	Podocarpaceae	*Dacrydium* sp.	Saccate, Rugulate	Min 58µm, Med 58µm, Max 58µm
Plate 2.6	Cyatheaceae	*Cyathea* sp.	Trilete, Granulate	Min 31µm, Med 34µm, Max 37µm
Plate 2.7	Cyatheaceae	*Cyathea* sp.	Trilete, Psilate	Min 29µm, Med 31µm, Max 33µm
Plate 2.8	Indet	Indet	Trilete, Psilate	Min 21µm, Med 22µm, Max 22µm
Plate 2.9	Mimosaceae	Indet	Trilete, Granulate	Min 18µm, Med 18µm, Max 28µm
Plate 2.10	Indet	Indet	Trilete, Psilate	Min 23µm, Med 25µm, Max 26µm
Plate 2.11	Ericaceae	*Piptadenia* or *Rhododendron*	Tetrad, Psilate	Min 26µm, Med 31µm, Max 32µm
Plate 2.12	Ericaceae	Indet	Tetrad, Granulate	Min 31µm, Med 34µm, Max 36µm
Plate 2.13	Ericaceae	Indet	Tetrad, Psilate	Min 25µm, Med 29µm, Max 30µm
Plate 2.14	Ericaceae	Indet	Tetrad, Psilate	Min 21µm, Med 25µm, Max 27µm
Plate 2.15	Ericaceae	Indet	Tetrad, Psilate	Min 23µm, Med 25µm, Max 28µm
Plate 3.1	Malvaceae	Indet	Echinate	Min 34µm, Med 36µm, Max 37µm
Plate 3.2	Malvaceae	Indet	Echinate	Min 27µm, Med 33µm, Max 35µm
Plate 3.3	Malvaceae	Indet	Echinate	Min 28µm, Med 30µm, Max 31 µm
Plate 3.4	Malvaceae	Indet	Echinate	Min 23µm, Med 25µm, Max 27µm
Plate 3.5	Malvaceae	Indet	Echinate	Min 22µm, Med 23µm, Max 24µm
Plate 3.6	Malvaceae	Indet	Echinate	Min 19µm, Med 25µm, Max 26µm
Plate 3.7	Indet	Indet	Echinate	Min 25µm, Med 27µm, Max 29µm
Plate 3.8	Indet	Indet	Echinate	Min 17µm, Med 19µm, Max 20µm
Plate 3.9	Indet	Indet	Echinate	Min 21µm, Med 22µm, Max 24µm
Plate 3.10	Malvaceae	Indet	Echinate	Min 18µm, Med 20µm, Max 22µm
Plate 3.11	Malvaceae	Indet	Echinate	Min 19µm, Med 20µm, Max 22µm
Plate 3.12	Indet	Indet	Echinate	Min 20µm, Med 21µm, Max 23µm
Plate 3.13	Indet	Indet	Echinate	Min 19µm, Med 22µm, Max 23µm
Plate 3.14	Indet	Indet	Echinate	Min 6µm, Med 7µm, Max 7µm
Plate 3.15	Arecaceae	*Arenga* sp.	Monoporate, Echinate	Length 18µm, Width 13µm
Plate 3.16	Pandanaceae	*Pandanus* sp.	Monoporate, Echinate	Length16–17µm, Width 11–13µm

Plate 3.17	Pandanaceae	*Pandanus* sp.	Monoporate, Echinate	Length 14–15µm, Width 10–11µm
Plate 4.1	Zygnemataceae	*Concentricystes* sp.	Inaperturate Striate	Min 44µm, Med 45µm, Max 46µm
Plate 4.2	Zygnemataceae	*Concentricystes* sp.	Inaperturate Striate	Min 40µm, Med 43µm, Max 44µm
Plate 4.3	Zygnemataceae	*Concentricystes* sp.	Striate	Min 35µm, Med 36µm, Max 38µm
Plate 4.4	Zygnemataceae	*Concentricystes* sp.	Striate	Min 40µm, Med 41µm, Max 42µm
Plate 4.5	Zygnemataceae	*Concentricystes* sp.	Striate	Min 29µm, Med 30µm, Max 32µm
Plate 4.6	Poaceae	Indet	Monoporate, Granulate	Min 14µm, Med 15µm, Max 16µm
Plate 4.7	Poaceae	Indet	Monoporate, Psilate	Min 13µm, Med 14µm, Max 14µm
Plate 4.8	Poaceae	Indet	Monoporate, Psilate	Min 14µm, Med 15µm, Max 16µm
Plate 4.9	Poaceae	Indet	Monoporate, Granulate	Min 23µm, Med 24µm, Max 25µm
Plate 4.10	Poaceae	Indet	Monoporate, Psilate	Min 12µm, Med 13µm, Max 15µm
Plate 4.11	Poaceae	Indet	Monoporate, Psilate	Min 13µm, Med 13µm, Max 14µm
Plate 4.12	Poaceae	Indet	Monoporate, Psilate	Min 11µm, Med 12µm, Max 13µm
Plate 4.13	Poaceae	Indet	Monoporate, Psilate	Min 15µm, Med 17µm, Max 18µm
Plate 4.14	Poaceae	Indet	Monoporate, Granulate	Min 28µm, Med 28µm, Max 29µm
Plate 4.15	Poaceae	Indet	Monoporate, Psilate	Min 8µm, Med 9µm, Max 10µm
Plate 4.16	Poaceae	Indet	Monoporate, Psilate	Min 8µm, Med 8µm, Max 8µm
Plate 4.17	Poaceae	Indet	Monoporate, Psilate	Min 8µm, Med 9µm, Max 10µm
Plate 4.18	Pandanaceae	*Freycinetia* sp.	Monoporate, Psilate	Length 9–12µm, Width 4–5µm
Plate 4.19	Pandanaceae	*Freycinetia* sp.	Monoporate, Psilate	Length 12–14µm, Width 9–10µm
Plate 4.20	Pandanaceae	*Freycinetia* sp.	Monoporate, Psilate	Length17–19 µm, Width 8–10µm
Plate 4.21	Pandanaceae	*Freycinetia* sp.	Monoporate, Psilate	Length 12–13µm, Width 7–8µm
Plate 5.1	Indet	Indet	Scabrate	Min 43µm, Med 45µm, Max 47µm
Plate 5.2	Indet	Indet	Scabrate	Min 26µm, Med 27µm, Max 27µm
Plate 5.3	Polygonaceae	*Polygonum* sp.	Scabrate	Min 29µm, Med 33µm, Max 34µm
Plate 5.4	Indet	Indet	Papillate	Min 29µm, Med 30µm, Max 32µm
Plate 5.5	Indet	Indet	Scabrate	Min 23µm, Med 27µm, Max29 µm
Plate 5.6	Indet	Indet	Papillate	Min 22µm, Med 25µm, Max 27µm
Plate 5.7	Indet	Indet	Papillate	Min 23µm, Med 26µm, Max 28µm
Plate 5.8	Indet	Indet	Scabrate	Min 20µm, Med 22µm, Max 25µm
Plate 5.9	Indet	Indet	Scabrate	Min 18µm, Med 20µm, Max 21µm
Plate 5.10	Indet	Indet	Papillate	Min 21µm, Med 24µm, Max 26µm
Plate 5.11	Indet	Indet	Papillate	Min 17µm, Med 19µm, Max 20µm
Plate 5.12	Indet	Indet	Papillate	Min 12µm, Med 13µm, Max 14µm
Plate 5.13	Indet	Indet	Scabrate	Min 22µm, Med 23µm, Max 24µm
Plate 5.14	Indet	Indet	Papillate	Min 19µm, Med 20µm, Max 21µm
Plate 5.15	Indet	Indet	Papillate	Min 18µm, Med 18µm, Max 19µm
Plate 5.16	Arecaceae	Indet	Granulated	Min 18µm, Med 20µm, Max 21 µm
Plate 5.17	Indet	Indet	Scabrate	Min 11µm, Med 12µm, Max 13µm
Plate 6.1	Rubiaceae	Indet	Triporate, Granulate	Min 26µm, Med 27µm, Max 29µm
Plate 6.2	Rubiaceae	Indet	Triporate, Granulate	Min 25µm, Med 26µm, Max 26µm
Plate 6.3	Rubiaceae	Indet	Triporate, Granulate	Min 24µm, Med 24µm, Max 25 µm
Plate 6.4	Rubiaceae	Indet	Triporate, Scabrate	Min 25µm, Med 25µm, Max 25µm
Plate 6.5	Indet	Indet	Triporate, Psilate	Min 21µm, Med 21µm, Max 22µm
Plate 6.6	Indet	Indet	Triporate, Psilate	Min 20µm, Med 20µm, Max 21µm
Plate 6.7	Rubiaceae	Indet	Triporate, Granulate	Min 33µm, Med 33µm, Max 33µm
Plate 6.8	Indet	Indet	Triporate, Psilate	Min 25µm, Med 27µm, Max 37µm
Plate 6.9	Stemonuraceae	*Stemonurus* sp.	Triporate, Psilate	Min 24µm, Med 25µm, Max 26µm
Plate 6.10	Indet	Indet	Triporate, Granulate	Min 26µm, Med 26µm, Max 26µm
Plate 6.11	Stemonuraceae	*Stemonurus* sp.	Triporate, Psilate	Min 20µm, Med 20µm, Max 21µm
Plate 6.12	Stemonuraceae	*Stemonurus* sp.	Triporate, Psilate	Min 21µm, Med 22µm, Max 25µm
Plate 7.1	Indet	Indet	5-porate, Granulate	Min 34µm, Med 34µm, Max 34µm
Plate 7.2	Indet	Indet	5-porate, Psilate	Min 18µm, Med 18µm, Max 18µm
Plate 7.3	Indet	Indet	5-porate, Granulate	Min 21µm, Med 21µm, Max 21µm
Plate 7.4	Indet	Indet	4-porate, Granulate	Min 29µm, Med 29µm, Max 30µm
Plate 7.5	Indet	Indet	Triporate, Granulate	Min 21µm, Med 22µm, Max 24µm
Plate 7.6	Indet	Indet	Triporate, Granulate	Min 23µm, Med 24µm, Max 24µm
Plate 7.7	Indet	Indet	4-porate, Granulate	Min 26µm, Med 27µm, Max 29µm
Plate 7.8	Indet	Indet	Triporate, Granulate	Min 19µm, Med 20µm, Max 20µm
Plate 7.9	Indet	Indet	4-porate, Psilate	Min 20µm, Med 21µm, Max 22µm
Plate 7.10	Indet	Indet	4-porate, Psilate	Min 20µm, Med 20µm, Max 21µm
Plate 7.11	Indet	Indet	Triporate, Psilate	Min 18µm, Med 20µm, Max 20µm
Plate 7.12	Indet	Indet	Triporate, Psilate	Min 15µm, Med 17µm, Max 18µm
Plate 7.13	Indet	Indet	4-porate, Psilate	Min 18µm, Med 19µm, Max 22µm
Plate 8.1	Indet	Indet	Triporate, Scabrate	Min 18µm, Med 19µm, Max 20µm
Plate 8.2	Indet	Indet	Triporate, Scabrate	Min 18µm, Med 19µm, Max 18µm

Plate 8.3	Indet	Indet	4-porate, Granulate	Min 20µm, Med 20µm, Max 21µm
Plate 8.4	Indet	Indet	4-porate, Psilate	Min 15µm, Med 16µm, Max 17µm
Plate 8.5	Indet	Indet	Triporate, Granulate	Min 17µm, Med 17µm, Max 18µm
Plate 8.6	Indet	Indet	Triporate, Psilate	Min 15µm, Med 15µm, Max 16µm
Plate 8.7	Indet	Indet	Triporate, Psilate	Min 14µm, Med 15µm, Max 15µm
Plate 8.8	Indet	Indet	Triporate, Granulate	Min 17µm, Med 17µm, Max 17µm
Plate 8.9	Indet	Indet	Triporate, Granulate	Min 15µm, Med 16µm, Max 17µm
Plate 8.10	Indet	Indet	Triporate, Psilate	Min 14µm, Med 15µm, Max 15 µm
Plate 8.11	Indet	Indet	Triporate, Granulate	Min 14µm, Med 15µm, Max 15µm
Plate 8.12	Indet	Indet	Triporate, 4-porate, Psilate	Min 14µm, Med 14µm, Max 15µm
Plate 8.13	Moraceae	Indet	Triporate, Psilate	Min 13µm, Med 14µm, Max 15µm
Plate 8.14	Moraceae	Indet	Triporate, Psilate	Min 11µm, Med 12µm, Max 12µm
Plate 8.15	Moraceae	Indet	Triporate, Psilate	Min 10µm, Med 11µm, Max 11µm
Plate 8.16	Indet	Indet	Triporate, Psilate	Min 14µm, Med 14µm, Max 15µm
Plate 8.17	Indet	Indet	Triporate, Psilate	Min 15µm, Med 16µm, Max 18µm
Plate 8.18	Stemonuraceae	Indet	Triporate, Psilate	Min 20µm, Med 20µm, Max 20µm
Plate 8.19	Indet	Indet	Triporate, Psilate	Min 14µm, Med 14µm, Max 14µm
Plate 9.1	Myrtaceae	*Syzigium* sp.	Parasyncolpate, Syncolpate, Triporate	Min 17µm, Med 17µm, Max 17µm
Plate 9.2	Myrtaceae	*Syzigium* sp.	Parasyncolpate, Syncolpate, Triporate	Min 13µm, Med 14µm, Max 14µm
Plate 9.3	Myrtaceae	*Syzigium* sp.	Parasyncolpate, Syncolpate, Triporate	Min 12µm, Med 12µm, Max 13µm
Plate 9.4	Myrtaceae	*Syzigium* sp.	Parasyncolpate, Syncolpate, Triporate	Min 9µm, Med 10µm, Max 11µm
Plate 9.5	Myrtaceae	*Syzigium* sp.	Parasyncolpate, Syncolpate, Triporate	Min 9µm, Med 10µm, Max 11µm
Plate 9.6	Indet	Indet	Triporate	Min 11µm, Med 12µm, Max 13µm
Plate 9.7	Myrtaceae	*Syzigium* sp.	Parasyncolpate, Syncolpate, Triporate	Min 10µm, Med 11µm, Max 12µm
Plate 9.8	Myrtaceae	*Syzigium* sp.	Parasyncolpate, Syncolpate, Triporate	Min 9µm, Med 10µm, Max 10µm
Plate 9.9	Myrtaceae	*Syzigium* sp.	Parasyncolpate, Syncolpate, Triporate	Min 9µm, Med 9µm, Max 10µm
Plate 9.10	Indet	Indet	Triporate	Min 10µm, Med 11µm, Max 11µm
Plate 9.11	Myrtaceae	*Syzigium* sp.	Parasyncolpate, Syncolpate, Triporate	Min 9µm, Med 10µm, Max 10µm
Plate 9.12	Myrtaceae	*Syzigium* sp.	Parasyncolpate, Syncolpate, Triporate	Min 8µm, Med 9µm, Max 9µm
Plate 9.13	Myrtaceae	*Syzigium* sp.	Parasyncolpate, Syncolpate, Triporate	Min 7µm, Med 8µm, Max 9µm
Plate 9.14	Indet	Indet	Triporate	Min 9µm, Med 10µm, Max 10µm
Plate 9.15	Myrtaceae	*Syzigium* sp.	Parasyncolpate, Syncolpate, Triporate	Min 7µm, Med 7µm, Max 8µm
Plate 9.16	Myrtaceae	*Syzigium* sp.	Parasyncolpate, Syncolpate, Triporate	Min 6µm, Med 7µm, Max 7µm
Plate 9.17	Myrtaceae	*Syzigium* sp.	Parasyncolpate, Syncolpate, Triporate	Min 6µm, Med 6µm, Max 7µm
Plate 9.18	Myrtaceae	*Syzigium* sp.	Parasyncolpate, Syncolpate, Triporate	Min 4µm, Med 4µm, Max 6µm
Plate 10.1	Fagaceae	Indet	Heterocolpate, Psilate	Min23 µm, Med 24µm, Max 25µm
Plate 10.2	Fagaceae	*Nothofagus* sp	Heterocolpate, Psilate	Equatorial 15µm, Polar 17µm
Plate 10.3	Indet	Indet	Heterocolpate, 6-colpate, Granulate	Equatorial 22µm, Polar 32µm
Plate 10.4	Indet	Indet	Heterocolpate, 6-colpate, Psilate	Equatorial 16–19µm, Polar 19–22µm
Plate 10.5	Indet	Indet	Heterocolpate, 8-colpate, Psilate	Equatorial 16µm, Polar 16–17µm
Plate 10.6	Combretaceae	Indet	Heterocolpate, 6-colpate, Psilate	Equatorial 11–13µm, Polar 17–20µm
Plate 10.7	Combretaceae	Indet	Heterocolpate, 6-colpate, Psilate	Equatorial 14–15µm, Polar 15–18µm
Plate 10.8	Combretaceae	Indet	Heterocolpate, 6-colpate, Psilate	Equatorial 9–10µm, Polar 13–14µm
Plate 10.9	Combretaceae	Indet	Heterocolpate, 6-colpate, Psilate	Equatorial 81-0µm, Polar 12µm
Plate 10.10	Combretaceae	Indet	Heterocolpate, 6-colpate, Psilate	Equatorial 9–10µm, Polar 11–12µm
Plate 10.11	Combretaceae	Indet	Heterocolpate, 6-colpate, Psilate	Equatorial 10–11 µm, Polar 9–11µm
Plate 10.12	Combretaceae	Indet	Heterocolpate, 6-colpate, Psilate	Equatorial 7–8µm, Polar 10–11µm
Plate 10.13	Combretaceae	Indet	Heterocolpate, 6-colpate, Psilate	Equatorial 8–9µm, Polar 9–10µm
Plate 10.14	Combretaceae	Indet	Heterocolpate, 6-colpate, Psilate	Equatorial 7–8µm, Polar 9–10µm
Plate 11.1	Sapotaceae	*Palaquium* sp.	5-Colporate, Granulate	Equatorial 39–43µm, Polar 41–46µm
Plate 11.2	Sapotaceae	*Palaquium* sp.	4-Colporate, Psilate	Equatorial 37–40µm, Polar 38–43µm
Plate 11.3	Sapotaceae	*Palaquium* sp.	5-Colporate, Psilate	Equatorial 33–36µm, Polar 37–39µm
Plate 11.4	Sapotaceae	*Palaquium* sp.	5-Colporate, Psilate	Equatorial 34–37µm, Polar 40–42µm
Plate 11.5	Sapotaceae	*Palaquium* sp.	5-Colporate, Granulate	Equatorial 36–38µm, Polar 39–41µm
Plate 12.1	Sapotaceae	*Palaquium* sp.	4-Colporate, Psilate	Equatorial 35–37µm, Polar36–40 µm
Plate 12.2	Sapotaceae	*Palaquium* sp.	5-Colporate, Reticulated	Equatorial 31–33µm, Polar 34–38µm
Plate 12.3	Sapotaceae	*Palaquium* sp.	4-Colporate, Psilate	Equatorial 23–27µm, Polar 28–31µm
Plate 12.4	Sapotaceae	*Palaquium* sp.	5-Colporate, Psilate	Equatorial 33–34µm, Polar 37–40µm
Plate 12.5	Sapotaceae	*Palaquium* sp.	5-Colporate, Psilate	Equatorial 29µm, Polar30µm
Plate 12.6	Sapotaceae	*Palaquium* sp.	4-Colporate, Psilate	Equatorial 32–34µm, Polar 35–38µm
Plate 12.7	Sapotaceae/Burseraceae	Indet	Tricolporate, Psilate	Equatorial 31µm, Polar 34µm
Plate 12.8	Sapotaceae	*Palaquium* sp.	5-Colporate, Psilate	Equatorial 30µm, Polar 31µm
Plate 12.9	Meliaceae	Indet	4-Colporate, Psilate	Equatorial 26µm, Polar 34µm
Plate 13.1	Meliaceae	Indet	4-Colporate, Psilate	Equatorial 27µm, Polar 37µm
Plate 13.2	Meliaceae	Indet	5-Colporate, Psilate	Equatorial 22–24µm, Polar 29–34µm
Plate 13.3	Meliaceae	Indet	4-Colporate, Psilate	Equatorial 23µm, Polar 29µm

Plate 13.4	Meliaceae	Indet	4-Colporate, Psilate	Equatorial 21µm, Polar 31µm
Plate 13.5	Meliaceae	Indet	5-Colporate, Psilate	Equatorial 18µm, Polar 23µm
Plate 13.6	Meliaceae	Indet	4-Colporate, Psilate	Equatorial 15–17µm, Polar 22–24µm
Plate 13.7	Meliaceae	Indet	4-Colporate, Psilate	Equatorial 17µm, Polar 24µm
Plate 13.8	Meliaceae	Indet	5-Colporate, Psilate	Equatorial 14–16µm, Polar 22µm
Plate 13.9	Meliaceae	Indet	4-Colporate, Psilate	Equatorial 16–17µm, Polar 19–21µm
Plate 13.10	Meliaceae	Indet	5-Colporate, Psilate	Equatorial 15µm, Polar 21µm
Plate 13.11	Indet	Indet	5-Colporate, Psilate	Equatorial 13µm, Polar 19µm
Plate 13.12	Burseraceae	Indet	5-Colporate, Psilate	Equatorial 20µm, Polar 20µm
Plate 13.13	Indet	Indet	4-Colporate, Psilate	Equatorial 14–16µm, Polar 15–16µm
Plate 13.14	Indet	Indet	4-Colporate, Psilate	Equatorial 13–14µm, Polar13–14 µm
Plate 13.15	Indet	Indet	4-Colporate, Psilate	Equatorial 13µm, Polar 16µm
Plate 14.1	Clusiaceae	*Callophyllum* sp.	Triporate, Granulate	Equatorial 25–30µm, Polar 30–33µm
Plate 14.2	Clusiaceae	*Callophyllum* sp.	Triporate, Psilate	Equatorial 31–34µm, Polar 26–30µm
Plate 14.3	Indet	Indet	Triporate, Granulate	Equatorial 27–29µm, Polar 33–36µm
Plate 14.4	Indet	Indet	Triporate, Granulate	Equatorial 39µm, Polar 28µm
Plate 14.5	Clusiaceae	*Callophyllum* sp.	Triporate, Psilate	Equatorial 31µm, Polar 31µm
Plate 14.6	Clusiaceae	*Callophyllum* sp.	Triporate, Granulate	Equatorial 25–27µm, Polar 24–25µm
Plate 14.7	Indet	Indet	Triporate, Granulate	Equatorial 26–28µm, Polar 26–29µm
Plate 14.8	Rubiaceae	*Ixora* sp.	Triporate, Psilate	Equatorial 24–26µm, Polar 28µm
Plate 14.9	Indet	Indet	Triporate, Granulate	Equatorial 30µm, Polar 27µm
Plate 14.10	Indet	Indet	Triporate, Psilate	Equatorial 22–23µm, Polar 21–23µm
Plate 14.11	Clusiaceae	*Callophyllum* sp.	Triporate, Psilate	Equatorial 26–29µm, Polar 27–30µm
Plate 14.12	Clusiaceae	*Callophyllum* sp.	Triporate, Psilate	Equatorial 25–28µm, Polar24–25µm
Plate 14.13	Indet	Indet	Triporate, Psilate	Equatorial 27–28µm, Polar 27–29µm
Plate 14.14	Indet	Indet	Triporate, Psilate	Equatorial 20–22µm, Polar 20–23µm
Plate 15.1	Dipterocarpaceae	*Shorea* sp.	Triporate, Granulate	Equatorial 30µm, Polar 31µm
Plate 15.2	Dipterocarpaceae	*Shorea* sp.	Triporate, Granulate	Equatorial 23–24µm, Polar 22–24µm
Plate 15.3	Dipterocarpaceae	*Shorea* sp.	Triporate, Granulate	Equatorial 19–20µm, Polar 22–23µm
Plate 15.4	Dipterocarpaceae	*Shorea* sp.	Triporate, Granulate	Equatorial 19–20µm, Polar 22–24µm
Plate 15.5	Dipterocarpaceae	*Shorea* sp.	Triporate, Granulate	Equatorial 19–21 µm, Polar 18–22µm
Plate 15.6	Dipterocarpaceae	Indet	Triporate, Psilate	Equatorial 17–19µm, Polar 17–19µm
Plate 15.7	Dipterocarpaceae	Indet	Triporate, Psilate	Equatorial 22–23µm, Polar17–20 µm
Plate 15.8	Dipterocarpaceae	Indet	Triporate, Psilate	Equatorial 18µm, Polar 20–21µm
Plate 15.9	Dipterocarpaceae	Indet	Triporate, Granulate	Equatorial 17–18µm, Polar 15–17µm
Plate 15.10	Dipterocarpaceae	Indet	Triporate, Psilate	Equatorial 14–17µm, Polar17–18 µm
Plate 15.11	Dipterocarpaceae	Indet	Triporate, Granulate	Equatorial 20–22µm, Polar12–14 µm
Plate 15.12	Dipterocarpaceae	Indet	Triporate, Granulate	Equatorial 20–22µm, Polar 14–16µm
Plate 16.1	Dipterocarpaceae	Indet	Triporate, Psilate	Equatorial 18µm, Polar 18–20µm
Plate 16.2	Dipterocarpaceae	Indet	Triporate, Psilate	Equatorial 15–17µm, Polar 18µm
Plate 16.3	Dipterocarpaceae	Indet	Triporate, Psilate	Equatorial 14–15µm, Polar 12–14µm
Plate 16.4	Dipterocarpaceae	Indet	Triporate, Psilate	Equatorial 16–17µm, Polar 15–16µm
Plate 16.5	Dipterocarpaceae	Indet	Triporate, Psilate	Equatorial 13–15µm, Polar 14–16µm
Plate 16.6	Dipterocarpaceae	Indet	Triporate, Psilate	Equatorial 13–15µm, Polar 14–15µm
Plate 16.7	Dipterocarpaceae	*Vatica* sp.	Triporate, Psilate	Equatorial 12–14µm, Polar 12–14µm
Plate 16.8	Dipterocarpaceae	*Vatica* sp.	Triporate, Psilate	Equatorial 14µm, Polar 12µm
Plate 16.9	Dipterocarpaceae	*Vatica* sp.	Triporate, Psilate	Equatorial 11µm, Polar 12µm
Plate 16.10	Sapindaceae	Indet	Triporate, Psilate	Equatorial 17µm, Polar 17–18µm
Plate 16.11	Sapindaceae	Indet	Triporate, Psilate	Equatorial 14µm, Polar 15–16µm
Plate 16.12	Sapindaceae	Indet	Triporate, Psilate	Equatorial 13–14µm, Polar 16–17µm
Plate 16.13	Sapindaceae	Indet	Triporate, Psilate	Equatorial 16µm, Polar 15µm
Plate 16.14	Sapindaceae	Indet	Triporate, Psilate	Equatorial 18µm, Polar 20µm
Plate 16.15	Sapindaceae	Indet	Triporate, Psilate	Equatorial 11µm, Polar 15µm
Plate 16.16	Sapindaceae	Indet	Triporate, Psilate	Equatorial 8µm, Polar 11µm
Plate 16.17	Indet	Indet	Triporate, Psilate	Equatorial 19µm, Polar 29µm
Plate 16.18	Indet	Indet	Triporate, Psilate	Equatorial 21µm, Polar 22µm
Plate 16.19	Indet	Indet	Triporate, Psilate	Equatorial 13µm, Polar 18µm
Plate 16.20	Indet	Indet	Triporate, Psilate	Equatorial 15µm, Polar 9µm
Plate 16.21	Indet	Indet	Triporate, Psilate	Equatorial 16µm, Polar 18µm
Plate 16.22	Lamiaceae	*Calicarpa* sp	Triporate, Granulate	Equatorial 26µm, Polar 11–13µm
Plate 16.23	Lamiaceae	*Calicarpa* sp	Triporate, Granulate	Equatorial 27–29µm, Polar 15–116µm
Plate 16.24	Lamiaceae	*Gomphostemma* sp.	Triporate, Granulate	Equatorial 34–35µm, Polar 17–23µm
Plate 16.25	Lamiaceae	*Gomphostemma* sp.	Triporate, Granulate	Equatorial 33–26µm, Polar 27µm
Plate 17.1	Anacardiaceae	Indet	Triporate, Granulate	Equatorial 25µm, Polar 42µm
Plate 17.2	Anacardiaceae	Indet	Triporate, Granulate	Equatorial 23–25µm, Polar 38–39µm

Plate 17.3	Anacardiaceae	Indet	Triporate, Granulate	Equatorial 21–23µm, Polar 32–34µm
Plate 17.4	Indet	Indet	Triporate, Granulate	Equatorial 16–18µm, Polar 32–35µm
Plate 17.5	Indet	Indet	Triporate, Granulate	Equatorial 18–20µm, Polar 30–33µm
Plate 17.6	Indet	Indet	Triporate, Granulate	Equatorial 18–21µm, Polar 28–31µm
Plate 17.7	Indet	Indet	Triporate, Granulate	Equatorial 17–19µm, Polar 27–29µm
Plate 17.8	Ebenaceae	*Diospyros* sp	Triporate, Psilate	Equatorial 15–18µm, Polar 23–27µm
Plate 17.9	Indet	Indet	Triporate, Psilate	Equatorial 15–16µm, Polar 24–27µm
Plate 17.10	Ebenaceae	*Diospyros* sp	Triporate, Psilate	Equatorial 13–14µm, Polar 19–20µm
Plate 17.11	Indet	Indet	Triporate, Granulate	Equatorial 16µm, Polar 27µm
Plate 17.12	Ebenaceae	*Diospyros* sp	Triporate, Psilate	Equatorial 14–16µm, Polar 20–21µm
Plate 17.13	Fagaceae	Lithocarpus sp	Triporate, Psilate	Equatorial 12–14µm, Polar 21–23µm
Plate 17.14	Fagaceae	Lithocarpus sp	Triporate, Psilate	Equatorial 14µm, Polar 28µm
Plate 17.15	Fagaceae	Lithocarpus sp	Triporate, Psilate	Equatorial 13–14µm, Polar 21–23µm
Plate 17.16	Fagaceae	Lithocarpus sp	Triporate, Psilate	Equatorial 12–13µm, Polar 19–20µm
Plate 17.17	Fagaceae	Lithocarpus sp	Triporate, Granulate	Equatorial 13µm, Polar 22µm
Plate 18.1	Indet	Indet	Triporate, Baculate	Equatorial 23µm, Polar 27µm
Plate 18.2	Indet	Indet	Triporate, Baculate	Equatorial 23µm, Polar 26µm
Plate 18.3	Fagaceae	Indet	Triporate, Baculate	Equatorial 19–20µm, Polar 22–23µm
Plate 18.4	Fagaceae	Indet	Triporate, Baculate	Equatorial 17–18µm, Polar 19–20µm
Plate 18.5	Fagaceae	Indet	Triporate, Baculate	Equatorial 14–16µm, Polar 14–16µm
Plate 18.6	Indet	Indet	Triporate, Baculate	Equatorial 12–13µm, Polar 15–16µm
Plate 18.7	Indet	Indet	Triporate, Psilate	Equatorial 14–16µm, Polar 19–20µm
Plate 18.8	Indet	Indet	Triporate, Psilate	Equatorial 12–14µm, Polar 16–18µm
Plate 18.9	Indet	Indet	Triporate, Psilate	Equatorial 10–11µm, Polar 16–17µm
Plate 18.10	Indet	Indet	Triporate, Psilate	Equatorial 9–11µm, Polar 14–16µm
Plate 18.11	Indet	Indet	Triporate, Psilate	Equatorial 9–11µm, Polar 17µm
Plate 18.12	Indet	Indet	Triporate, Psilate	Equatorial 11–12µm, Polar 16–17µm
Plate 18.13	Indet	Indet	Triporate, Psilate	Equatorial 10–11µm, Polar 13–15µm
Plate 18.14	Indet	Indet	Triporate, Psilate	Equatorial 10–11 µm, Polar 13µm
Plate 18.15	Indet	Indet	Triporate, Psilate	Equatorial 9–10µm, Polar 11–12µm
Plate 18.16	Indet	Indet	Triporate, Psilate	Equatorial 8–10µm, Polar 12–13µm
Plate 18.17	Indet	Indet	Triporate, Psilate	Equatorial 8–9µm, Polar 9–10µm
Plate 18.18	Indet	Indet	Triporate, Psilate	Equatorial 9–10µm, Polar 8µm
Plate 18.19	Indet	Indet	Triporate, Psilate	Equatorial 7µm, Polar 9–10µm
Plate 18.20	Aquifoliaceae	*Ilex* sp.	Triporate, Psilate	Equatorial 9–10µm, Polar 17–19µm
Plate 18.21	Aquifoliaceae	*Ilex* sp.	Triporate, Psilate	Equatorial 8–9µm, Polar 15µm
Plate 18.22	Aquifoliaceae	*Ilex* sp.	Triporate, Psilate	Equatorial 8–9µm, Polar 16–18µm
Plate 18.23	Aquifoliaceae	*Ilex* sp.	Triporate, Psilate	Equatorial 9µm, Polar 15µm
Plate 18.24	Aquifoliaceae	*Ilex* sp.	Triporate, Psilate	Equatorial 7µm, Polar 13–14µm
Plate 18.25	Aquifoliaceae	*Ilex* sp.	Triporate, Psilate	Equatorial 7–8µm, Polar 10–11µm
Plate 18.26	Aquifoliaceae	*Ilex* sp.	Triporate, Psilate	Equatorial 9µm, Polar 13µm

Plate 1. Monolete Spore.

1. Indet.
2. Indet.
3. Indet.
4. Indet.
5. Indet.
6. Indet.
7. Indet.
8. Indet.
9. Indet.
10. (Davaliaceae) *Davalia* sp.
11. Indet.
12. Indet.
13. Indet.
14. Indet.
15. Indet.
16. Indet.
17. Indet.

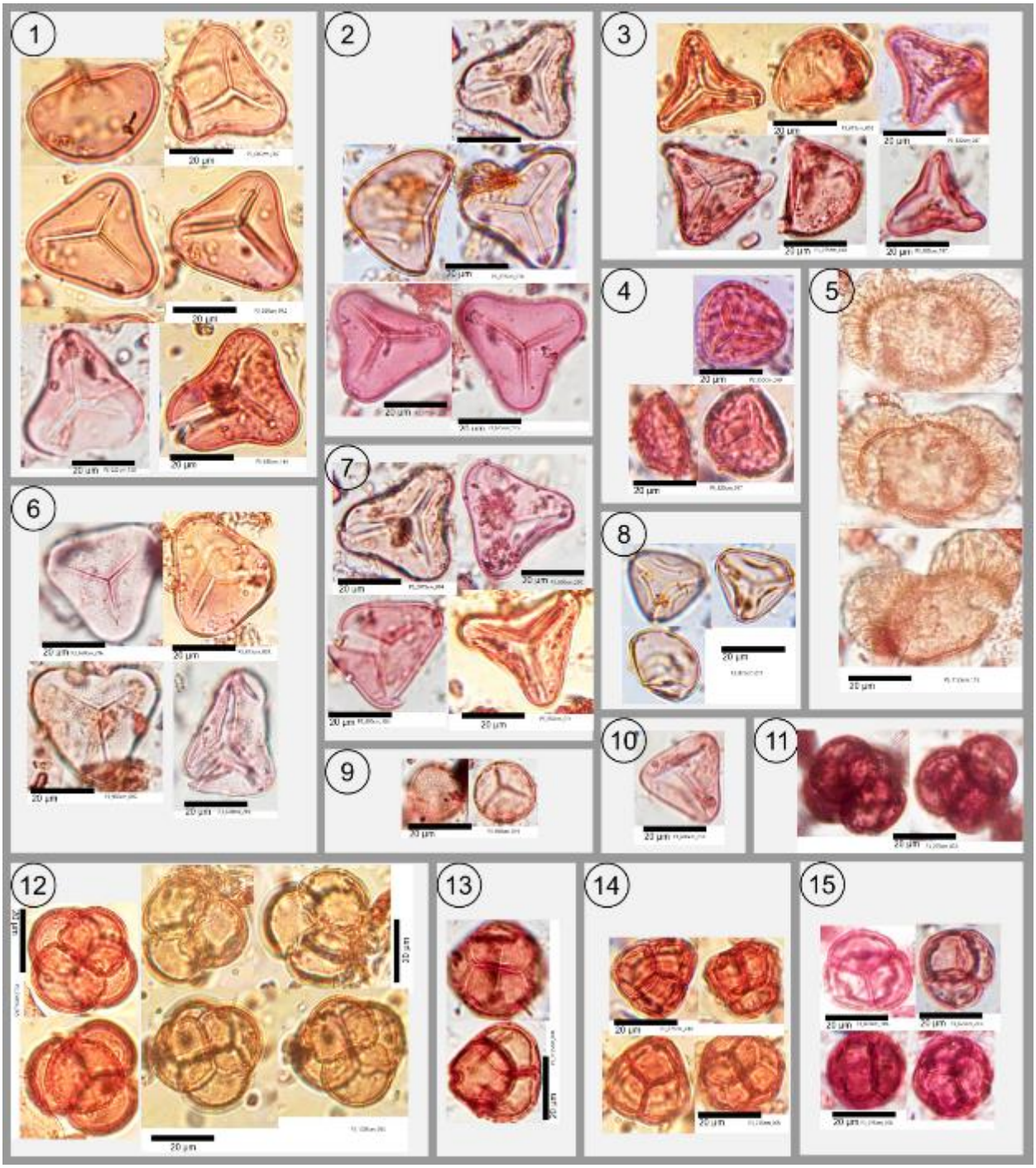

Plate 2. Trilete, Saccate, Tetrad.

1. (Cyatheaceae) *Cyathea* sp.
2. (Cyatheaceae) *Cyathea* sp.
3. Indet.
4. (Lycopodiaceae) *Lycopodiella* sp.
5. (Podocarpaceae) *Dacrydium* sp.
6. (Cyatheaceae) *Cyathea* sp.
7. (Cyatheaceae) *Cyathea* sp.
8. Indet.
9. Mimosaceae
10. Indet.
11. (Ericaceae) *Piptadenia* sp. or *Rhododendron* sp.
12. Ericaceae
13. Ericaceae
14. Ericaceae
15. Ericaceae

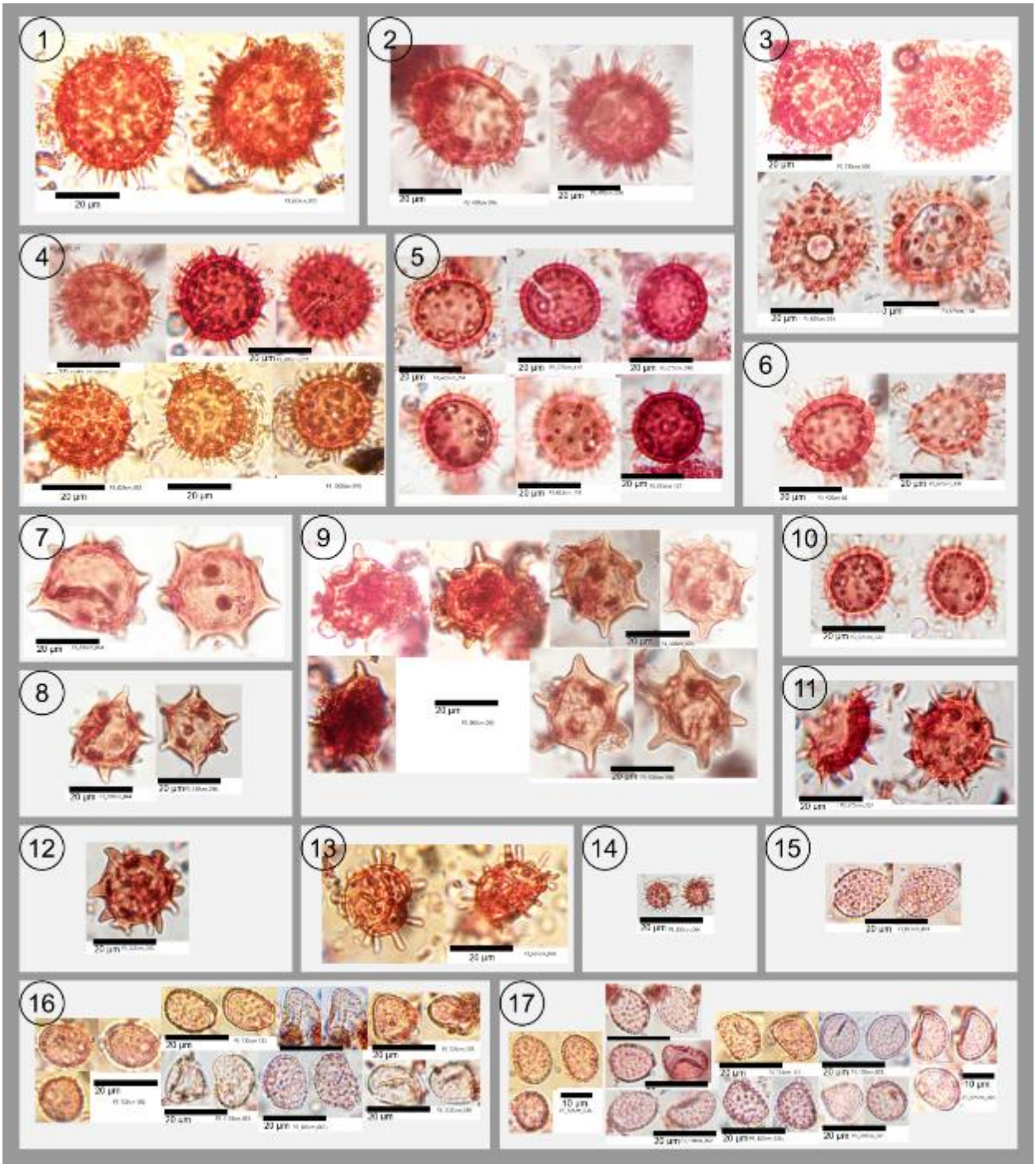

Plate 3. Echinate.
1. Malvaceae
2. Malvaceae
3. Malvaceae
4. Malvaceae
5. Malvaceae
6. Malvaceae
7. Indet.
8. Indet.
9. Indet.
10. Malvaceae
11. Malvaceae
12. Indet.
13. Indet.
14. Indet.
15. (Arecaceae) *Arenga* sp.
16. (Pandanaceae) *Pandanus* sp.
17. (Pandanaceae) *Pandanus* sp.

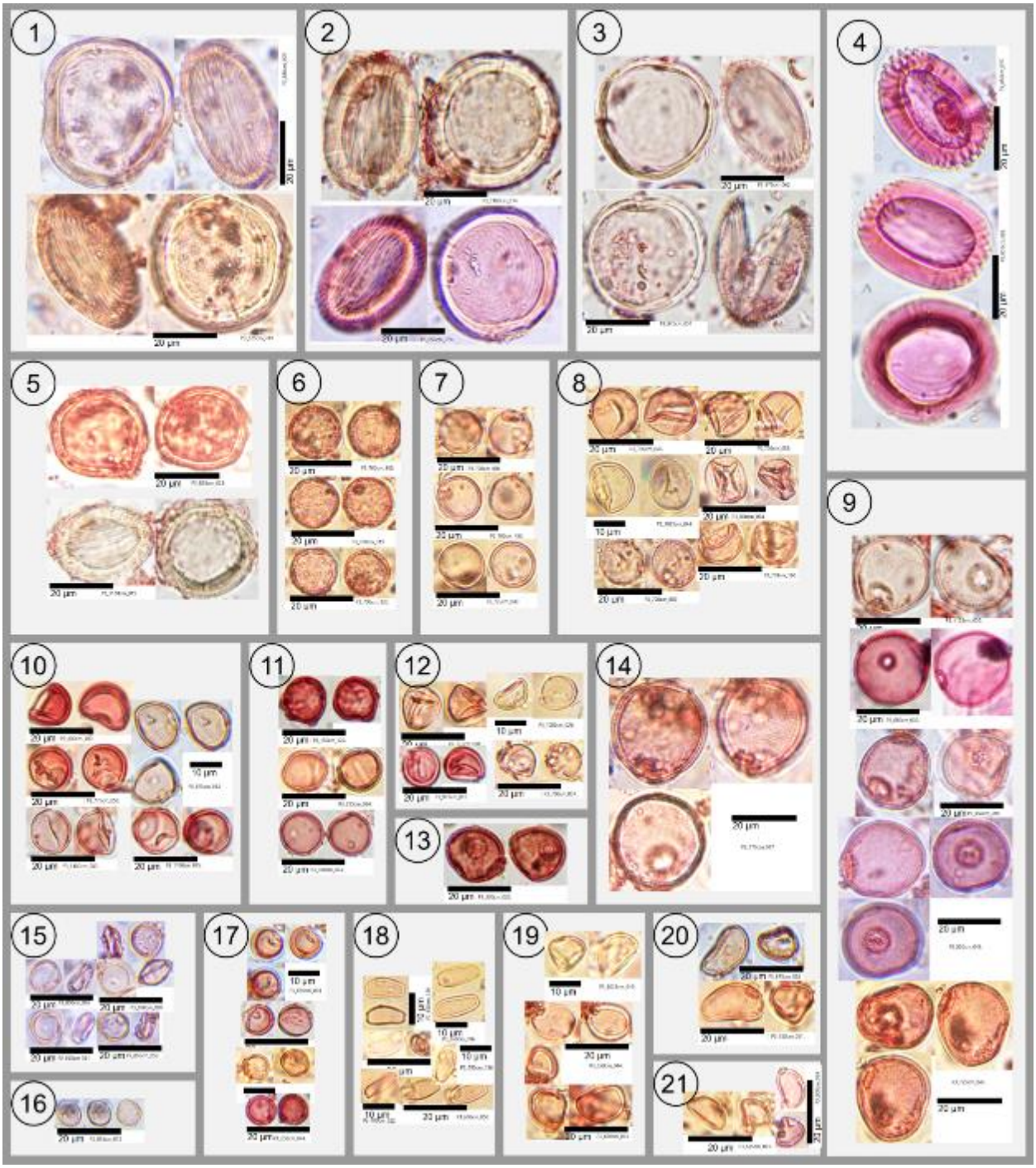

Plate 4. Inaperturate, Monoporate.

1. (Zygnemataceae) *Concentricystes* sp.
2. (Zygnemataceae) *Concentricystes* sp.
3. (Zygnemataceae) *Concentricystes* sp.
4. (Zygnemataceae) *Concentricystes* sp.
5. (Zygnemataceae) *Concentricystes* sp.
6. Poaceae
7. Poaceae
8. Poaceae
9. Poaceae
10. Poaceae
11. Poaceae
12. Poaceae
13. Poaceae
14. Poaceae
15. Poaceae
16. Poaceae
17. Poaceae
18. (Pandanaceae) *Freycinetia* sp.
19. (Pandanaceae) *Freycinetia* sp.
20. (Pandanaceae) *Freycinetia* sp.
21. (Pandanaceae) *Freycinetia* sp.

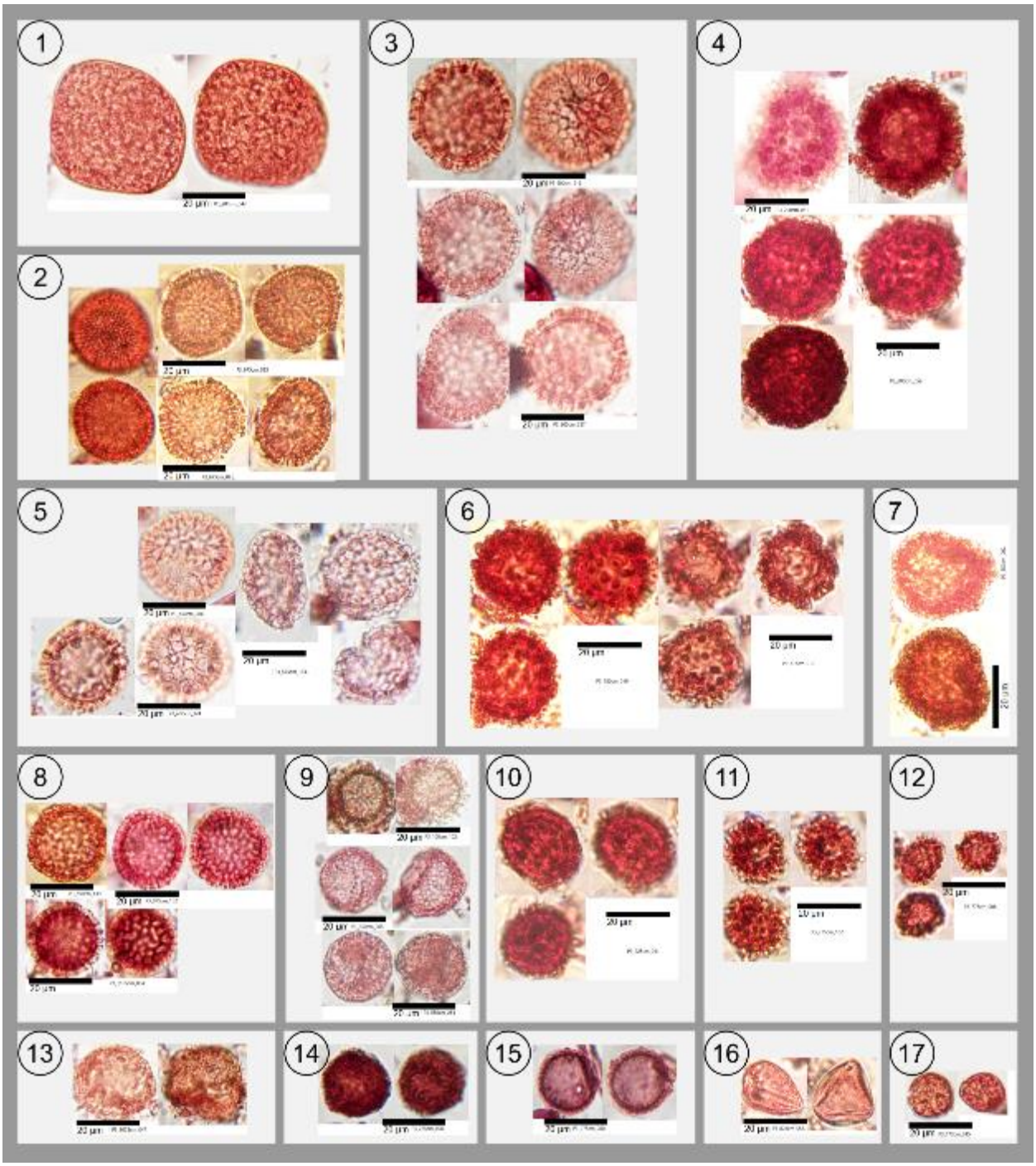

Plate 5. Inaperturate.

1. Indet.
2. Indet.
3. (Polygonaceae) *Polygonum* sp.
4. Indet.
5. Indet.
6. Indet.
7. Indet.
8. Indet.
9. Indet.
10. Indet.
11. Indet.
12. Indet.
13. Indet.
14. Indet.
15. Indet.
16. Arecaceae
17. Indet.

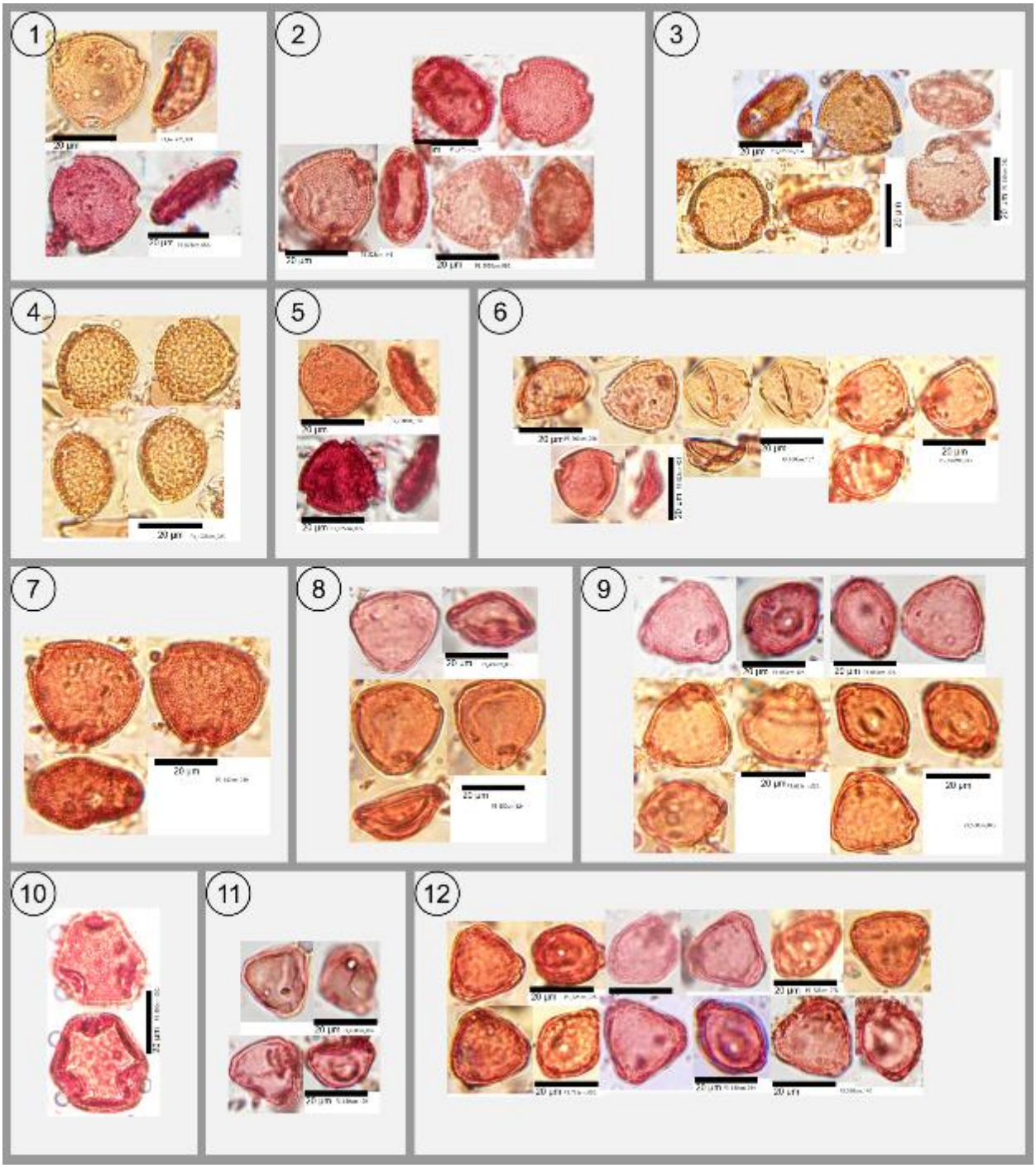

Plate 6. Porate.

1. Rubiaceae
2. Rubiaceae
3. Rubiaceae
4. Rubiaceae
5. Indet.
6. Indet.
7. Rubiaceae
8. Indet.
9. *Stemonurus* sp.
10. Indet.
11. *Stemonurus* sp.
12. *Stemonurus* sp.

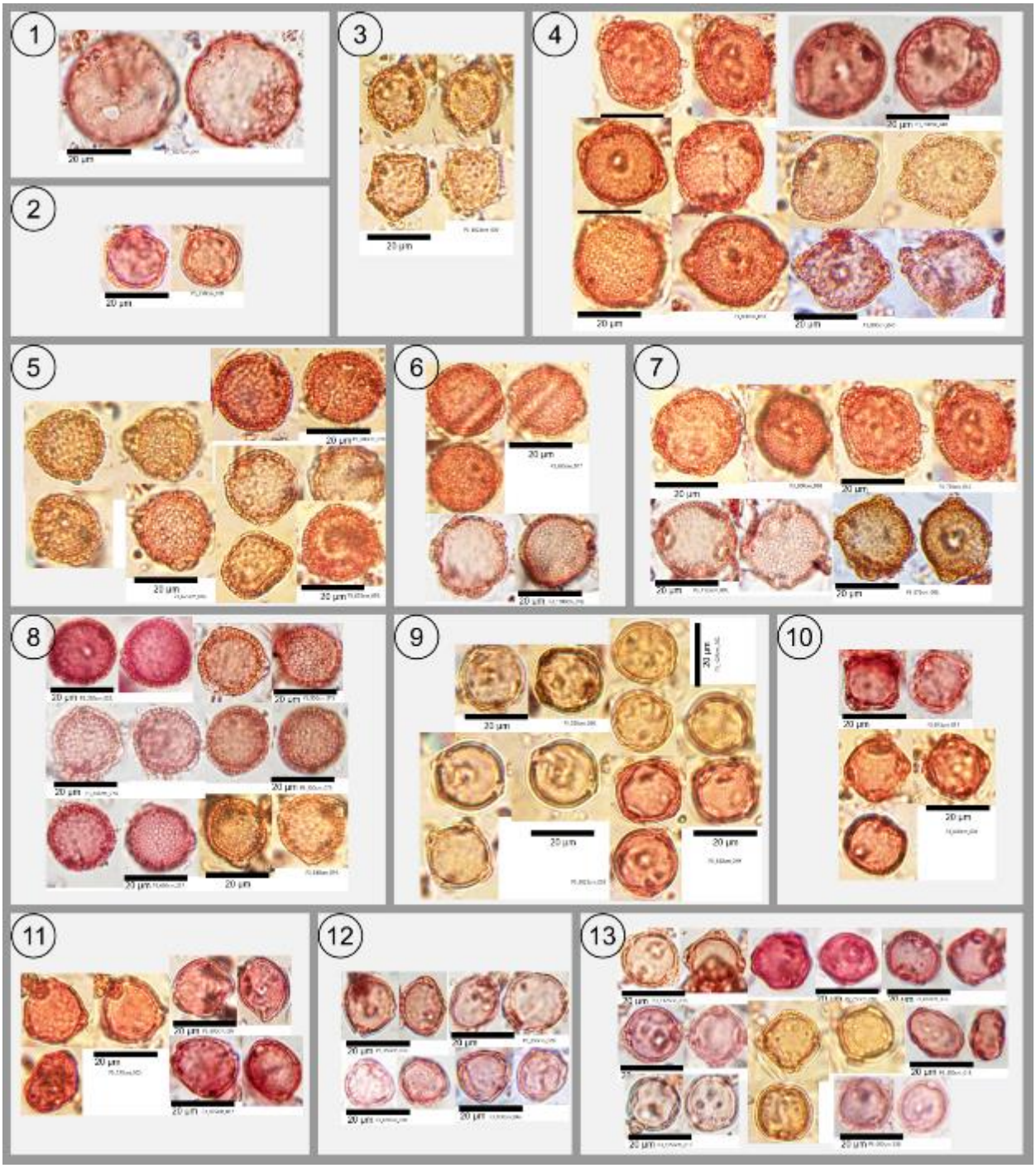

Plate 7. Porate.

1. Indet.
2. Indet.
3. Indet.
4. Indet.
5. Indet.
6. Indet.
7. Indet.
8. Indet.
9. Indet.
10. Indet.
11. Indet.
12. Indet.
13. Indet.

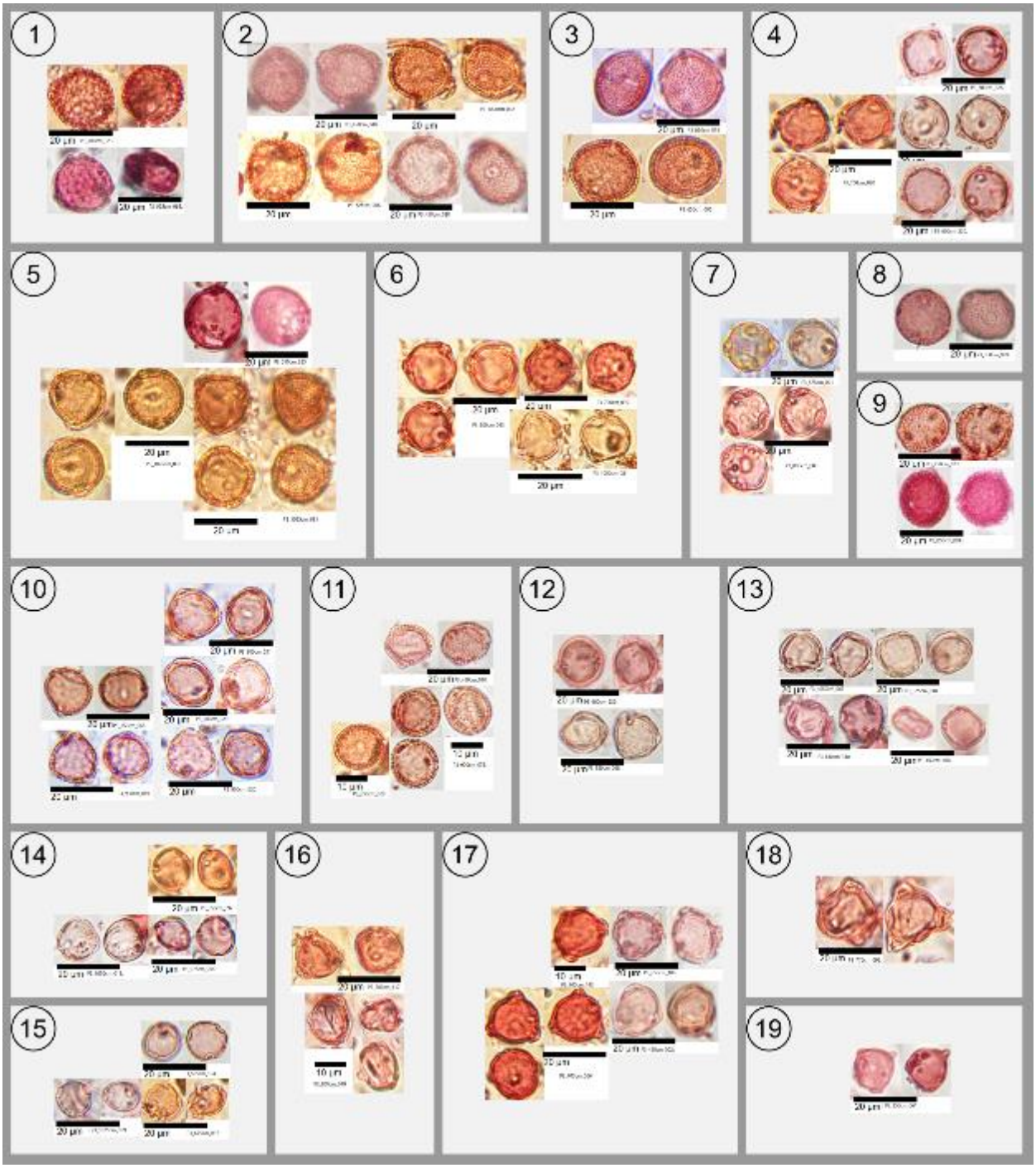

Plate 8. Porate.

1. Indet.
2. Indet.
3. Indet.
4. Indet.
5. Indet.
6. Indet.
7. Indet.
8. Indet.
9. Indet.
10. Indet.
11. Indet.
12. Indet.
13. Moraceae
14. Moraceae
15. Moraceae
16. Indet.
17. Indet.
18. Stemonuraceae
19. Indet.

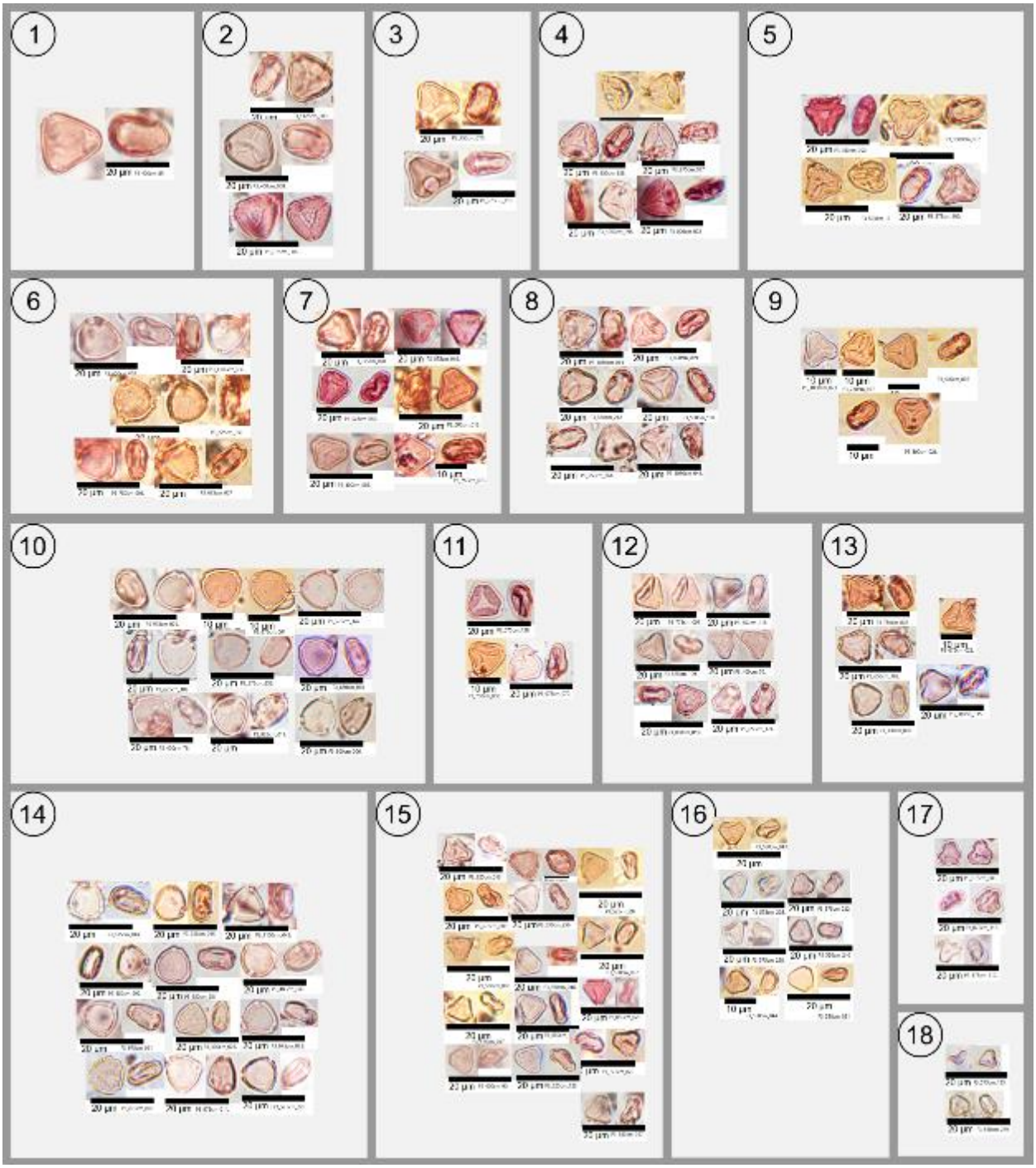

Plate 9. Porate, Syncolpate-Syncolporate.

1. Myrtaceae, *Syzigium* sp.
2. Myrtaceae, *Syzigium* sp.
3. Myrtaceae, *Syzigium* sp.
4. Myrtaceae, *Syzigium* sp.
5. Myrtaceae, *Syzigium* sp.
6. Indet.
7. Myrtaceae, *Syzigium* sp.
8. Myrtaceae, *Syzigium* sp.
9. Myrtaceae, *Syzigium* sp.
10. Indet.
11. Myrtaceae, *Syzigium* sp.
12. Myrtaceae, *Syzigium* sp.
13. Myrtaceae, *Syzigium* sp.
14. Indet.
15. Myrtaceae, *Syzigium* sp.
16. Myrtaceae, *Syzigium* sp.
17. Myrtaceae, *Syzigium* sp.
18. Myrtaceae, *Syzigium* sp.

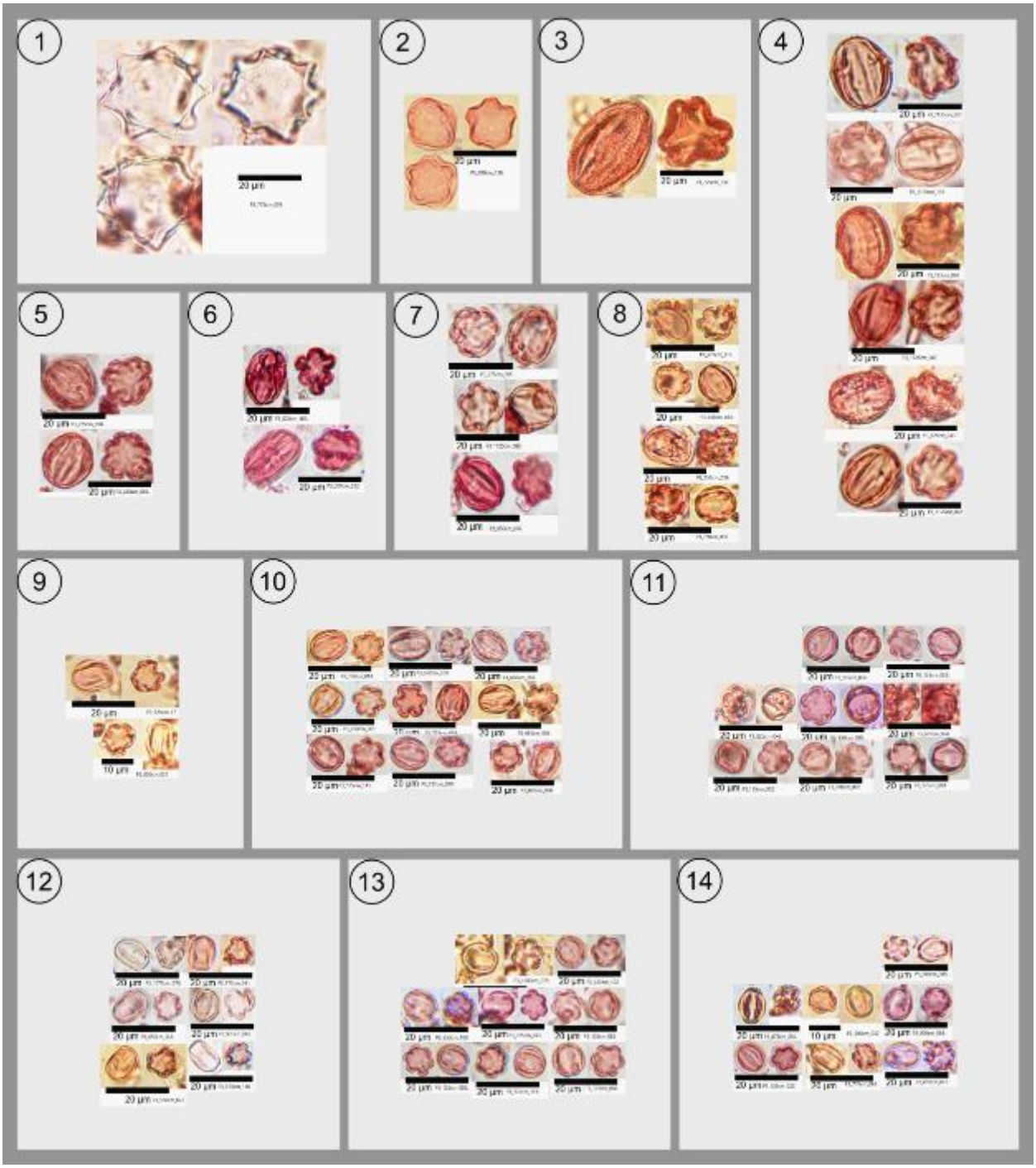

Plate 10. Heterocolpate.

1. Indet
2. (Fagaceae) *Nothofagus* sp
3. Indet.
4. Indet.
5. Indet.
6. Combretaceae
7. Combretaceae
8. Combretaceae
9. Combretaceae
10. Combretaceae
11. Combretaceae
12. Combretaceae
13. Combretaceae
14. Combretaceae

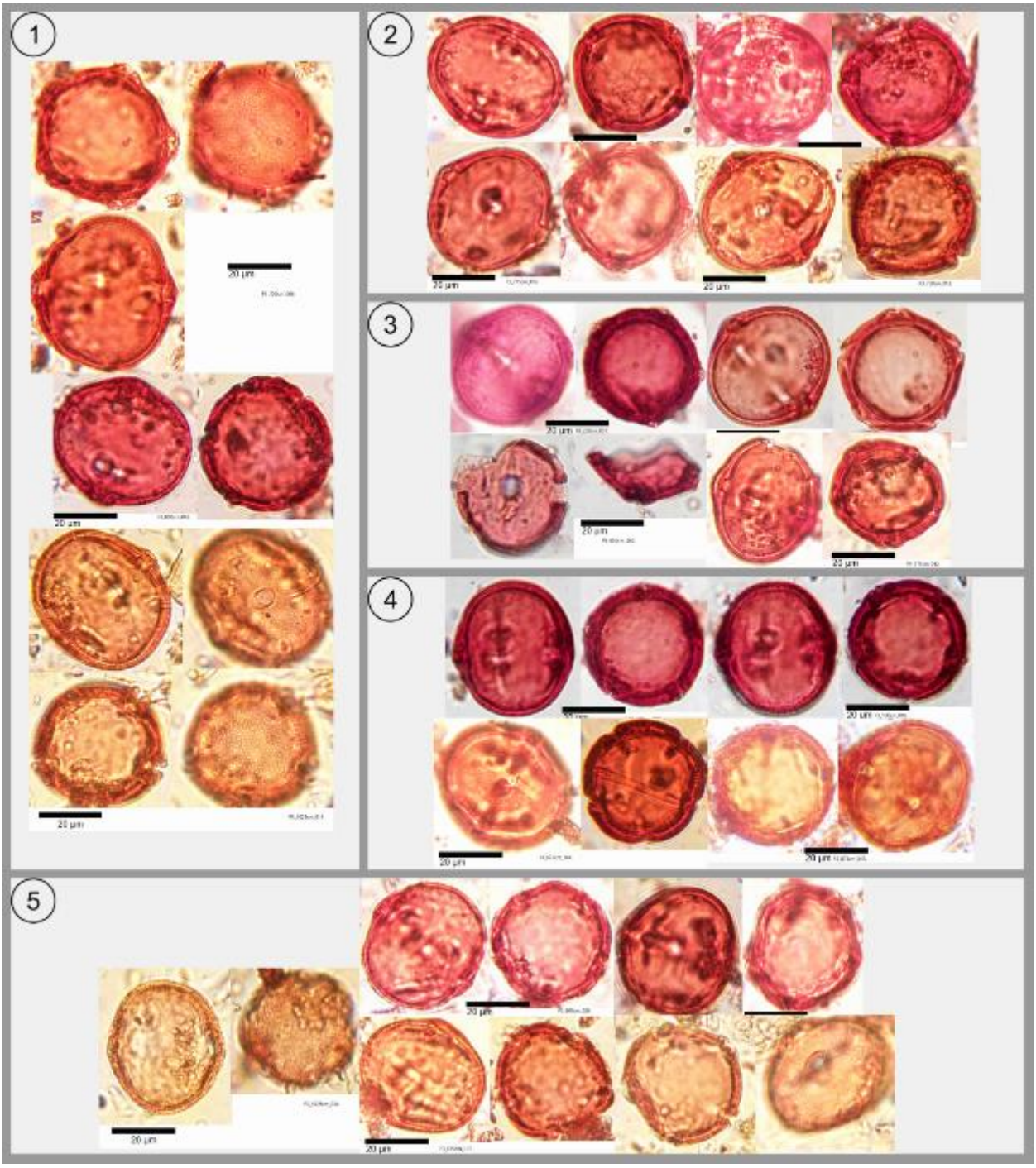

Plate 11. 4–5-colpate, 4–5-colporate.
1. (Sapotaceae) *Palaquium* sp.
2. (Sapotaceae) *Palaquium* sp.
3. (Sapotaceae) *Palaquium* sp.
4. (Sapotaceae) *Palaquium* sp.
5. (Sapotaceae) *Palaquium* sp.

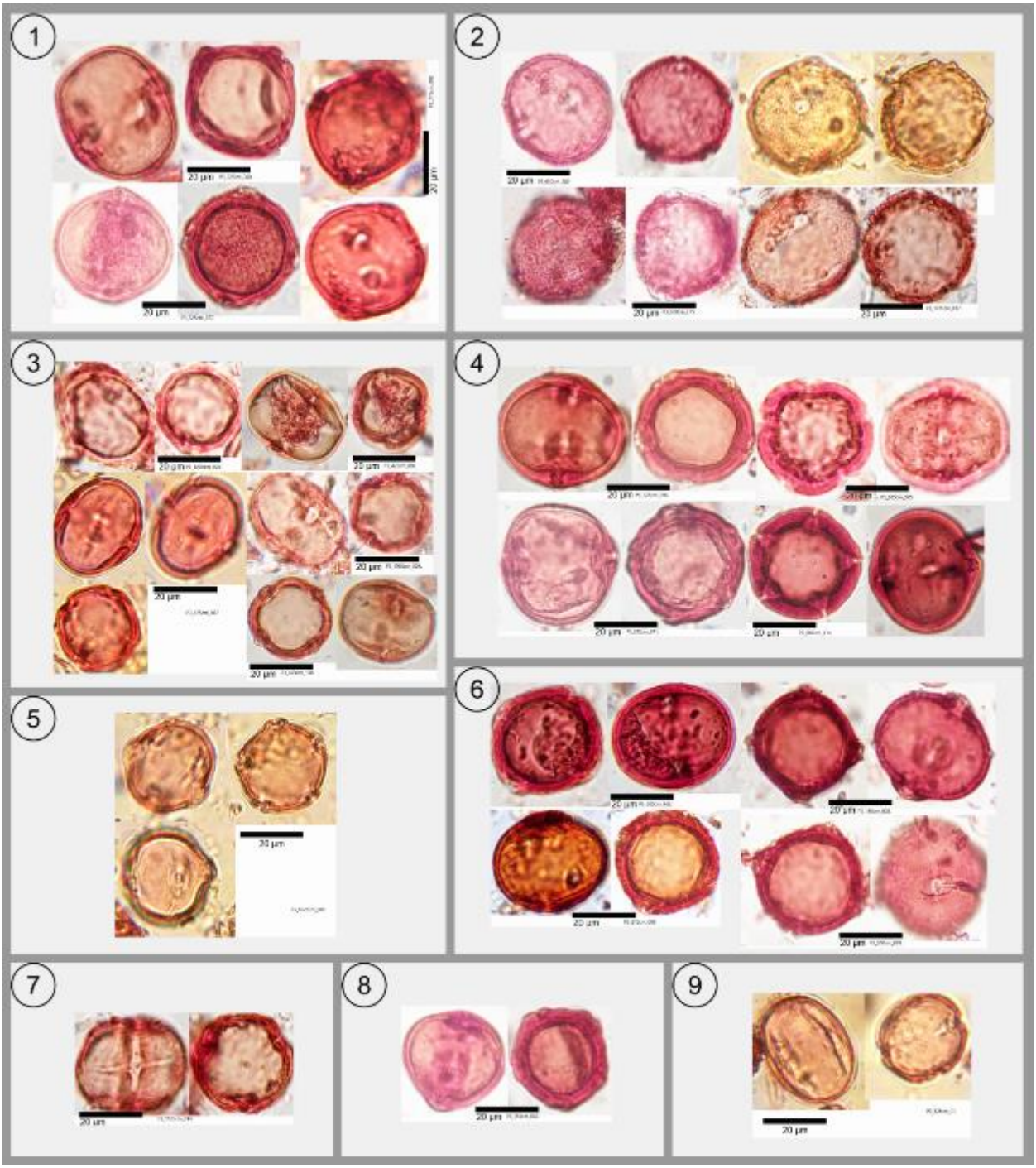

Plate 12. 4–5-colpate, 4–5-colporate

1. (Sapotaceae) *Palaquium* sp.
2. (Sapotaceae) *Palaquium* sp.
3. (Sapotaceae) *Palaquium* sp.
4. (Sapotaceae) *Palaquium* sp.
5. Indet.
6. (Sapotaceae) *Palaquium* sp.
7. Sapotaceae/Burseraceae
8. (Sapotaceae) *Palaquium* sp.
9. Meliaceae

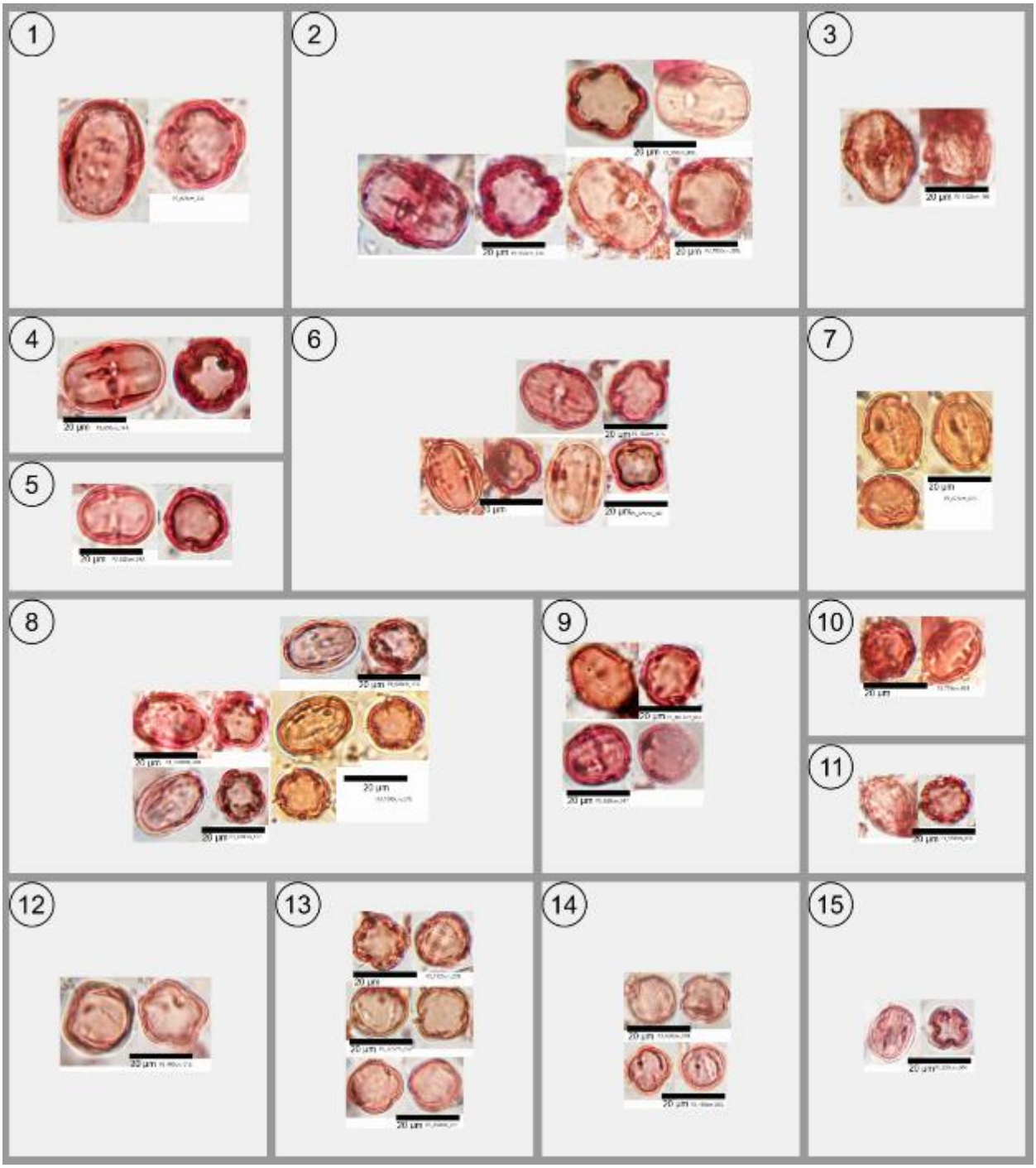

Plate 13. 4–5-colpate, 4–5-colporate

1. Meliaceae
2. Meliaceae.
3. Meliaceae.
4. Meliaceae.
5. Meliaceae
6. Meliaceae.
7. Meliaceae.
8. Meliaceae.
9. Meliaceae
10. Meliaceae.
11. Indet
12. Burseraceae
13. Indet
14. Indet
15. Indet

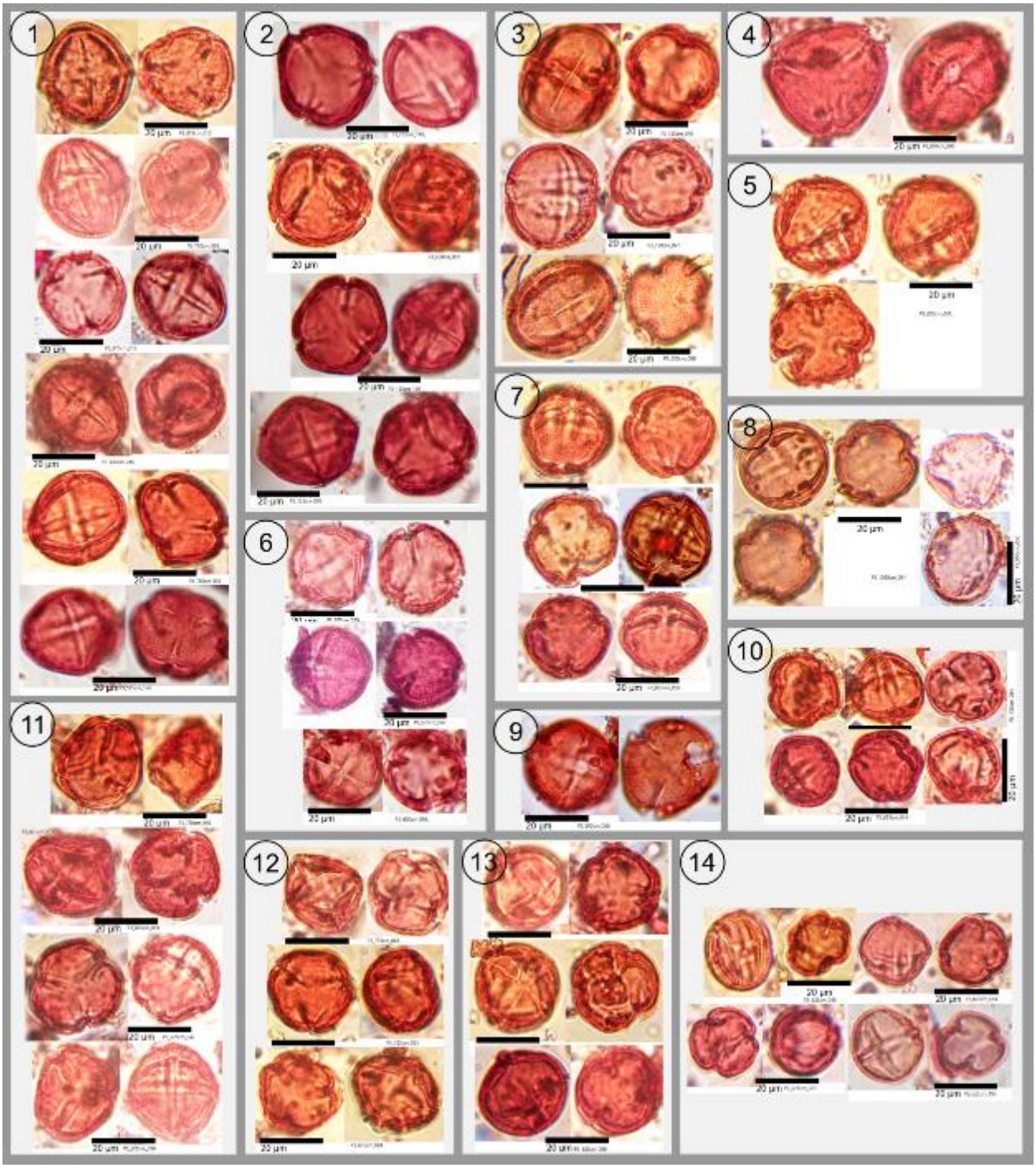

Plate 14. Tricolpate, Tricolporate

1. (Clusiaceae) *Callophyllum* sp.
2. (Clusiaceae) *Callophyllum* sp.
3. Indet.
4. Indet.
5. (Clusiaceae) *Callophyllum* sp.
6. (Clusiaceae) *Callophyllum* sp.
7. Indet.
8. (Rubiaceae) *Ixora* sp.
9. Indet.
10. Indet.
11. (Clusiaceae) *Callophyllum* sp.
12. (Clusiaceae) *Callophyllum* sp.
13. Indet.
14. Indet.

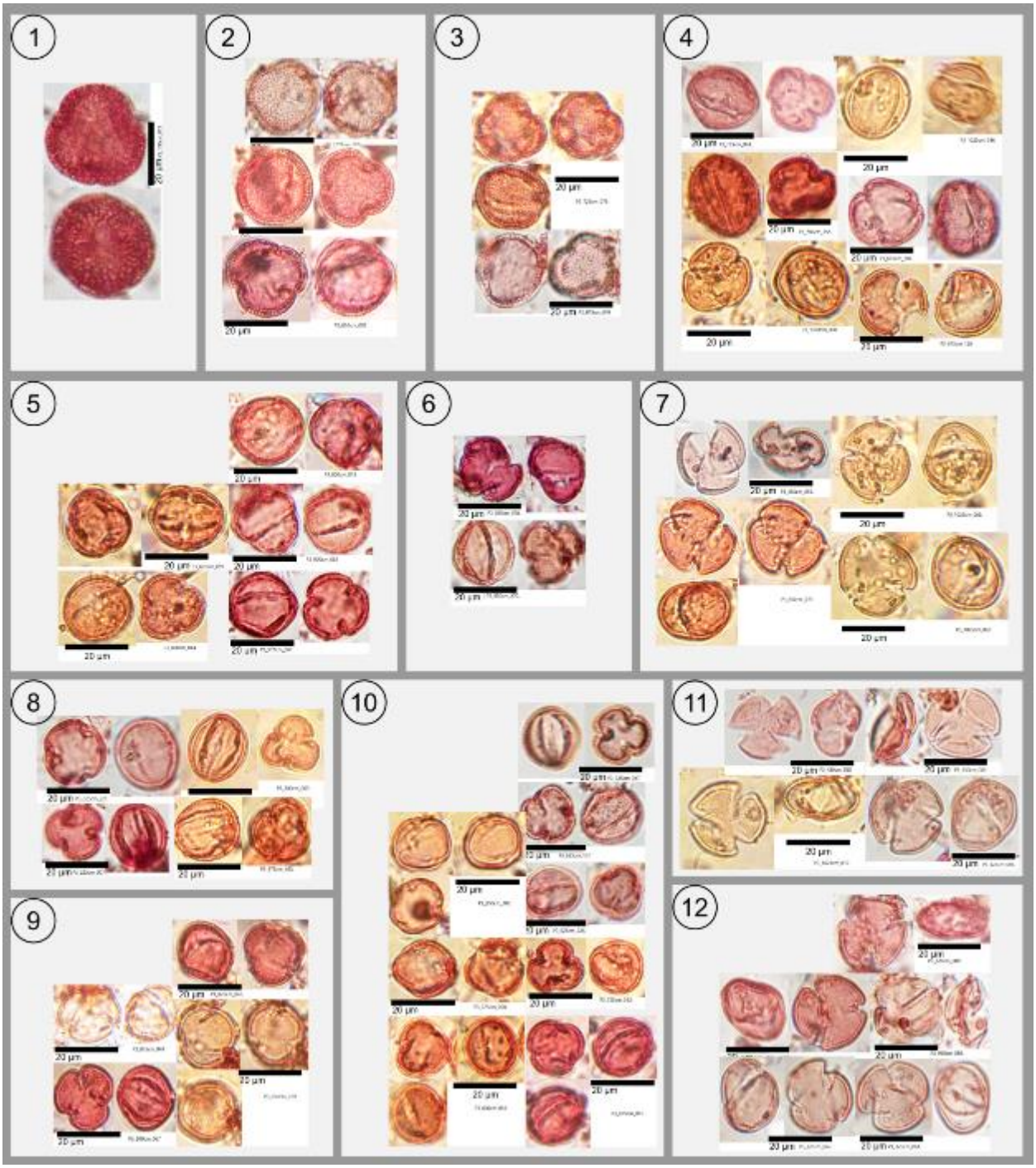

Plate 15. Tricolpate, Tricolporate

1. (Dipterocarpaceae) *Shorea* sp.
2. (Dipterocarpaceae) *Shorea* sp.
3. (Dipterocarpaceae) *Shorea* sp.
4. (Dipterocarpaceae) *Shorea* sp.
5. (Dipterocarpaceae) *Shorea* sp.
6. Dipterocarpaceae
7. Dipterocarpaceae
8. Dipterocarpaceae
9. Dipterocarpaceae
10. Dipterocarpaceae
11. Dipterocarpaceae.
12. Dipterocarpaceae

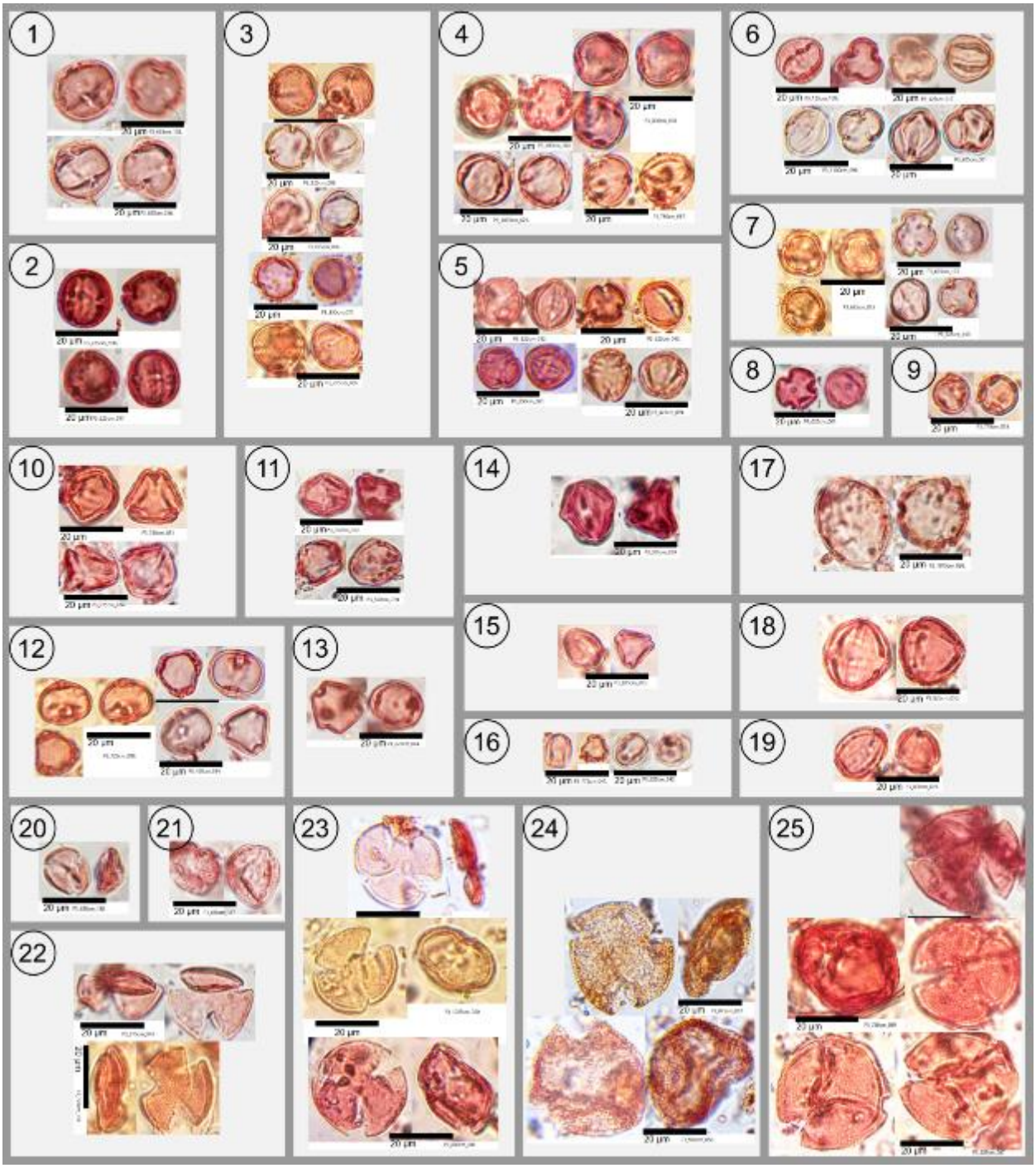

Plate 16. Tricolpate, Tricolporate

1. Dipterocarpaceae
2. Dipterocarpaceae
3. Dipterocarpaceae
4. Dipterocarpaceae
5. Dipterocarpaceae
6. Dipterocarpaceae
7. (Dipterocarpaceae) *Vatica* sp.
8. (Dipterocarpaceae) *Vatica* sp.
9. (Dipterocarpaceae) *Vatica* sp.
10. Sapindaceae
11. Sapindaceae
12. Sapindaceae
13. Sapindaceae
14. Sapindaceae
15. Sapindaceae
16. Sapindaceae
17. Indet
18. Indet
19. Indet
20. Indet
21. Indet
22. (Lamiaceae) *Calicarpa* sp.
23. (Lamiaceae) *Calicarpa* sp.
24. (Lamiaceae) *Gomphostemma* sp.
25. (Lamiaceae) *Gomphostemma* sp.

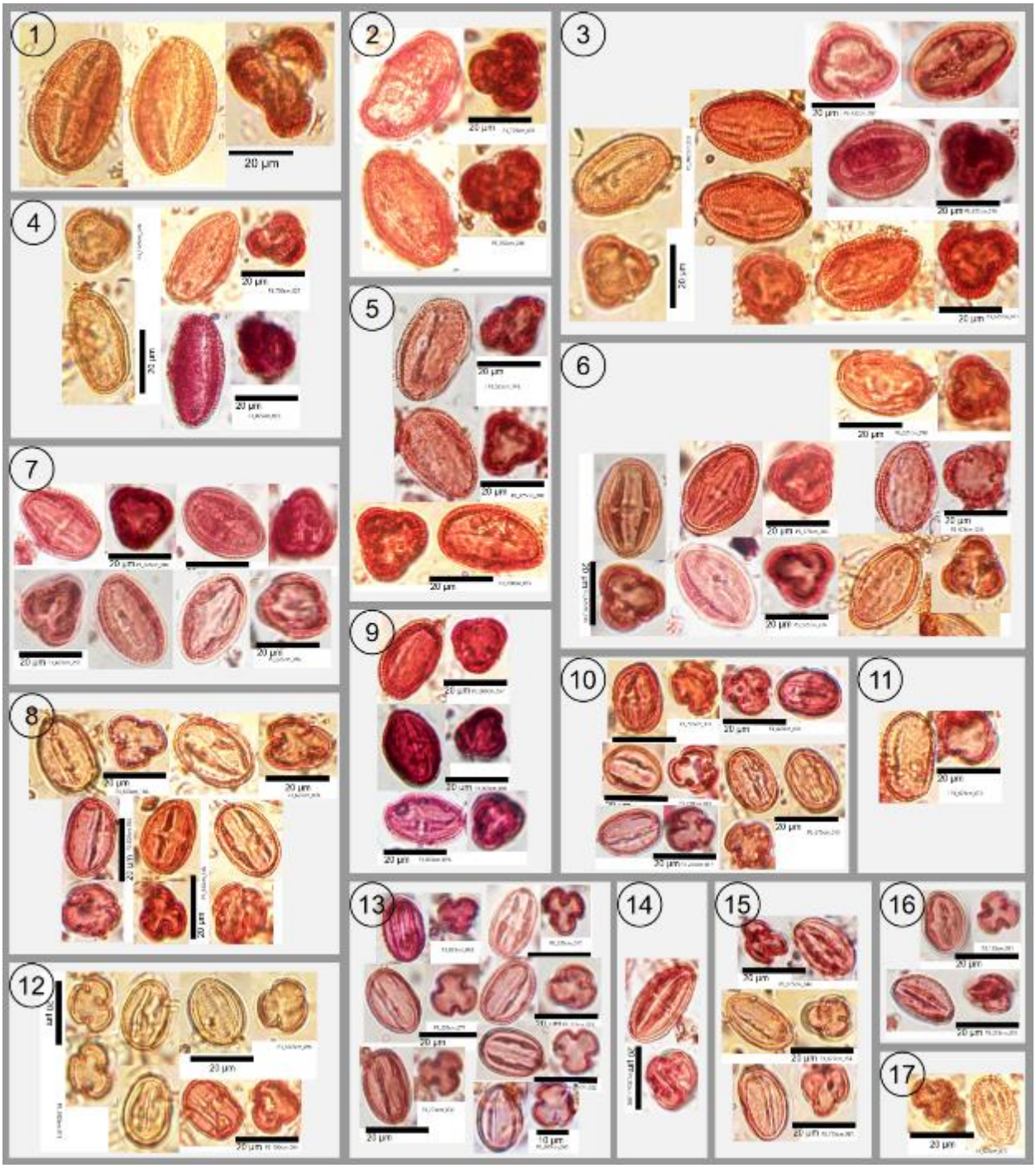

Plate 17. Tricolpate, Tricolporate

1. Anacardiaceae
2. Anacardiaceae
3. Anacardiaceae
4. Indet
5. Indet
6. Indet
7. Indet
8. (Ebenaceae) *Diospyros* sp.
9. Indet
10. (Ebenaceae) *Diospyros* sp.
11. Indet
12. (Ebenaceae) *Diospyros* sp.
13. (Fagaceae) *Lithocarpus* sp.
14. (Fagaceae) *Lithocarpus* sp.
15. (Fagaceae) *Lithocarpus* sp.
16. (Fagaceae) *Lithocarpus* sp.
17. (Fagaceae) *Lithocarpus* sp.

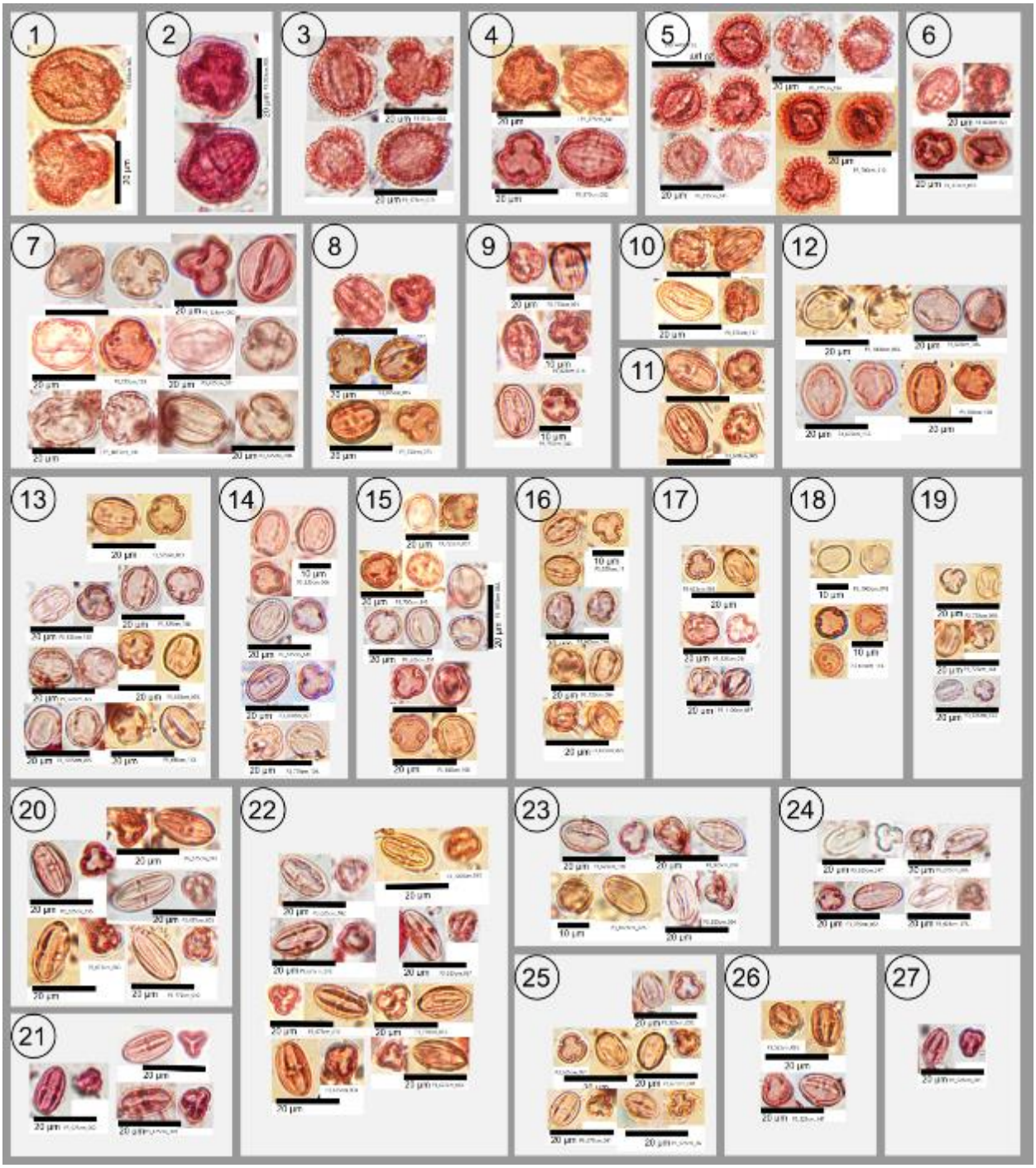

Plate 18. Tricolpate, Tricolporate

1. Indet
2. Indet
3. Fagaceae
4. Fagaceae
5. Fagaceae
6. Indet
7. Indet
8. Indet
9. Indet
10. Indet
11. Indet
12. Indet
13. Indet
14. Indet
15. Indet
16. Indet
17. Indet
18. Indet
19. Indet
20. (Aquifoliaceae) *Ilex* sp.
21. (Aquifoliaceae) *Ilex* sp.
22. (Aquifoliaceae) *Ilex* sp.
23. (Aquifoliaceae) *Ilex* sp.
24. (Aquifoliaceae) *Ilex* sp.
25. (Aquifoliaceae) *Ilex* sp.
26. (Aquifoliaceae) *Ilex* sp.
27. (Aquifoliaceae) *Ilex* sp.

References

Anderson, J. and Muller, J. (1975) 'Palynological study of a Holocene peat and a Miocene coal deposit from NW Borneo', Review of Palaeobotany and Palynology, 19(4), pp. 291–351.

Anshari, G. et al. (2004) 'Environmental change and peatland forest dynamics in the Lake Sentarum area, West Kalimantan, Indonesia', Journal of Quaternary Science, 19(7), pp. 637–655. Available at: https://doi.org/10.1002/jqs.879.

Anshari G, Gusmayanti E, Afifudin M and Widhanarto G (2012) A study of carbon balance in customary peat forest (Hutan Nung) in Taman Nasional Danau Sentarum (No.ENV0100-USA19-DM3, TA: USA193000) CIFOR

Anshari, G., Peter Kershaw, A. and van der Kaars, S. (2001) 'A Late Pleistocene and Holocene pollen and charcoal record from peat swamp forest, Lake Sentarum Wildlife Reserve, West Kalimantan, Indonesia', Palaeogeography, Palaeoclimatology, Palaeoecology, 171(3–4), pp. 213–228. Available at: https://doi.org/10.1016/S0031-0182(01)00246–2.

Barrington, D. S., Patel, N. R., & Southgate, M. W. (2020). Inferring the impacts of evolutionary history and ecological constraints on spore size and shape in the ferns. Applications in Plant Sciences, 8(4), e11339.

Biagioni, S. et al. (2015) '8000years of vegetation dynamics and environmental changes of a unique inland peat ecosystem of the Jambi Province in Central Sumatra, Indonesia', Palaeogeography, Palaeoclimatology, Palaeoecology, 440, pp. 813–829. Available at: https://doi.org/10.1016/j.palaeo.2015.09.048.

Bindler, R. (2006) 'Mired in the past — looking to the future: Geochemistry of peat and the analysis of past environmental changes', Global and Planetary Change, 53(4), pp. 209–221. Available at: https://doi.org/10.1016/j.gloplacha.2006.03.004.

Blackford, J. (2000) 'Palaeoclimatic records from peat bogs', Trends in Ecology & Evolution, 15(5), pp. 193–198.

Chambers, F.M. and Charman, D.J. (2004) 'Holocene environmental change: contributions from the peatland archive', The Holocene, 14(1), pp. 1–6. Available at: https://doi.org/10.1191/0959683604hl684ed.

Chambers, F.M. and van Geel, B. (2011) 'Considerations for the preparation of peat samples for palynology, and for the counting of pollen and non-pollen palynomorphs'.

Cole, L. E., Bhagwat, S. A., & Willis, K. J. (2015). Long-term disturbance dynamics and resilience of tropical peat swamp forests. Journal of Ecology, 103(1), 16-30.

Dennis, R., Erman, A. and Meijaard, E., 2000. Fire in the Danau Sentarum landscape: historical, present perspectives. Borneo Research Bulletin, pp.123-138.

Faegri, K., Kaland, P. E., & Krzywinski, K. (1989). Textbook of pollen analysis (No. Ed. 4). John Wiley & Sons Ltd..

Grant-Downton, R. (2009) Pollen terminology. An illustrated handbook. Annals of Botany Company.

Haberle, S. (2018) 'The Australasian Pollen and Spore Atlas (APSA)'.

Hamilton, R., Hall, T., Stevenson, J., & Penny, D. (2019). Distinguishing the pollen of Dipterocarpaceae from the seasonally dry and moist tropics of south-east Asia using light microscopy. Review of Palaeobotany and Palynology, 263, 117-133.

Hapsari, K.A. et al. (2017) 'Environmental dynamics and carbon accumulation rate of a tropical peatland in Central Sumatra, Indonesia', Quaternary Science Reviews, 169, pp. 173–187. Available at: https://doi.org/10.1016/j.quascirev.2017.05.026.

Hapsari, K.A. et al. (2018) 'Resilience of a peatland in Central Sumatra, Indonesia to past anthropogenic disturbance: Improving conservation and restoration designs using palaeoecology', Journal of Ecology, 106(6), pp. 2473–2490. Available at: https://doi.org/10.1111/1365-2745.13000.

Hodgkins, S.B. et al. (2018) 'Tropical peatland carbon storage linked to global latitudinal trends in peat recalcitrance', Nature Communications, 9(1), pp. 1–13. Available at: https://doi.org/10.1038/s41467-018-06050-2.

Jones, S. (2012) Late Quaternary environmental history from the Kelabit Highlands of Sarawak, Malaysian Borneo: A record of climate, vegetation and land-use.

Osaki, M. and Tsuji, N. (2016) Tropical peatland ecosystems. Springer.

Polak, B. (1949) De Rawa Lakbok, een eutroof laagveen op Java. Archipel Drukkerij.

Polak, E. (1933) Ueber Torf und Moor in Niederländisch Indien. Verhandelingen der Koninklijke Academie van Wetenschappen te Amsterdam, vol 3. Afdeeling Natuurkunde (tweede sectie). North-Holland Publishing Company, Amsterdam.

Poliakova, A. and Behling, H. (2016) 'Pollen and fern spores recorded in recent and late Holocene marine sediments from the Indian Ocean and Java Sea in Indonesia', Quaternary International, 392, pp. 251–314. Available at: https://doi.org/10.1016/j.quaint.2015.06.046.

Punt, W. et al. (2007) 'Glossary of pollen and spore terminology', Review of palaeobotany and palynology, 143(1–2), pp. 1–81.

Ruwaimana, M. et al. (2020) 'The oldest extant tropical peatland in the world: a major carbon reservoir for at least 47,000 years', Environmental Research Letters [Preprint]. Available at: https://doi.org/10.1088/1748-9326/abb853.

Simbolon, H., & Mirmanto, E. (2000). Cheklist of Plant Species in the Peat Swamp Forest of Central Kalimantan Indonesia. hlm 179–190. In Proceedings of the International Symposium on Tropical peat Lands.

Slik, J. W. F., Poulsen, A. D., Ashton, P. S., Cannon, C. H., Eichhorn, K. A. O., Kartawinata, K., ... & Wilkie, P. (2003). A floristic analysis of the lowland dipterocarp forests of Borneo. Journal of Biogeography, 30(10), 1517–1531.

Tuah, S. J., Jamal, Y. M., & Limin, S. H. (2003). Nutritional characteristics in leaves of plants native to tropical peat swamps and heath forests of Central Kalimantan, Indonesia. Tropics, 12(3), 221-245.

Williams, J.W. et al. (2018) 'The Neotoma Paleoecology Database, a multiproxy, international, community-curated data resource', Quaternary Research, 89(1), pp. 156–177. Available at: https://doi.org/10.1017/qua.2017.105.

Yulianto, E. et al. (2005) 'A Holocene pollen record of vegetation and coastal environmental changes in the coastal swamp forest at Batulicin, South Kalimantan, Indonesia', Journal of Asian Earth Sciences, 25(1), pp. 1–8.

V. CONCLUDING SUMMARY

This research provided answers to most of the questions that we posed. Here, I reiterate the question and their answers in the following paragraphs. However, besides the planned questions, our research also provided some unexpected but important findings. Our first unexpected highlight is the age and the depth of the tropical inland peat, with a depth of 15–18m and age of more than 50,000 years, one of our sites is currently the most carbon-dense ecosystems in the world and the oldest extant peatland in the world. The second unexpected highlight is the finding of the flood as one of the main factors that shaped the stratigraphy of the peatland, as flooding is rarely mentioned as an important factor that affects peatland development and change over time.

Our first question is about initiation and formation of peatland and how it is related to the past climate and sea level changes. We answer this question by conducting radiocarbon dating analysis and combine the with previous published radiocarbon dates of peatlands throughout Kalimantan to create a synthesis of peatland formation. Before our research, only three radiocarbon-dated series were available in West Kalimantan: one inland peat dating to 45.6 ka (Anshari et al., 2001), and two coastal peat cores dating to 4.1 ka (Anshari et al., 2010) and 4.5 ka (Neuzil, 1997). This limited available data prompted us to provide more information on the peat age in this area. Thus, from our sample, we eventually conducted 41 radiocarbon dates, and 32 dates reported in the first published paper. We combined our data with 37 other radiocarbon dates from other studies all across Borneo and create a synthesis which shows a hiatus in peat genesis during a cool and dry period from to 20–30 ka. We highlight the inland peat, where the peat is exceptionally deep, reaching a maximum depth of 18 m and aged more than 50,000 years. Our best estimate of mean peat depth over 3833 km^2 of the Upper Kapuas is 5.16 ± 2.66 m, corresponding to a carbon density of 2,790 ± 1,440 Mg C/ha. This result suggests that our inland peat site is one of the most carbon dense ecosystems. It withstood the glacial-interglacial climate transition and remains mostly intact but is increasingly threatened by land-use change.

Our second question is about tropical peatlands carbon dynamic throughout times and its response to factors such as climate, fire, and humans. We answered this question by conducting stratigraphic physical and geochemical analyses, following widely applied rationale and methods (Bindler 2006). We collected and intensively radiocarbon-dated peat cores from two peat domes, inland peat of Putussibau and coastal peat of Rasau Jaya. We visualized their cross-sectional profiles of geochemical properties and developed three macrocharcoal records from each peat

dome. We found the young (4500 yr) and shallow (6 m) coastal peat has a simple and linear age-depth relationship, showing stable accumulation of carbon during the late Holocene. In contrast, the older (ca. 40,000 yr) and deeper (15 m) inland peat shows a more complex history, where we observed age reversals and hiatuses, likely caused by climate variability from the Last Glacial Maximum (LGM) to the Holocene. We also conducted analysis on charcoal as a proxy for fire occurrence. The charcoal record reveals a continuous presence of low severity fire as indicated by charcoal morphotypes, though fire frequency increased after agriculture established. An age reversal during the LGM was likely caused by a flood. Two periods of hiatuses occurred, each several millennia in length, at the end of the LGM and during the early Holocene. One cause of the hiatuses may have been a climatically-halted peat formation from low precipitation and cooler climate during the LGM. Another cause may have been that severe fires consumed thousands of years of accumulated peat. If the hiatuses were entirely due to fire, the carbon released from these paleo-fire events (600 t/ha) suggests several times the impact of the most intense modern peat fires.

Our third question is about tropical peatland vegetation change. As the previous chapter dealt with the physical and chemical properties of peat stratigraphy analysis, the last question deals on biological analysis which mainly focuses on pollen. Despite its relatively poor nutrients, tropical peatlands still support a high plant biodiversity (Lawrence, 2004; Page et al., 2012). These plants will produce either pollen or spores, which will be preserved in the peat layer. By identifying and quantifying the pollen and spore within a layer, we can infer the vegetation composition change and its response to factors such as climate, fire, and flood. Previous studies on peatland in Indonesia resulting on around 60–90 plant taxa, but mostly only identified to family level (Anshari et al., 2001; Hapsari et al., 2017; Yulianto et al., 2005). Studies of the pollen diversity of Southeast Asia peatlands are still non-existent, thus in this chapter we catalogued the pollen diversity of the peat. This resulted in 287 pollen and spore morphotypes. However, creating a pollen morphotypes atlas is only the first part of answering the question, as we need to complete a full analysis (of about 350 identified pollen per level in the core) to create a stratigraphic graph.

There are multiple challenges that we encounter during this research. First, with respect to the sampling process, we did not predict that the peat would be deeper than our coring equipment could reach. Most of the previous studies only predicted the peat depth at about 12 m (Belyea

and Baird, 2006; Page et al., 2004) thus we only brough the equipment that enough to core 15m. Fortunately one of our author, Gusti Anshari has another project that obtained a core at another site nearby, which found a total peat depth of 17–18 m, which may be the maximum depth at our site. Second, the coring equipment that we used, Russian Peat Corer, is designed for coring temperate peat, in which the main vegetation is sphagnum moss with occasional shrubs. However, tropical peat often has hardwood trees that grow to 1 to 2 m diameter, and even though theses trees, after falling onto the peat surface, slowly decay in the peat for thousands years, it is still difficult to core through them. Hence, coring was often halted, especially in the deep inland peat. This suggests that tropical peat probably needs better equipment and sampling method to collect a complete core at depths as great as 18 m. Third, our oldest peat sample is at the limit of radiocarbon dating, thus we can only say it is more than 50,000 years but we cannot confirm the real age. Other methods such as luminescence dating are probably applicable for dating basal sands below the peat (Lian and Roberts, 2006; Preusser et al., 2008) but this will require re-sampling. Fourth, despite already conducting 41 radiocarbon dates, which is a costly process, we could still be benefitted from more radiocarbon dating to create more detail age profile of our peat cores. And lastly, we underestimated the workload of the last research question. Unlike pollen research in northern temperate regions that has fewer species and a well referenced palynoflora, there is a much higher plant biodiversity and much more limited reference materials for tropical pollen. Thus, we limit our study on creating the pollen morphotype atlas and will continue this research after this dissertation.

References

Anshari, G., Peter Kershaw, A., van der Kaars, S., 2001. A Late Pleistocene and Holocene pollen and charcoal record from peat swamp forest, Lake Sentarum Wildlife Reserve, West Kalimantan, Indonesia. Palaeogeography, Palaeoclimatology, Palaeoecology, Quaternary Environmental Change in the Indonesian Region 171, 213–228. https://doi.org/10.1016/S0031-0182(01)00246-2

Anshari, G.Z., Afifudin, M., Nuriman, M., Gusmayanti, E., Arianie, L., Susana, R., Nusantara, R.W., Sugardjito, J., Rafiastanto, A., 2010. Drainage and land use impacts on changes in selected peat properties and peat degradation in West Kalimantan Province, Indonesia. Biogeosciences 7, 3403–3419.

Belyea, L.R., Baird, A.J., 2006. Beyond "the limits to peat bog growth": Cross-scale feedback in peatland development. Ecological Monographs 76, 299–322.

Bindler, R., 2006. Mired in the past — looking to the future: Geochemistry of peat and the analysis of past environmental changes. Global and Planetary Change, Peatlands: records of global environmental changes 53, 209–221. https://doi.org/10.1016/j.gloplacha.2006.03.004

Bridgham, S.D., Pastor, J., Dewey, B., Weltzin, J.F., Updegraff, K., 2008. Rapid carbon response of peatlands to climate change. Ecology 89, 3041–3048.

Cochrane, M.A., 2003. Fire science for rainforests. Nature 421, 913–919. https://doi.org/10.1038/nature01437

Dommain, R., Couwenberg, J., Glaser, P.H., Joosten, H., Suryadiputra, I.N.N., 2014. Carbon storage and release in Indonesian peatlands since the last deglaciation. Quaternary Science Reviews 97, 1–32. https://doi.org/10.1016/j.quascirev.2014.05.002

Dommain, R., Couwenberg, J., Joosten, H., 2011. Development and carbon sequestration of tropical peat domes in south-east Asia: links to post-glacial sea-level changes and Holocene climate variability. Quaternary Science Reviews 30, 999–1010. https://doi.org/10.1016/j.quascirev.2011.01.018

Haberle, S.G., Behling, H., Dupont, L., Kirleis, W., 2010. Introduction: Tropical palaeoecology and global change. Global Change Biology 16, 1645–1646. https://doi.org/10.1111/j.1365-2486.2010.02231.x

Hapsari, K.A., Biagioni, S., Jennerjahn, T.C., Reimer, P.M., Saad, A., Achnopha, Y., Sabiham, S., Behling, H., 2017. Environmental dynamics and carbon accumulation rate of a tropical peatland in Central Sumatra, Indonesia. Quaternary Science Reviews 169, 173–187. https://doi.org/10.1016/j.quascirev.2017.05.026

Lawrence, D., 2004. Erosion of tree diversity during 200 years of shifting cultivation in Bornean rain forest. Ecological Applications 14, 1855–1869. https://doi.org/10.1890/03-5321

Lian, O.B., Roberts, R.G., 2006. Dating the Quaternary: progress in luminescence dating of sediments. Quaternary Science Reviews 25, 2449–2468.

Neuzil, S.G., 1997. Onset and rate of peat and carbon accumulation in four domed ombrogenous peat deposits, Indonesia. Biodiversity and sustainability of tropical peatland.

Page, S., Hooijer, A., Rieley, J., Banks, C., Hoscilo, A., 2012. The tropical peat swamps of Southeast Asia: human impacts on biodiversity, hydrology and carbon dynamics, in: Rosen, B., Gower, D., Richardson, J., Johnson, K., Rüber, L., Williams, S. (Eds.), Biotic Evolution and Environmental Change in Southeast Asia, Systematics Association Special Volume Series. Cambridge University Press, Cambridge, pp. 406–433. https://doi.org/10.1017/CBO9780511735882.018

Page, S.E., Rieley, J.O., Banks, C.J., 2011. Global and regional importance of the tropical peatland carbon pool. Global Change Biology 17, 798–818. https://doi.org/10.1111/j.1365-2486.2010.02279.x

Page, S.E., Wűst, R. a. J., Weiss, D., Rieley, J.O., Shotyk, W., Limin, S.H., 2004. A record of Late Pleistocene and Holocene carbon accumulation and climate change from an equatorial peat bog (Kalimantan, Indonesia): implications for past, present and future carbon dynamics. J. Quaternary Sci. 19, 625–635. https://doi.org/10.1002/jqs.884

Preusser, F., Degering, D., Fuchs, M., Hilgers, A., Kadereit, A., Klasen, N., Krbetschek, M., Richter, D., Spencer, J.Q., 2008. Luminescence dating: basics, methods and applications. E&G Quaternary Science Journal 57, 95–149.

Young, D.M., Baird, A.J., Gallego-Sala, A.V., Loisel, J., 2021. A cautionary tale about using the apparent carbon accumulation rate (aCAR) obtained from peat cores. Sci Rep 11, 9547. https://doi.org/10.1038/s41598-021-88766-8

Yulianto, E., Rahardjo, A.T., Noeradi, D., Siregar, D.A., Hirakawa, K., 2005. A Holocene pollen record of vegetation and coastal environmental changes in the coastal swamp forest at Batulicin, South Kalimantan, Indonesia. Journal of Asian Earth Sciences 25, 1–8.

SUPPLEMENTARY DOCUMENTS

Supplementary for Chapter 2

We estimated the total carbon stock of peats in Upper Kapuas Basin following equation provided by Yu (2012) and Lawson (2015):

$Cs = A \times \overline{D} \times \overline{BD} \times \overline{CC}$

where:
Cs = carbon stock (kg)
A = area of the peat (m^2)
$\overline{D}$ = mean peat thickness / depth (m)
$\overline{BD}$ = mean bulk density (kg/m^3)
$\overline{CC}$ = mean carbon content (% dry mass)

Area of the peat

As there is uncertainty of the total peat coverage in this region, we calculated the area based on two available maps, one from Global Forest Watch which covers an area of 2,461.32 km^2 and one from *Badan Restorasi Gambut* (BRG, Peat Restoration Agency) from the Indonesian Government which covers an area of 3,833.2 km^2 (Fig S2.1).

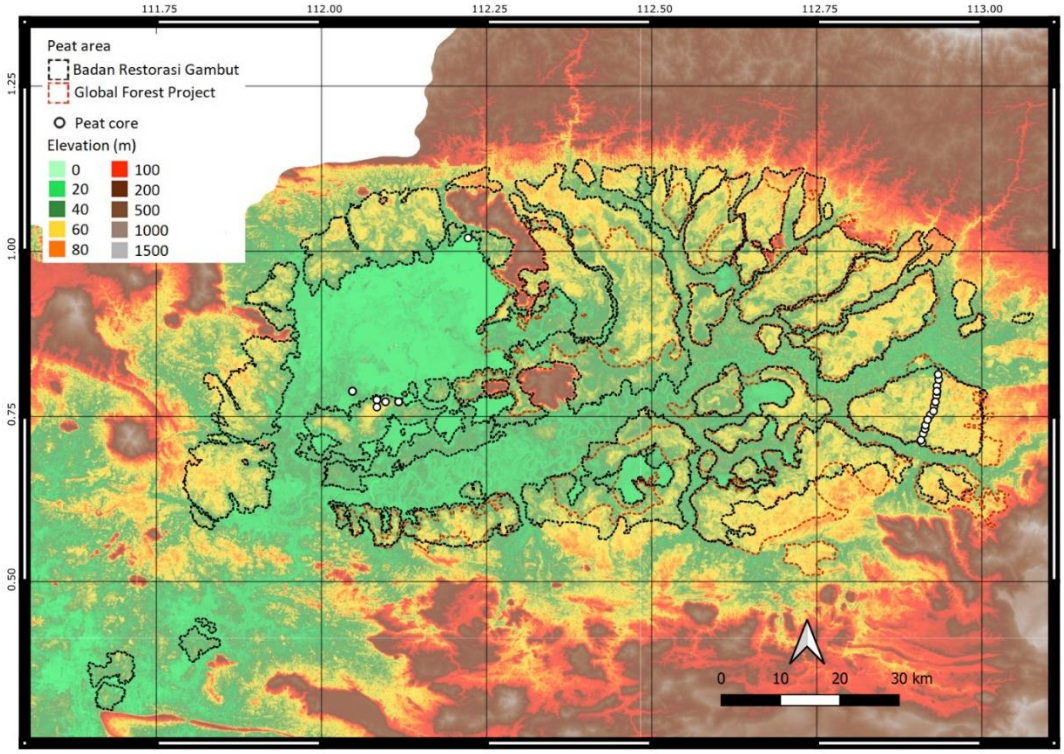

Figure S2.1 Map of Upper Kapuas Basin peat area. The map from Global Forest Project is delineated by a red line, while the map from Badan Restorasi Gambut Indonesia is delineated by a black line.

BD, LOI, CD per volume and CC per sample

We divided the cores into 25-cm-segments and resample 10 cm of the cores for bulk density analysis (Fig S2.2). Volume of each sample was measured by water displacement. After measuring dry mass, the same sample was used for loss-on-ignition (LOI) analysis (at 550°C). To calculate the carbon density per volume, we assumed that 54% of the LOI is carbon, as indicated by a previous study in the same region using an elemental analyzer (Anshari et al., 2010). As we have not yet used an elemental analyzer to measure the percent total organic carbon, we resorted to using LOI measurements to estimate CC. Based on Anshari et al. (2010), we expect this approach to result in only a ca. 4% error.

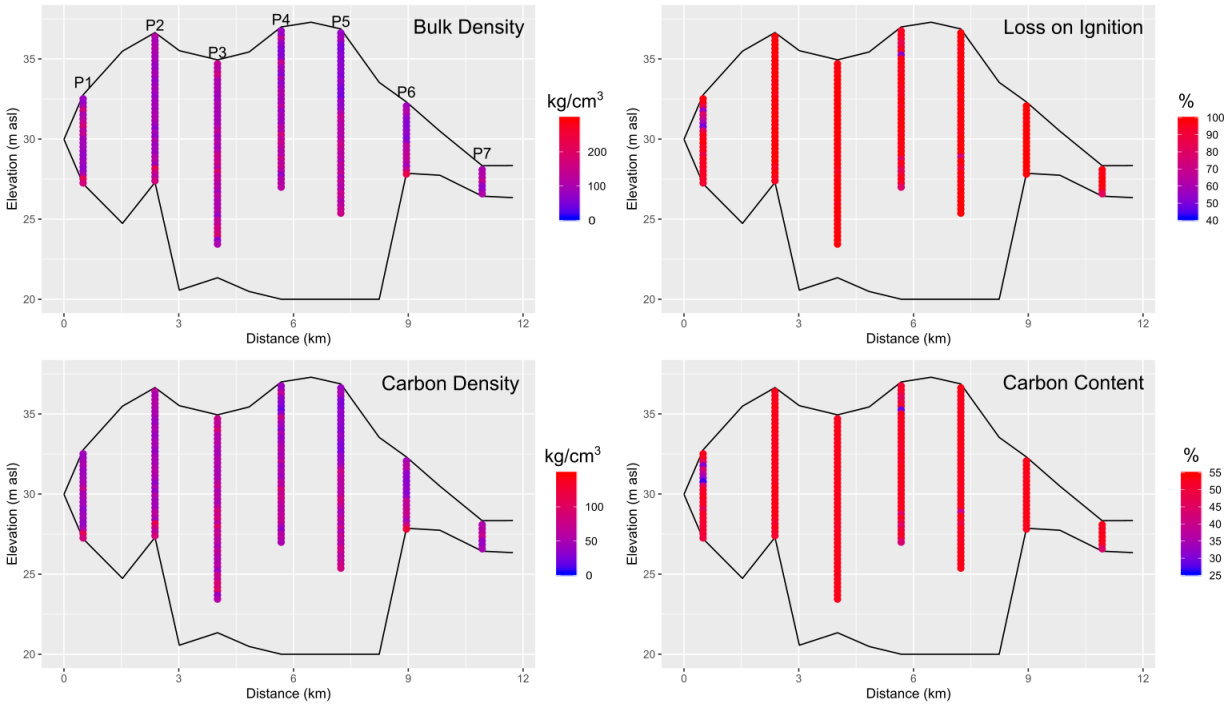

Figure S2.2. Value of bulk density, loss on ignition, carbon density per volume and carbon content for each 25 cm segments (n = 217). For core P3, P4 and P5 we able to get deeper to collect small 5 cm sample for radiocarbon, however, due to technical constrain (the peat corer was broken) we were not able to collect the 25 cm segment sample from depths below 10-11 m.

BD, LOI, CD and CC per core

We calculated the mean and standard deviation of BD, LOI, CD and CC per each core and for all sample. We calculated carbon density per unit area (Megagram per hectare – Mg/ha) by sum up the carbon density across the core. For the cores (P3, P4 and P5) that do not have complete samples until the bottom, we used average value of other samples in the same core.

Table S2.1. Mean and standard deviation of BD, LOI, CD and CC per core

Core	Depth	N sample	BD (kg/m^3)	LOI (%)	CD (kg/m^3)	CC (%)	CD (Mg/ha)
P1	5.5	22	110 ± 42	87.072 ± 15.17	50 ± 18	47.02 ± 8.19	2740 ± 997
P2	9.4	37	99 ± 30	98.828 ± 0.98	53 ± 16	53.37 ± 0.53	4922 ± 1452
P3	13.6	46	116 ± 29	99.134 ± 0.66	62 ± 15	53.53 ± 0.36	8417 ± 2067
P4	17.0	40	102 ± 30	94.558 ± 8.56	52 ± 16	51.06 ± 4.62	8858 ± 2679
P5	16.9	46	96 ± 34	98.172 ± 4.24	51 ± 18	53.01 ± 2.29	8576 ± 3099
P6	4.5	18	101 ± 45	99.321 ± 0.40	54 ± 24	53.63 ± 0.22	2444 ± 1093
P7	1.9	7	101 ± 25	96.192 ± 6.36	53 ± 14	51.94 ± 3.43	998 ± 260
Mean			**103 ± 6**	**96.182 ± 4.06**	**53 ± 4**	**51.94 ± 2.19**	**5279 ± 3081**

Local depth

Beside the main cores where we collected the core, we also conducted depth survey between the cores. We calculate the local depth based on these 14 points.

Table S2.2. Peat depth of the cores and sampling points in between cores.

Pointname	Depth (m)
P1	5.55
P1.5	10.75
P2	9.35
P2.5	14.95
P3	13.6
P3.5	14.95
P4	17
P4.5	17.29
P5	16.87
P5.5	13.53
P6	4.45
P6.5	2.75
P7	1.9
P7.5	2
Mean	**10.35**
SD	**5.71**

Modelling depth

As our local depth in our transect may not correctly represent the entire Upper Kapuas Basin, we tried to predict that value based on correlation with distance to the river and distance to the edge of peat dome. As we only have a small number of data point and they are not normally distributed, we used Kendall correlation method. We find that depth is more correlated to the distance to the peat edge than to the water (table S1.3 and S1.4)

Table S2.3. Distance to the river and peat edge for each sampling points and Kendall correlation value between peat depth, CD and distance to the river and to the peat edges.

Point	Depth (m)	Distance to (m)		
		River	GFW peat edge	BRG peat edge
P1	5.6	1787	79	236
P1.5	10.8	2922	1247	1358
P2	9.4	3776	2113	2221
P2.5	15.0	4370	2745	2854
P3	13.6	5377	3751	3859
P3.5	15.0	6236	4588	4695
P4	17.0	7115	5438	5543
P4.5	17.3	7043	5473	5719
P5	16.9	6386	4718	5054
P5.5	13.5	5594	3760	4255
P6	4.5	5139	3130	3697
P6.5	2.8	4757	2450	2816
P7	1.9	3812	1509	1726
P7.5	2.0	3160	1110	888
Kendal correlation value		**0.574594**	**0.662994**	**0.662994**

Afterward, we test simple linear and multiple polynomial regression betweendepth to the distance to the peat edge, however, AIC and BIC value suggest that simple linear correlation is better than the others. Here we only presented fit line and linear model that we use to predict the depth (Fig S2.3)

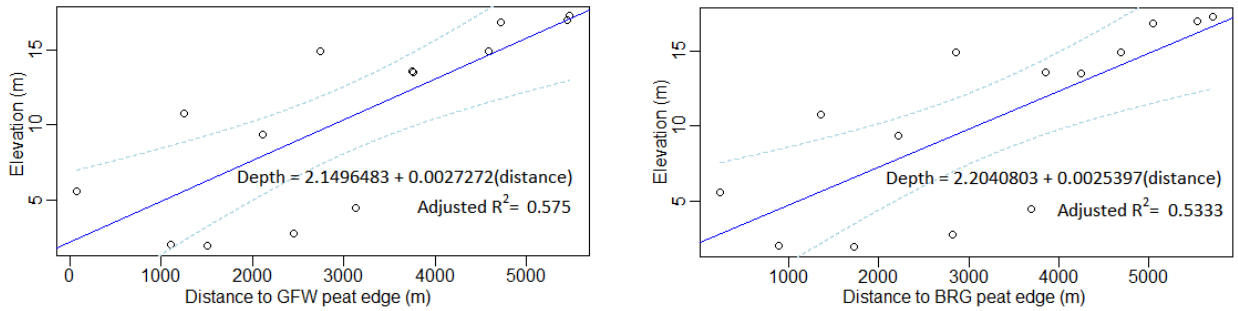

Figure S2.3. Linear equations used for predicting the depth based on their distance to the peat edge. Light dotted blue line shows 95% confidence interval

We use equations above to predict the depth at 1 km grid, and based on that we calculate the mean, upper and lower estimate of the depth (Fig S2.4.)

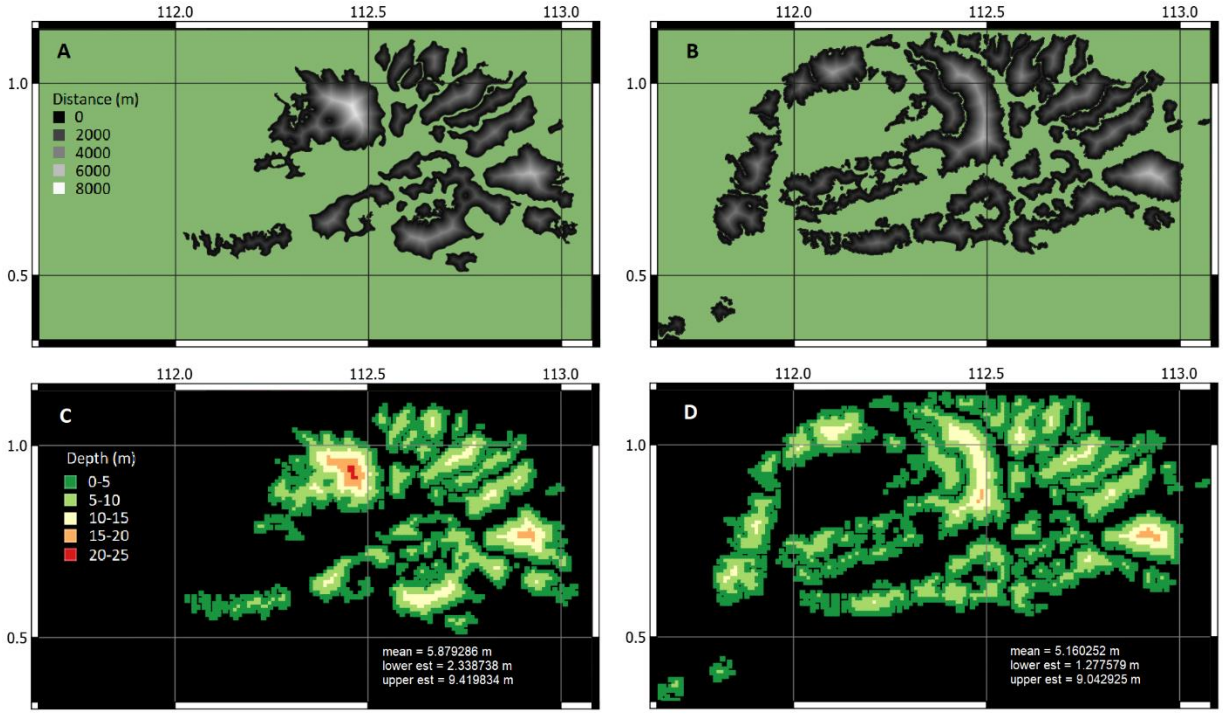

Figure S2.4. A & B - Distance to the peat edge for Global Forest Watch (A) and *Badan Restorasi Gambut* (B). C & D - Predicted depth based on the distance to the peat edge of each map, with lower and upper estimate with 95% confidence interval

Calculating the total carbon for Upper Kapuas Basin

We put the value of area, carbon density, depth, bulk density and carbon content based on data and calculation above to the equation:

Cs = $A \times \overline{D} \times \overline{BD} \times \overline{CC}$

where:

A = area of the peat:
- 2,461,320,000 m^2 (GFW)
- 3,833,200,000 m^2 (BRG)

$\overline{D}$ = mean peat depth:
- 10.35 m (sampling site)
- 5.88 m (predicted based on GFW map)
- 5.16 m (predicted based on BRG map)

$\overline{BD}$ = mean bulk density: 103 kg/m^3

$\overline{CC}$ = mean carbon content: 51.94 %

Table S2.4. Carbon store estimation in Upper Kapuas Basin. Area values are based on either GFW or BRG map, and the depth are based on mean sampling sites or based on modelling.

Area and depth value sources	Area (m^2)	Depth (m)	BD (kg/m^3)	CC (%)	total (kg)	lower est (kg)	upper est (kg)
GFW map, sampling sites depth	2,461,320,000	10.35 ± 5.71 (SD)	103.8 ± 6.1	51.95 ± 2.1	1,373,879,639,905	553,412,391,661	2,359,172,447,312
BRG map, sampling sites depth	3,833,200,000				2,139,646,789,398	861,871,020,312	3,674,117,881,883
GFW, modelled depth	2,461,320,000	5.88 ± 3.54 (95% CI)			780,522,925,859	279,091,594,070	1,383,773,627,253
BRG, modelled depth	3,833,200,000	5.16 ± 2.66 (95% CI)			1,066,722,457,323	464,370,161,806	1,789,016,303,632

Calculating carbon density per hectare

Mean carbon density in our sample is 53±4 kg/m^3 and carbon density per hectare on our sampling site is 5279±3081 MgC/ha (Table S1.1). However, to state the value of carbon density of the Upper Kapuas Basin, we also use the modelled depth to calculate the value of carbon density (Table S1.5).

Table S2.5. Carbon density estimation based on modelled depth.

Depth value sources	Depth (m)	CD (kg/m^3)	CD (kg/m^2)	lower est (kg/m^2)	upper est (kg/m^2)
Modelled depth of GFW map	5.88 ± 3.54 (95% CI)	53.4 ± 3.7	313.992	116.298	468.174
Modelled depth of BRG map	5.16 ± 2.66 (95% CI)		275.544	124.25	388.654

Table S2.6. List of Radiocarbon dates used for Figure 2.4.

ID	Material	Location	Lat	Long	Study	Basal	Depth (m)	Top elevation	Bottom elevation	Lab code	Age	Error	Cal year mean	Cal year min	Cal year max
IF I	Bulk peat (125-500 µm)	Gunung Palung	-1.21	110.098	This study	Y	0.15	10	9.85	NOSAMS-156265	35	20	NA	NA	NA
IF II	Bulk peat (125-500 µm)	Gunung Palung	-1.21	110.098	This study	Y	0.15	10	9.85	NOSAMS-156266	0	0	NA	NA	NA
TZ I	Bulk peat (125-500 µm)	Gunung Palung	-1.206	110.097	This study	Y	1.24	10	8.76	NOSAMS-156276	1120	15	1020	980	1060
TZ II	Bulk peat (125-500 µm)	Gunung Palung	-1.207	110.096	This study	Y	0.90	10	9.1	NOSAMS-156277	7260	30	8090	8010	8160
TZ III	Bulk peat (125-500 µm)	Gunung Palung	-1.206	110.094	This study	Y	1.32	10	8.68	NOSAMS-156278	8290	35	9310	9140	9420
KP I	Bulk peat (125-500 µm)	Gunung Palung	-1.209	110.097	This study	Y	0.15	10	9.85	NOSAMS-156267	275	20	310	160	430
KP II	Bulk peat (125-500 µm)	Gunung Palung	-1.209	110.097	This study	Y	0.30	10	9.7	NOSAMS-156268	3500	20	3770	3700	3830
RC1	Macrofossil (>500 µm)	Ketapang	-1.582	110.431	This study	Y	8.47	NA	NA	NOSAMS-156271	9640	50	10970	10780	11190
RC1	Macrofossil (>500 µm)	Ketapang	-1.582	110.431	This study	Y	8.47	NA	NA	NOSAMS-156269	9610	40	10940	10780	11160
RC1	Bulk peat (125-500 µm)	Ketapang	-1.582	110.431	This study	Y	8.47	NA	NA	NOSAMS-156270	9560	45	10930	10720	11100
RC2	Macrofossil (>500 µm)	Ketapang	-1.598	110.480	This study	Y	4.87	NA	NA	NOSAMS-156272	5750	25	6550	6480	6640
RC2	Bulk peat (125-500 µm)	Ketapang	-1.598	110.480	This study	Y	4.87	NA	NA	NOSAMS-156273	4690	25	5390	5320	5570
RC3	Macrofossil (>500 µm)	Ketapang	-1.618	110.449	This study	Y	3.18	NA	NA	NOSAMS-156274	6180	25	7080	7000	7160
RC3	Bulk peat (125-500 µm)	Ketapang	-1.618	110.449	This study	Y	3.18	NA	NA	NOSAMS-156275	6120	25	6990	6910	7160
P1	Bulk peat (125-500 µm)	Putussibau	0.714	112.908	This study	Y	5.55	32.76	27.21	NOSAMS-161956	31700	730	35710	34350	37620
P3	Bulk peat (125-500 µm)	Putussibau	0.745	112.918	This study	Y	13.60	34.94	21.34	NOSAMS-161957	26200	370	30410	29610	31020
P4	Bulk peat (125-500 µm)	Putussibau	0.758	112.927	This study	N	15.00	37	22	NOSAMS-161958	46100	5200	47850	44890	>50000
P5	Bulk peat (125-500 µm)	Putussibau	0.772	112.930	This study	N	12.00	36.87	24.87	NOSAMS-161959	35600	1400	40230	37660	42730
P6	Bulk peat (125-500 µm)	Putussibau	0.788	112.932	This study	Y	4.45	32.31	27.86	NOSAMS-161960	15450	110	18710	18490	18920
R3	Bulk peat (125-500 µm)	Rasau Jaya	-0.24	109.372	This study	Y	0.60	1.29	0.69	NOSAMS-161951	4010	20	4480	4420	4520
R5.5	Bulk peat (125-500 µm)	Rasau Jaya	-0.205	109.396	This study	Y	5.85	7.08	1.23	NOSAMS-161952	3920	20	4360	4290	4420
R6	Bulk peat (125-500 µm)	Rasau Jaya	-0.199	109.398	This study	Y	6.00	7.54	1.54	NOSAMS-161953	3870	20	4310	4240	4410
R6.5	Bulk peat (125-500 µm)	Rasau Jaya	-0.191	109.405	This study	Y	4.80	6.31	1.51	NOSAMS-161954	3950	20	4420	4300	4510
R7	Bulk peat (125-500 µm)	Rasau Jaya	-0.184	109.408	This study	Y	3.40	5.64	2.24	NOSAMS-161955	3880	20	4330	4250	4410
T1P3	Bulk peat (125-500 µm)	Sentarum	0.772	112.117	This study	N	0.20	NA	NA	Wk-F32491	4587	59	5290	5050	5470
T1P3	Bulk peat (125-500 µm)	Sentarum	0.772	112.117	This study	N	7.80	NA	NA	Wk-F32485	12074	137	13940	13560	14370
T1P3	Bulk peat (125-500 µm)	Sentarum	0.772	112.117	This study	Y	9.00	NA	NA	Wk-F32492	11894	60	13700	13560	13940
T2P3	Bulk peat (125-500 µm)	Sentarum	0.772	112.097	This study	Y	6.92	NA	NA	Wk-F32488	12689	158	15040	14320	15600
T3P3	Bulk peat (125-500 µm)	Sentarum	0.775	112.084	This study	N	0.15	NA	NA	Wk-F32489	5716	66	6510	6320	6670
T3P3	Bulk peat (125-500 µm)	Sentarum	0.775	112.084	This study	Y	2.05	NA	NA	Wk-F32487	16444	121	19840	19540	20140
T4P3	Bulk peat (125-500 µm)	Sentarum	0.764	112.084	This study	Y	14.00	NA	NA	Wk-F32490	11693	160	13530	13200	13930
S2	Bulk peat (125-500 µm)	Sentarum	1.02	112.222	This study	N	0.05	18.42	18.37	NOSAMS-161950	9050	40	10220	10180	10250
BRO-1963	Bulk peat	Marudi	-1.1	114.133	(Anderson and Muller, 1975)	Y	NA	NA	NA	NA	4270	70	4840	4580	5040
Wk-5779	Bulk peat	Sentarum	0.788	112.047	(Anshari et al., 2004)	Y	1.24	NA	NA	Waikato	28780	100	32950	32560	33350
OZE148	Pollen	Sentarum	0.788	112.047	(Anshari et al., 2004)	Y	0.82	NA	NA	Waikato	42200	700	45570	44410	46910
OZE145	Pollen	Sentarum	0.788	112.047	(Anshari et al., 2004)	Y	0.99	NA	NA	Waikato	38800	450	42740	42150	43390
OZE141	Pollen	Sentarum	0.788	112.047	(Anshari et al., 2004)	Y	1.50	NA	NA	Waikato	32800	300	36850	36130	37910
Wk 26757	Bulk peat	Rasau Jaya	-0.21	109.396	(Anshari et al., 2010)	Y	7.00	NA	NA	Waikato	3784	40	4160	3990	4290
E2P23-3	Bulk peat (< 1 mm)	Kutai Basin	-0.163	116.290	(Hope et al., 2005)	Y	13.49	NA	NA	NA	7500	220	8320	7870	8970
MLT1-4	Bulk peat (< 1 mm)	Kutai Basin	-0.275	116.310	(Hope et al., 2005)	Y	8.70	NA	NA	NA	6610	200	7500	7160	7930
S3P31-1	Bulk peat (< 1 mm)	Kutai Basin	-0.063	116.760	(Hope et al., 2005)	Y	13.75	NA	NA	NA	5900	320	6760	6030	7430
TM3P7-1	Bulk peat (< 1 mm)	Kutai Basin	-0.09	116.480	(Hope et al., 2005)	Y	12.25	NA	NA	NA	5690	90	6490	6310	6660
K1P17-3	Bulk peat (< 1 mm)	Kutai Basin	0.189	116.620	(Hope et al., 2005)	Y	8.70	NA	NA	NA	5500	130	6290	5950	6600
D1P5-2	Bulk peat (< 1 mm)	Kutai Basin	0.151	116.840	(Hope et al., 2005)	Y	6.32	NA	NA	NA	4830	270	5550	4880	6180
SR3P500-2	Bulk peat (< 1 mm)	Kutai Basin	-0.069	116.580	(Hope et al., 2005)	Y	6.07	NA	NA	NA	4300	140	4890	4530	5300
PK5-C14	Bulk peat	Palangkaraya	-2.167	113.667	(Neuzil, 1995) in (Dommain et al., 2011)	Y	NA	NA	NA	NA	9510	200	10830	10260	11250
PK2-C14	Bulk peat	Palangkaraya	-2.067	113.783	(Neuzil, 1995) in (Dommain et al., 2011)	Y	NA	NA	NA	NA	8140	180	9070	8610	9470
Wk-3	Bulk peat	Teluk Keramat	1.422	109.144	(Neuzil, 1995) in (Dommain et al., 2011)	Y	6.50	9	2.5	NA	4040	170	4530	4010	4960
N2	Bulk peat	Barambai	-2.58	115.390	(Notohadiprawiro, 2006)	Y	1.00	NA	NA	NA	2310	90	2340	2120	2700
SA6.5	Bulk peat	Sebangau	-2.384	113.863	(Page et al., 2004)	Y	9.50	NA	NA	NA	20350	130	24460	24100	24940
T2-020	Bulk peat	Rajang River	-2.5	111.567	(Staub and Esterle, 1994)	Y	6.00	3.8	-2.2	NA	6105	105	6990	6750	7240
T3-080	Bulk peat	Rajang River	-2.5	111.567	(Staub and Esterle, 1994)	Y	3.00	6.15	3.15	NA	1245	120	1160	930	1350

Table S2.6. (Continued) List of Radiocarbon dates used for Figure 2.4.

ID	Material	Location	Lat	Long	Study	Basal	Depth (m)	Top elevation	Bottom elevation	Lab code	Age	Error	Cal year mean	Cal year min	Cal year max
T2-100	Bulk peat	Rajang River	-2.5	111.567	(Staub and Esterle, 1994)	Y	NA	NA	-0.3	NA	6405	120	7320	7020	7560
T2-140	Bulk peat	Rajang River	-2.5	111.567	(Staub and Esterle, 1994)	Y	NA	NA	-0.6	NA	5945	205	6800	6320	7260
T2-000	Bulk peat	Rajang River	-2.5	111.567	(Staub and Esterle, 1994)	Y	6.50	2.55	-3.95	NA	5610	195	6420	5950	6850
T3-120	Bulk peat	Rajang River	-2.5	111.567	(Staub and Esterle, 1994)	Y	4.00	7.6	3.6	NA	1635	140	1550	1300	1860
RB-01	Bulk peat	Rajang River	-2.4	111.750	(Staub, James R. and Gastaldo, 2003)	Y	NA	NA	-0.6	NA	7340	220	8160	7740	8580
R-090-3	Bulk peat	Rajang River	-2.7	111.867	(Staub, James R. and Gastaldo, 2003)	Y	NA	NA	-2.7	NA	7060	280	7910	7440	8400
R-090-4	Bulk peat	Rajang River	-2.7	111.867	(Staub, James R. and Gastaldo, 2003)	Y	NA	NA	-2.7	NA	6820	325	7700	7030	8360
RI-06	Bulk peat	Rajang River	-2.4	111.750	(Staub, James R. and Gastaldo, 2003)	Y	NA	NA	-1.6	NA	6080	100	6950	6720	7240
RL-03	Bulk peat	Rajang River	-2.4	111.750	(Staub, James R. and Gastaldo, 2003)	Y	NA	NA	-0.9	NA	6055	95	6920	6680	7160
R-116-2	Bulk peat	Rajang River	-2.7	111.867	(Staub, James R. and Gastaldo, 2003)	Y	NA	NA	-1	NA	5830	100	6640	6410	6880
B4	Bulk peat	Baram River	4.45	114.017	(Tie and Esterle, 1991) in (Dommain et al., 2011)	Y	NA	NA	NA	NA	3570	50	3870	3710	3980
KB3	Bulk peat	Baram River	4.533	114.000	(Tie and Esterle, 1991) in (Dommain et al., 2011)	Y	NA	NA	NA	NA	1140	50	1050	940	1180
UBA-10003	Bulk peat	Bario, Sarawak	3.733	115.484	(Treat et al., 2017)	Y	NA	NA	NA	NA	40397	436	43980	43210	44790
GRO-1963	Bulk peat	Baram River	4.15	114.233	(Wilford, 1959) in (Dommain et al., 2011)	Y	NA	NA	NA	NA	4270	70	4840	4580	5040
NZ-352	Bulk peat	Lawas River	4.917	114.417	(Wilford, 1959) in (Dommain et al., 2011)	Y	NA	NA	NA	NA	1950	70	1900	1720	2100
OZJ341	Pollen	Sebangau	-2.384	113.863	(Wüst et al., 2008)	Y	8.67	NA	NA	NA	33930	395	38390	37160	39340
LGK-1276	Bulk peat	Batu Licin	-3.317	116.117	(Yulianto et al., 2005)	Y	4.50	NA	NA	NA	5140	180	5900	5580	6290

Table S2.7. Correlation between depth and basal age for all dated core in Borneo, for our study only, and for each site

Sample	Number of basal-dated cores	Kendall correlation of depth and basal age
All Borneo	45	0.165
This study	24	0.321
Rasau*	5	-0.600
Putussibau	5	0.600
Sentarum**	9	-0.833
Gunung Palung	7	0.720
Ketapang***	3	0.333

*This negative correlation is due to disturbance, where the oldest core at R3 is very degraded and only 60 cm peat remains. Thus, we suggest do not take this value into account as we could not predict what is real undisturbed peat depth in this site.

** We use data from our study (4 cores) and from Anshari, et al (2004) (5 cores).

*** We averaged the date of different dated material (bulk peat and macrofossil)

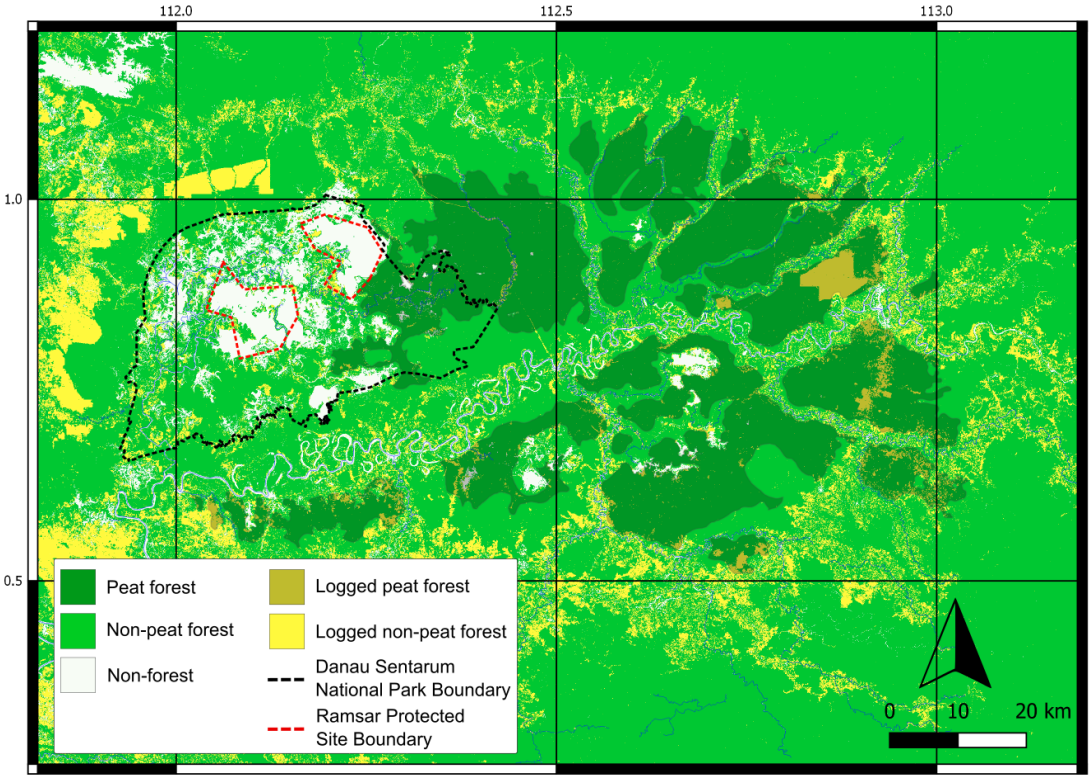

Figure S2.5 Logged forest area, protected areas, and peat extent in the upper Kapuas Basin. Non-peat areas include freshwater swamp forest and upland forest. The logged area estimate is from Global Forest Watch (Hansen et al., 2013) for the year 2000-2018. Summary statistics are in Table S3.

Table S2.8. Peat area, protected area and logged peat area in Upper Kapuas Basin

Land cover	**Area (ha)**	**Percentage**
Peat	246,132	100.0
Protected peat (within Danau Sentarum National Park)	58,123	23.6
Logged peat forest (2018)	17,173	7.0

Supplementary for Chapter 3

Table S3.1. Radiocarbon dates and resulting calibrated ages using rcarbon IntCal20

No	Core-Depth(cm)	Age	Err	Lab ID*	Age_min	Age_med	Age_max	Coord(lat;long)
1	P1-550	31700	730	OS-151563	34210	36660	39110	0.804;112.927
2	P2-945	44234	281	D-AMS 045876	45540	46760	47990	0.792;112.926
3	P3-85	1410	15	OS-155104	1280	1320	1360	0.780;112.925
4	P3-110	11300	75	OS-164600	12920	13190	13460	0.780;112.925
5	P3-150	10611	33	D-AMS 044484	12480	12620	12730	0.780;112.925
6	P3-200	11600	70	OS-155105	13180	13480	13760	0.780;112.925
7	P3-375	12750	90	OS-164601	14520	15130	15680	0.780;112.925
8	P3-500	15050	110	OS-155106	17940	18360	18770	0.780;112.925
9	P3-625	28131	96	D-AMS 044485	31600	32300	33000	0.780;112.925
10	P3-700	37900	2500	OS-164602	36290	41160	46030	0.780;112.925
11	P3-750	22400	300	OS-155107	25820	26730	27640	0.780;112.925
12	P3-1000	22800	360	OS-164603	25920	26920	27930	0.780;112.925
13	P3-1355	26200	370	OS-151564	29200	30230	31250	0.780;112.925
14	P4-250	1300	15	OS-164604	1180	1240	1300	0.768;112.922
15	P4-330	3867	25	D-AMS 045877	4100	4270	4420	0.768;112.922
16	P4-410	3527	30	D-AMS 045878	3640	3810	3980	0.768;112.922
17	P4-500	11521	37	D-AMS 044486	13240	13390	13580	0.768;112.922
18	P4-625	14225	47	D-AMS 045879	17040	17270	17500	0.768;112.922
19	P4-750	15850	140	OS-164605	18710	19160	19620	0.768;112.922
20	P4-825	27229	126	D-AMS 045880	31020	31370	31710	0.768;112.922
21	P4-995	24684	83	D-AMS 044489	28620	28920	29220	0.768;112.922
22	P4-1400	29921	133	D-AMS 045881	33980	34380	34770	0.768;112.922
23	P4-1495	46100	5200	OS-151672	40780	47890	55000	0.768;112.922
24	P5-95	425	18	D-AMS 044488	330	470	530	0.756;112.918
25	P5-250	3630	25	OS-164606	3780	3960	4140	0.756;112.918
26	P5-500	3906	25	D-AMS 041764	4150	4320	4520	0.756;112.918
27	P5-625	12000	85	OS-164607	13510	13870	14300	0.756;112.918
28	P5-750	12430	45	D-AMS 041765	14160	14590	15030	0.756;112.918
29	P5-1000	17630	53	D-AMS 044487	20930	21360	21790	0.756;112.918
30	P5-1050	28402	116	D-AMS 045882	31810	32540	33270	0.756;112.918
31	P5-1195	35600	1400	OS-151673	36270	39500	42730	0.756;112.918
32	P6-430	15450	110	OS-151674	18260	18690	19110	0.744;112.926
33	R3 -55	4010	20	OS-151558	4410	4500	4610	-0.240;109.372
34	R5.5-300	2920	20	OS-164597	2890	3070	3210	-0.205;109.396
35	R5.5-525	3920	20	OS-151559	4160	4350	4520	-0.205;109.396
36	R6-100	1390	15	OS-155108	1280	1310	1350	-0.199;109.398
37	R6-300	2530	20	OS-164598	2470	2620	2750	-0.199;109.398
38	R6-595	3870	20	OS-151560	4150	4280	4420	-0.199;109.398
39	R6.5-300	2540	25	OS-164599	2460	2610	2750	-0.191;109.405
40	R6.5-485	3950	20	OS-151561	4240	4380	4520	-0.191;109.405
41	R7-335	3880	20	OS-151562	4150	4280	4420	-0.184;109.408

*Lab ID
OS = NOSAMS Laboratory (Woods Hole, MA)
D-AMS = DirectAMS (Bothell WA)

Figure S3.1. Bacon Age-Depth model output of three deepest cores form each site (Rasau Jaya: R55, R6, R65, Putussibau: P3, P4 and P5). Each model shows the types of The Bayesian modeling applied for each core.

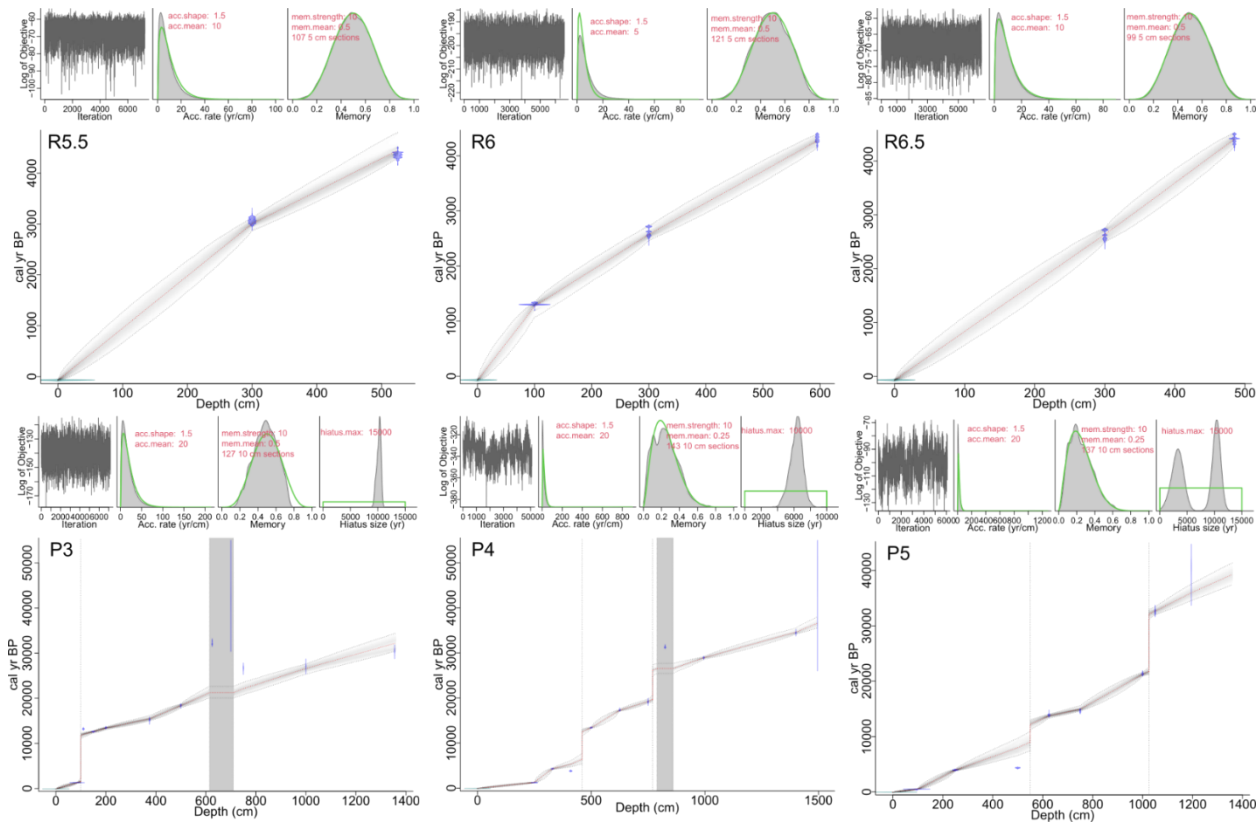

Figure S3.2. Vertical Profile of BD, LOI, C%, CD of Coastal (Rasau) and Inland (Putussibau) peat domes. Note that the color scale is unique for each graph.

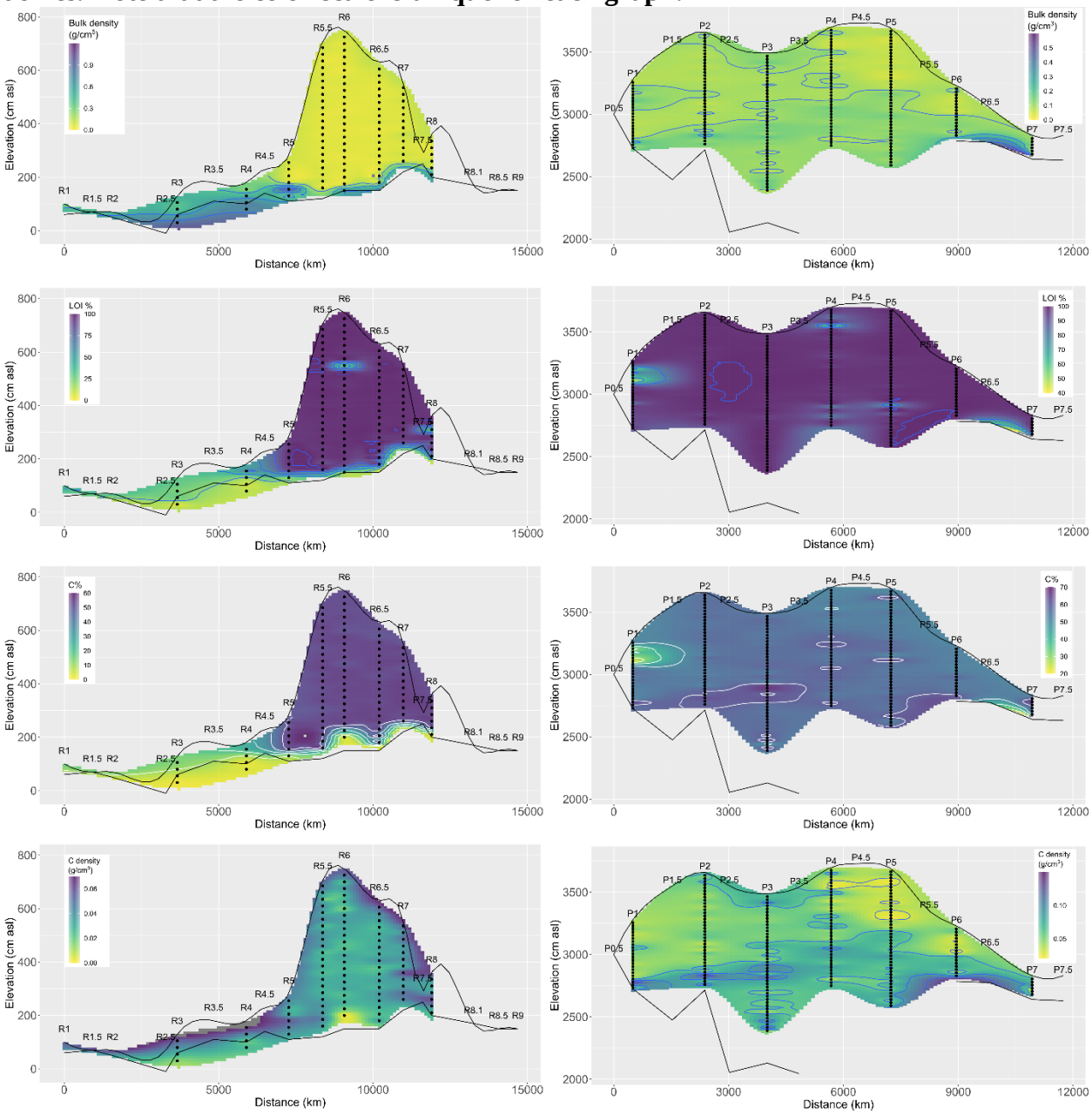

Figure S3.3. Vertical profile N%, CN, ^{13}C, ^{15}N of Coastal (Rasau) and Inland (Putussibau) peat domes. Note that the color scale is unique for each graph.

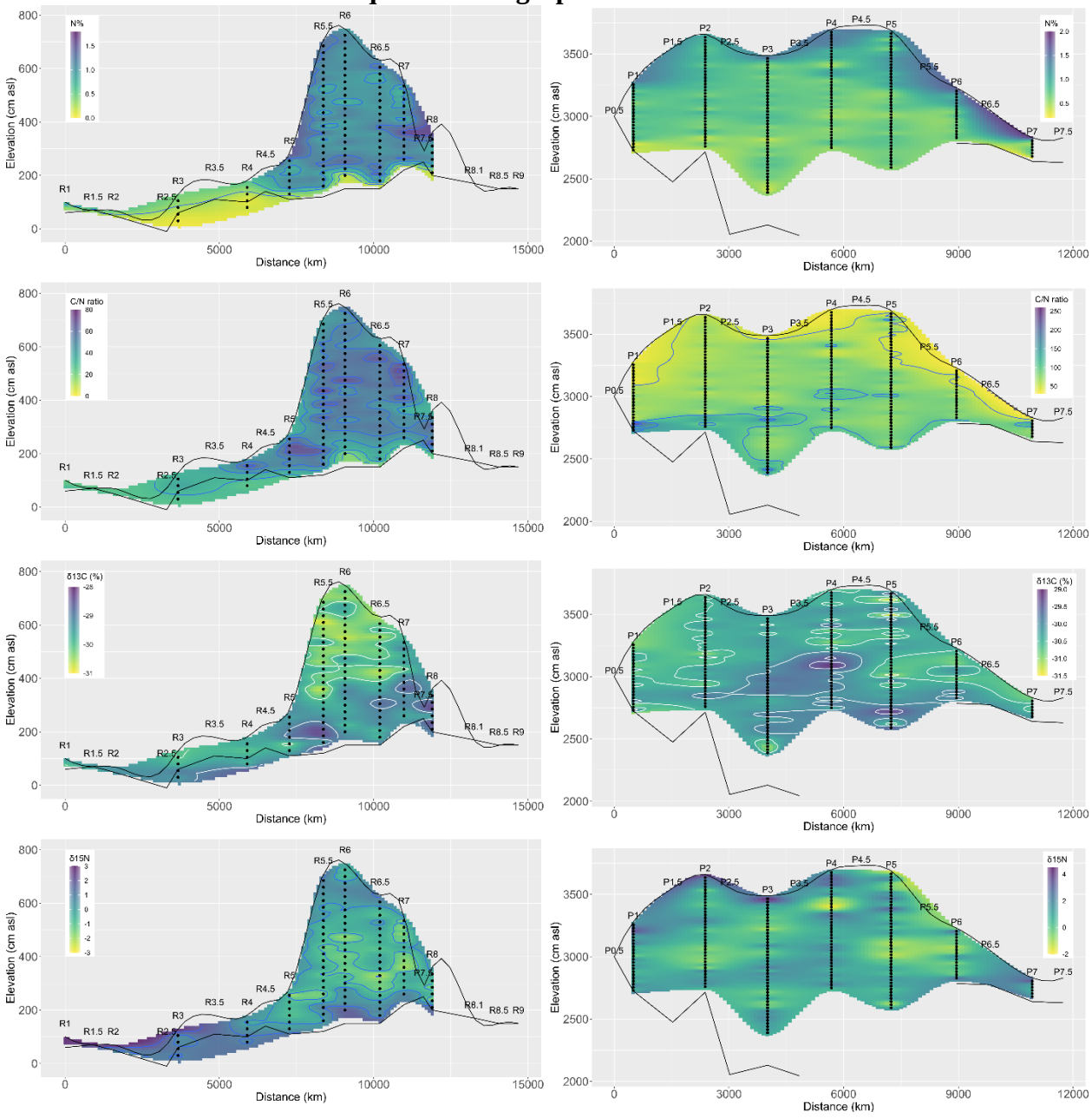

Figure S3.4. PUTUSSIBAU BD, aCAR, 13C, 15N, C%, N%, CN ratio. Light red block = hiatus, yellow line = slump

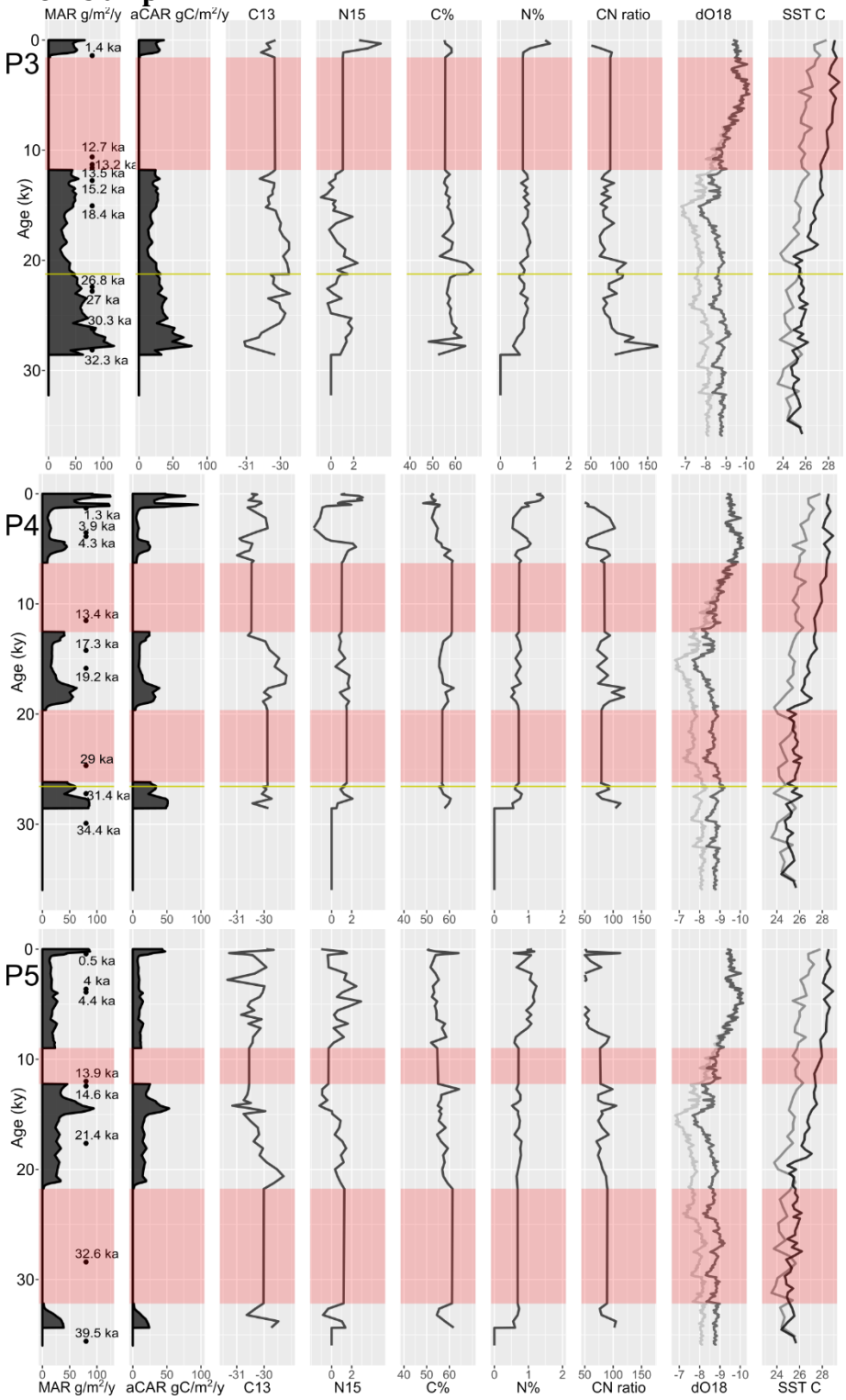

Figure S3.5. RASAU BD, aCAR, C13, N15, C%, N%, CN ratio.

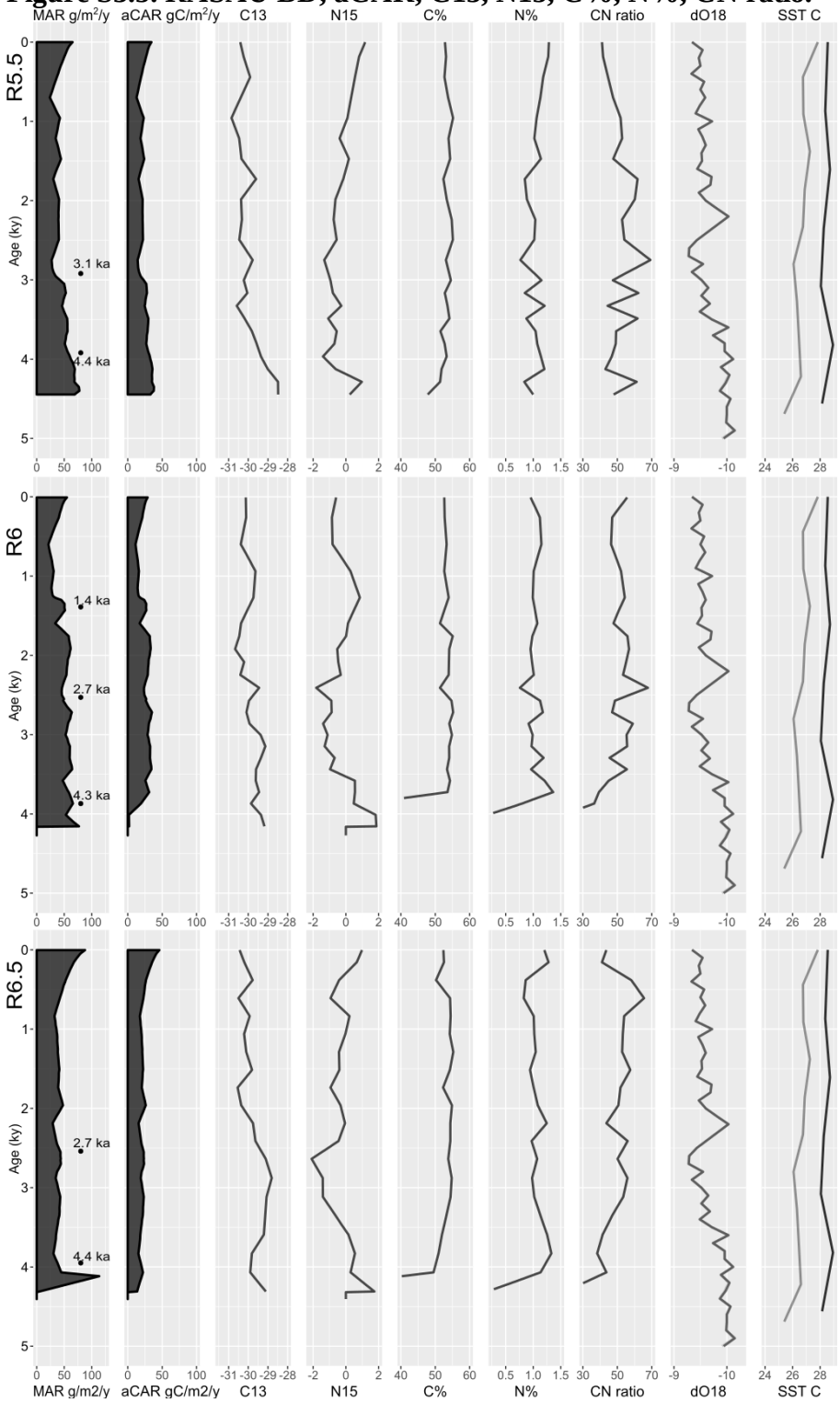

Figure S3.6. PUTUSSIBAU Charcoal types. Light red block = hiatus, yellow line = slump

Figure S3.7. RASAU Charcoal types.

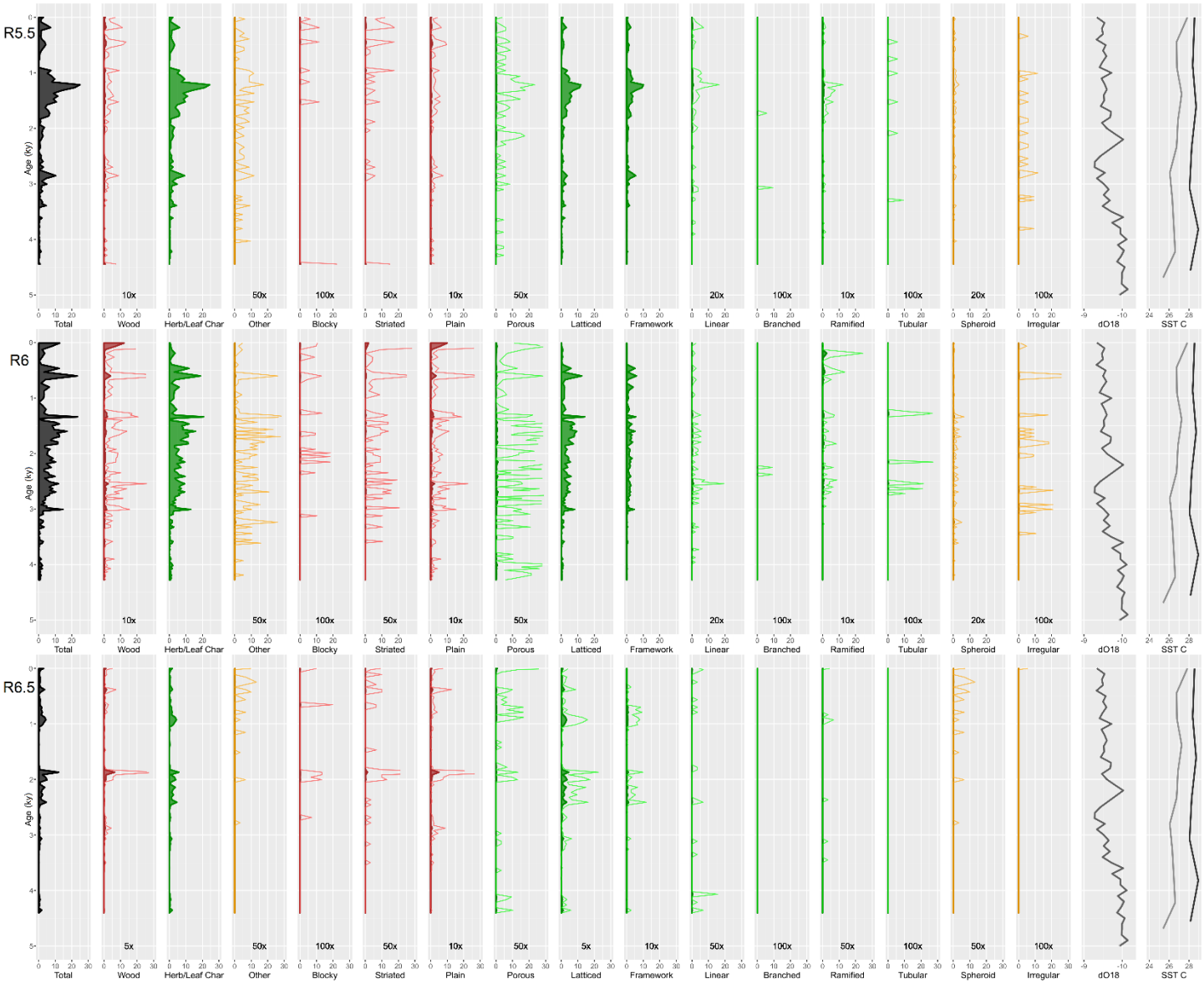

Figure S3.8. $\delta^{13}C$ NMR spectra of a non-charcoal sample, a charcoal sample, and the lattice morphotype

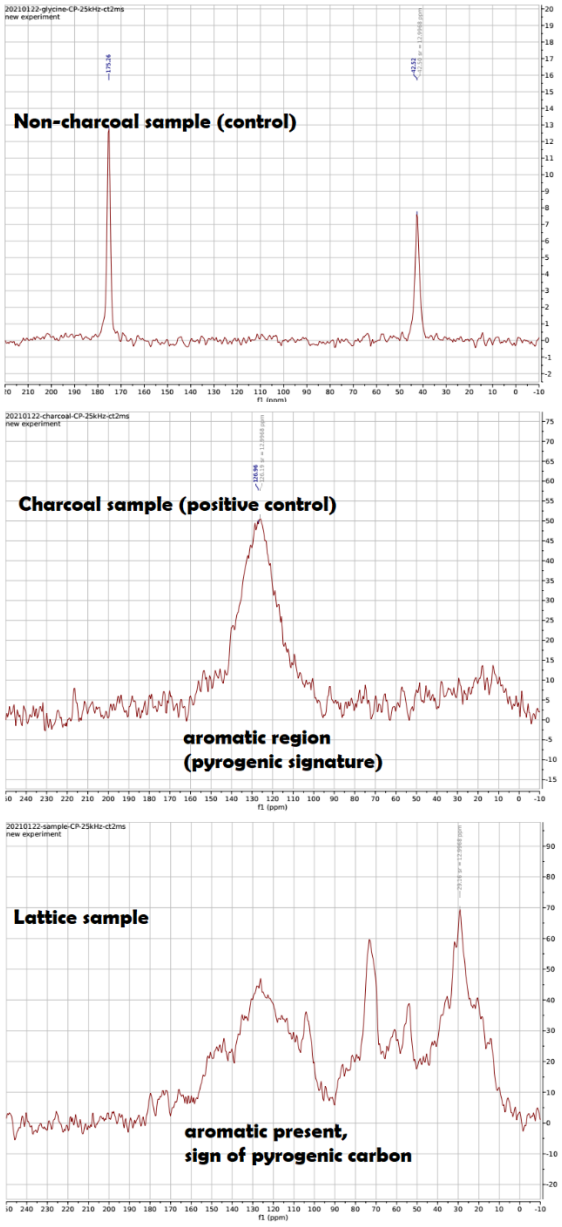

Figure S3.9. Silt deposit in cores P1.5 and P2 and its corresponding position in the peat dome